Final Technical Report

Project Title: Biorefinery and Hydrogen Fuel Cell Research

Award Number: DE-FG36-05GO85012

Recipient: Georgia Environmental Facilities Authority (Research subcontracted to The University of Georgia, Athens GA)

Project Location(s): University of Georgia, Athens GA 30602

Project Period: 1 July 2005 to 30 June 2010
Date of Report: April 2011
Written by: K.C. Das
Program Manager: K.C. Das

Principal Investigators: K.C. Das, Thomas T. Adams, Mark A. Eiteman, John Stickney, Joy Doran Peterson, James R. Kastner, Sudhagar Mani, Ryan Adolophson.

Subcontractors: The University of Georgia, Athens GA 30602

Cost-Sharing Partners: The University of Georgia, Athens GA 30602

DOE Project Team:

DOE Role – Person – Phone – Email
DOE-HQ contact: Natalie Roberts, 202-586-2325, natalie.roberts@ee.doe.gov
Field Project Officer: Jim Payne, 720-356-1744, jim.payne@go.doe.gov
Contract Specialist: Andrew Rittgers, 720-356-1769, Andrew.rittgers@go.doe.gov
Project Engineer: Evan Mueller, 720-356-1390, evan.mueller@go.doe.gov

Acknowledgment: This material is based upon work supported by the Department of Energy under Award Number DE-FG36-05GO85012.

Executive Summary

In this project we focused on several aspects of technology development that advances the formation of an integrated biorefinery. These focus areas include: [1] establishment of pyrolysis processing systems and characterization of the product oils for fuel applications, including engine testing of a preferred product and its pro forma economic analysis; [2] extraction of sugars through a novel hotwater extaction process, and the development of levoglucosan (a pyrolysis BioOil intermediate); [3] identification and testing of the use of biochar, the coproduct from pyrolysis, for soil applications; [4] developments in methods of atomic layer epitaxy (for efficient development of coatings as in fuel cells); [5] advancement in fermentation of lignocellulosics, [6] development of algal biomass as a potential substrate for the biorefinery, and [7] development of catalysts from coproducts. These advancements are intended to provide a diverse set of product choices within the biorefinery, thus improving the cost effectiveness of the system.

Technical effectiveness was demonstrated in the pyrolysis biooil based diesel fuel supplement, sugar extraction from lignocelluose, use of biochar, production of algal biomass in wastewaters, and the development of catalysts. Economic feasibility of algal biomass production systems seems attractive, relative to the other options. However, further optimization in all paths, and testing/demonstration at larger scales are required to fully understand the economic viabilities. The various coproducts provide a clear picture that multiple streams of value can be generated within an integrated biorefinery, and these include fuels and products.

Table of Contents

Introduction

This project conducted by the University of Georgia (UGA) involved research, development, and technology transfer of biorefinery technologies relating to the thermochemical and sugar platforms and contributions to the atomic layer epitaxy relating to fuel cell development. Additionally, the early part of the project addressed research capability development. The overall project goals were:

1. Develop pyrolysis-BioOil processing systems.
2. Laboratory development for fuels and chemicals.
3. Production, characterization and uses for pyrolysis-Char.
4. Develop Atomic layer epitaxy for fuel cell technology.
5. Develop fermentation-based conversion of biomass to fuels and products.
6. Develop biomass production technologies (e.g. algae).
7. Develop and test catalysts for biomass conversion to products.
8. Technology transfer and education.
9. Project Management and Reporting.

Georgia is a leading producer of biomass from forest, agriculture and other industries. Biorefining provides opportunities for economic development, particularly in rural areas. Outcomes from this project include new technology for production of fuels and products from biomass; developments in biomass production (algae) methods, pretreatments and related logistics; and technology and education of a workforce familiar with biorefining. A team of researchers from multiple disciplines were brought together at UGA and worked on various aspects of the biomass to biofuels pathways. This was accomplished by establishing a program titled Biorefining and Carbon Cycling Program with a vision as outlined in Figure 1.

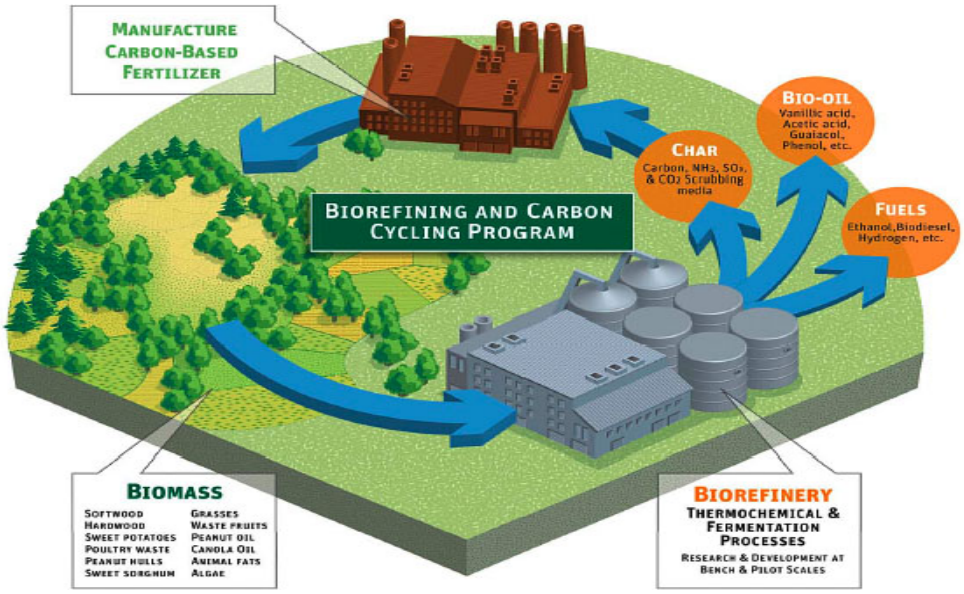

Figure 1. Schematic description of the Univeristy of Georgia Biorefining and Carbon Cycling Program R&D activities.

This multi-year project is divided into nine separate tasks that address a variety of areas including thermochemical conversion technology development, research capability development, co-product strategy, biomass resource development, fermentation technology development, catalyst testing, technology transfer and reporting. This report is structured by task and subtask and highlights the methods used and results obtained.

Task 1.0 Develop pyrolysis BioOil processing systems.

Our goal was to develop research infrastructure relating to pyrolysis, including bench scale batch and continuous pyrolyzers, and generate and characterize BioOils from various biomass. A related aspect of this work was to characterize biochar co-product generated from pyrolysis (reported separately in Task 3.0). This overall task was divided into subtasks, namely: 1.1 Develop batch and continuous pyrolyzers; 1.2 Upgrade pyrolyzer with biomass metering devices (vibratory feeder) and pyrolyze different biomass and characterize BioOil and biochars; 1.3 Characterize BioOil as a fuel through stability testing and engine performance testing; 1.4 Perform a pro forma analysis of most successful method developed and 1.5 Scale up pyrolyzer capacity.

Subtasks 1.1 and 1.2 – Development of pyrolysis systems and generate BioOils from different biomass

Methodology and results described and summarized below have independently been reported in the following peer-reviewed publications:

1. *Garcia-Perez, M., T.T. Adams, J.W. Goodrum, D.P. Geller and K.C. Das. 2007. Production and fuel properties of pine chip BioOil/biodiesel blends. Energy and Fuels 21, 2363-2372.*

Our efforts to develop capabilities to conduct pyrolysis research focused on establishing 4-kg batch reactors systems, and one semi-continuous reactor system. Char and BioOil were produced in two different slow pyrolysis units operating at atmospheric pressure. The batch system was a 230 mm long and 255 mm diameter batch reactor (Figure 1.1). The reactor could be heated to 600^{o}C and maintained at that temperature using a 30400 thermolyne furnace. The pyrolysis vapors were rapidly evacuated across the biomass bed using 2 L/min of nitrogen as carrier gas. Four ice-cooled traps connected in series were used to condense the vapors. Samples of the non-condensable gases were collected and analyzed by GC (Agilent 3000A). The charcoal solid residue was left behind in the reactor under nitrogen until the reactor cooled to room temperature to avoid any oxidation.

Pyrolysis in the semi-continuous system was conducted in an indirectly heated continuous flow reactor (Figure 1.2). Biomass pellets were fed via a rotary valve at a feed rate of 1.5 kg/h. The average amount of biomass used in each run was 6 kg. The reactor consisted in a 100 mm diameter stainless steel tube placed in a Lindberg/Blue M (model: HTF55322A 1200°C) furnace with an auger driven by a ¼ hp motor. A cooler was installed between the hopper and the furnace to prevent the heating of the biomass in the hopper. The auger speed was maintained at 2.2 rpm. A solid retention time of 8.26 min in the whole Auger and 5.91 min of which was in the heated zone is

obtained at this speed. The charcoal was collected in a stainless steel container located downstream the Auger.

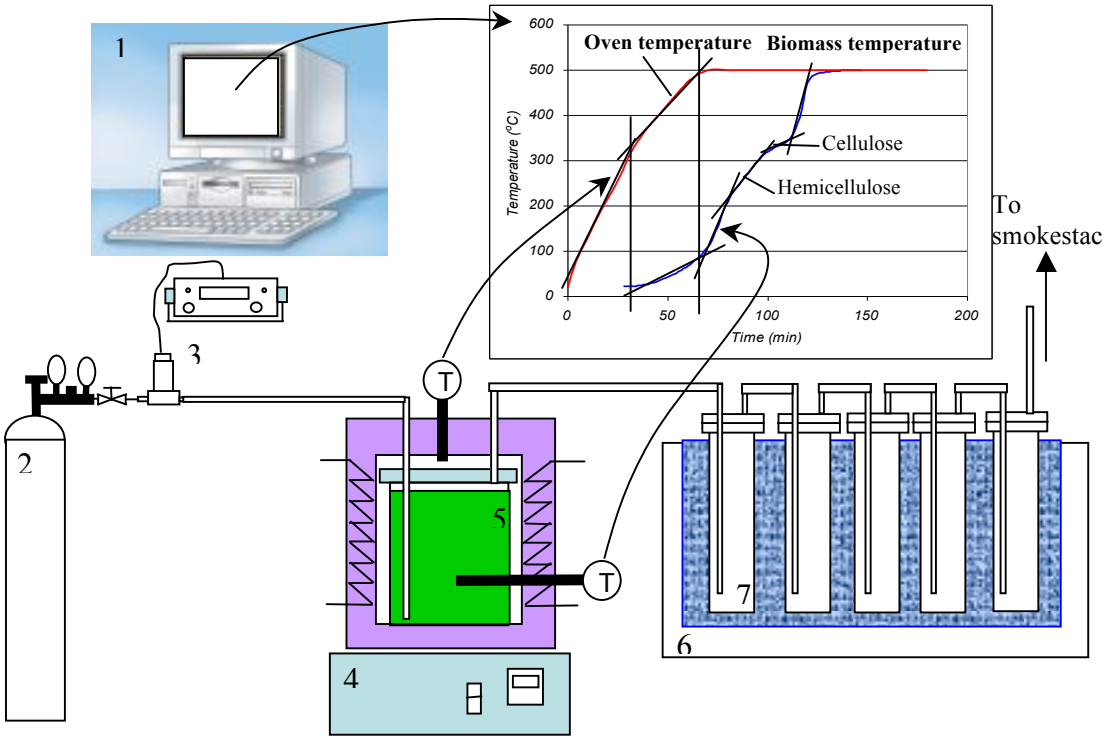

Figure 1.1. Batch Pyrolysis installations and typical oven and biomass temperature for pine chips (1) Computer connected to thermocouples, (2) Carrier gas cylinder, (3) Mass flow controller (4) Oven, (5) Pyrolysis reactor, (6) Chiller, (7) Condensing traps.

Upgrading of biomass feeding system

Subsequent to original installation where the biomass feed was either gravity feed or manually fed. We installed a vibratory metering feeder in the second version of the system. The unit installed was a Eriez Magnetics, precision vibratory feeder.

Installation of a fractional (sequential) condensing system

A vertical condenser followed by series of ice-cooled traps was used to condense the pyrolysis vapors (Figure 1.2). Contents from the BioOil traps (marked 10) were collected from individual receiving vessels, which were each at different temperatures as the cooling occurred. Initially, an effort was made to distinguish between fractions, however in order to determine total yield of BioOil, all contents were merged to form a single sample that was phase-separated.

The pressure inside the reactor was maintained a few millimeters of mercury under vacuum using a vacuum pump with a valve to control the pressure in the

pyrolysis reactors. 3 L min^{-1} of nitrogen was used as carrier gas to maintain an inert atmosphere inside the reactor.

Condensed liquids were separated into *aqueous* and *oily* phases (also known as decanted oil) in a separation funnel at 4 ^{o}C. The aqueous phase was subjected to an evaporation step at 60 ^{o}C under vacuum in a rotatory evaporator (Büchi, RE 111). The goal was to reduce the water content to values around 15 mass %. 5 mass % of methanol was added to all the resulting oils to improve their thermal stability.

Non-condensable gases were collected in sample bags and analyzed in a Agilent 3000 Gas Chromatograph. The Agilent 3000 Micro-Gas Chromatograph (GC) is formed of 4 independent channels (Molsive 5A Plot, 10 m x 32 mm; PLOT U, Aluminum PLOT and OV-1) designed for the analysis of specific gases. Each channel consists of an independent injector, a column, a flow control valve and a thermal conductivity detector. Argon and Helium are used as carrier gases. The columns are configured in such a way that each sample is completely analyzed in less than 10 minutes. The micro-GC was calibrated using Universal Gas Calibration Standard and costume made standards from National Specialty Gases.

Milestone 1.1: Successful implementation of reactor system completed.
Milestone 2.1: Successful implementation of feeder system completed.

Milestone 2.2: Successful implementation of fractional condenser completed and tested.

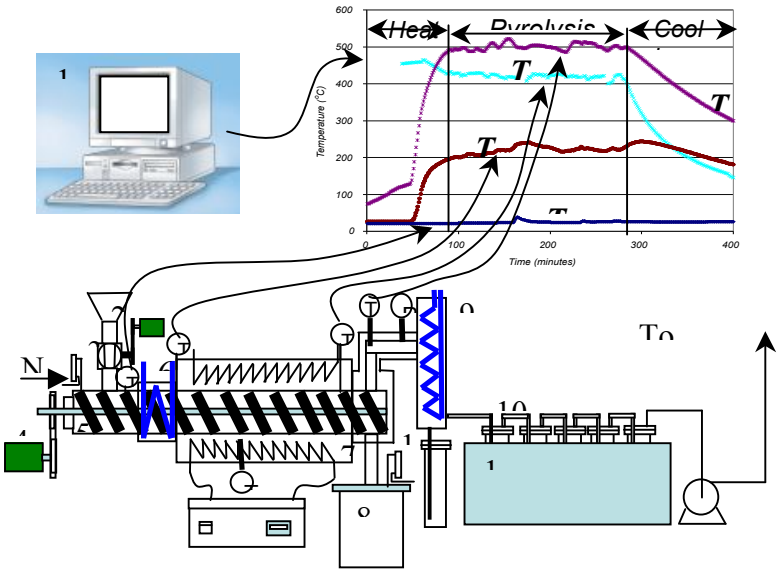

Figure 1.2. Continuous pyrolysis reactor used in the conversion of pine chip pellets. (1) Computer, (2) Feeding hopper, (3) Feeding valve, (4) Auger motor, (5) Auger Conveyer (6) Cooler, (7) Heater, (8) Char container, (9) Water cooler, (10) Bio-oil traps, (11) Ice chiller, (12) Vacuum pump.

Subtask 1.3 Characterize BioOil as a fuel through stability testing and engine performance testing

Water content of the bio-oils was determined by Karl Fisher titration (ASTM D-1744). Thermogravimetry analysis and GC/MS analyses were conducted for each of the obtained oils. Samples were diluted in 1:10 in methanol and analyzed using the HP 6890 GC oven with an HP 1973 MS detector in the scanning mode. Additional details are provided in the peer-reviewed publication.

A TG Mettler Toledo TGA/SDTA851e was used for the thermo-gravimetric tests using initial masses of 5 mg. An inert atmosphere and the removal of gases and condensable products were achieved using 50 cm^3 / min of nitrogen. The samples were heated from 25 to 600 ^oC at a heating rate of 10 ^oC / min.

The bio-oils were then fractionated using previously published schemes. Seven grams of bio-oil sample were first extracted using 200 mL of toluene. Waxy materials that remained in suspension in the toluene soluble fraction were separated using a Whatman N^o 42 filter (this type of filter was used in all filtrations). The toluene insoluble fraction was solubilized in 200 mL of MeOH and filtered in order to remove the char, non-polar waxy materials and other heavy compounds. The toluene was eliminated from filtrates in a rotary evaporator and the dry residue was weighed. The MeOH soluble compounds were added to 300 mL ice-cooled distilled water under strong agitation. The water insoluble fraction was removed by filtration. The solid residue was washed with distilled water during one hour. After this the solid residue was further extracted with dichloromethane until the filtrate was colorless. The solid remaining in the filter was dried at 105^oC over night. Part of the water present in the water soluble fraction was removed under vacuum at 60 ^oC. The water content remaining in that fraction was determined by Karl Fischer titration. As the result of this separation scheme, 6 fractions were obtained. The fractions were denominated as: 1) Toluene soluble fraction, 2) MeOH insoluble, 3) Water soluble, 4) Water-CH_2Cl_2 insoluble, 5) Water insoluble / CH_2Cl_2 soluble.

Biomass Characterization

The elemental analyses of pine chips and pine chip pellets studied are presented in Table 1.1. The results were very similar in both feedstocks and close to the ones reported for other woody biomasses. Table 1.2 presents the chemical proximate analysis for studied feedstocks. Both samples have very little content of fats (less than 1 mass %), protein (around 1 mass %) and ash (0.48 and 1.11 mass %) but are very rich in cellulose (more than 45 mass %), hemicellulose (around 10 mass %) and lignin (around 25 mass %). These results were expected for woody biomasses. The Pine chips have slightly larger content of cellulose and lignin.

Evaluation of products from the pyrolysis of pine chips and pine pellets

Mass balances for the pine chips and pine chip pellets pyrolysis tests carried out in the batch and in the continuous Auger reactors are presented in Table 1.3. The yields obtained for the charcoal was quite similar for both reactors (30 and 31 mass %) but was slightly larger to the one obtained by thermogravimetry (24 mass %). This result suggests that the reactions leading to the formation of additional char like the

secondary intra and extra-particle reactions are very similar for both systems and contributed to at least an increase in 5 mass % in the yield of char. These reactions could be mitigated reducing particle sizes and the residence time of pyrolysis vapors in contact with the partially converted biomass.

Table 1.1. Elemental of pine chips and pine chip pellets (mass %)

Feedstock	C	H	N	S	O*	Ash
	mass % organic basis					
Pine chips	49.5	6.05	0.06	0.02	43.79	0.49
Pine chip pellets	48.0	5.93	0.05	0.05	44.76	1.2

* by difference

Table 1.2. Proximate analysis of the two fractions (mass %)

Feedstock	Moisture	Cellulose	Hemi-cellulose	Lignin	Ash	Others (sugars, starch, pectins)
Pine chips	3.0	52.9	9.6	26.0	0.48	6.3
Pine chip pellets	7.7	45.0	11.4	23.2	1.11	10.1

Table 1.3. Yield of Products (mass %)

Products	Pine Chips (Batch reactor)	Pine Chip Pellets (Continuous reactors)
Char	31.2	30
Total Liquid	50.4	57.9
Water	26.2	30.9
Organics	24.2	26.9
TOP LAYER (AQUEOUS PHASE)	34.8	38.2
(%) Water	(69.98 %) 24.4	(74.06 %) 28.3
Organics	10.4	10.0
BOTTOM (OILY PHASE)	15.6	19.6
(%) Water	(11.81 %) 1.8	(13.50 %) 2.7
Organics	13.8	16.9
Gases (By difference)	18.4	12.1

The whole liquid condensed was separated into two phases (aqueous phase and oily phase). The phases were separated after cooling the oil to 4 ^{o}C. The aqueous phase represented 69 and 66 % the whole condensed liquid. This phase contained over 69 mass % of water. The oily phase that represented between 31 and 34 mass of the whole condensed liquid contained only 11.8 and 13.5 mass of water. This phase was very rich in organic compounds and is called in this paper oily phase.

Bio-oil characterization

On Figure 1.3 (left side) are presented the DTG curves corresponding to studied bio-oils. On heating a complex mixture under conditions of free gas exchange often realized in TG experiments, the lighter fractions will leave the sample first, and the heavier ones second, at progressively higher temperatures proportional to their molecular weight and boiling points. In the case of the pan has no covering lid, diffusion of gases from and to the sample is greatly accelerated due to good convection, the temperature gradients within the sample are minimal, and this enables the fractions of different volatility to leave the mixture consecutively at temperatures close to (but lower than) their saturation ones. Temperature intervals of bio-oil evaporation can be a very important tool to characterize bio-oils. TG vaporization and cracking curves with their characteristic profiles reflect the chemical composition of the sample.

The DTG curves were resolved in 5 major macro-families as follows using a method similar to the one described elsewhere[3] but in this case for the whole oils. The families identified were: *A:* Volatile compounds and water *B:* Mono-phenols and furans, *C:* Sugars, extractives derived compounds and dimmers, *D* and *E* oligomers.

The first group of compounds (family A) is mainly formed by organic compounds and water with boiling point under 200 ^{o}C. The main compound of this family is water. This family is formed of low molecular weight acids, aldehydes, alcohols (Molecular weight lower than 110 g/mol). These compounds are in general pointed as responsible for many of the poor fuel properties of bio-oils (low thermal stability, corrosion, low calorific value, high flash point) representing between 11 and 28 mass % of the volatiles generated by the studied oils.

Monolignols and furans are the main compounds forming the second group (family B). This family is associated to species that evaporate between 100 and 300 ^{o}C. The peak observed in the oils derived from the water soluble fractions are in general shifted to higher temperatures (perhaps a consequence of phenols and furans with higher polarity). This is the main fraction of studied oils contributing to between 31.8 and 51.0 mass % of the volatile compounds in the studied oils. The compounds commonly identified in this fraction (see Figure 1.4 and Table 1.4) are mainly alkylated and methoxylated phenols and benzenediols. Important amounts of furans must also form this family but unfortunately they are not commonly identified by GC/MS.[3] The compounds in this family have a boiling point similar to gasoline.

Family C is mainly formed of sugars, extractive derived compounds and dimmers. The peak assigned to this family are between 200 and 300 ^{o}C. These peaks include the evaporation of some mono-sugars and the cracking of poly-sugars. Only levoglucosane (M_w= 162 g/mol) is commonly detected by GC/MS chromatograms.

The oils derived from the aqueous phase are expected to be rich in sugars while the bottom oils will be richer in extractives derived compodi-phenols. The extractive derived compounds are also liked to appear in this family. Those species are mainly fatty and resin acids, paraffines and phenanthrenes (see Figure 1.4 and Table 1.4). Products of reaction between monomers (dimmers) are likely to be the main compounds forming he family in the bottom phases.

Families D and E cannot be identified by GC/MS due to their extremely high molar mass. The heavy compounds of lower molecular weight can be water soluble or water insoluble but CH_2Cl_2 soluble. These compounds will have molecular weights between 500 and 1000 g/mol. The heavier oligomers (molecular mass larger than 1000 g/mol) will not be insoluble in water and CH_2Cl_2.

The studied bio-oils were also analyzed using a conventional separation scheme described elsewhere.[3] Table 1.5 presents the composition of pine chip and pine chip pellet derived oils. The *water content* of the oils from pine chips was lower than the one for pine chip pellets. The water content of the aqueous phases depends of the intensity of the process used to remove the water. The *Methanol-insoluble fractions* are mainly formed by char and waxy materials in fresh oils. The content of this fraction in the produced oil was lower than 1 mass %. Low values of toluene soluble factions were observed in the aqueous phase (6.6 and 2.2 mass %) while the Oily phases were very rich in this fraction (58.5 and 45.3 mass %). The compounds soluble in toluene are mainly formed by mono-phenols, extractive derived compounds and low molecular weight non-polar oligomeric compounds. The *water soluble fraction* is the main fraction found in the bio-oils derived from the aqueous phase (52.3 and 41.7 mass %). This fraction is usually composed of sugars, furans, phenols and polar oligomers. The content of volatile compounds lost during the removal of solvents ranges from around 7.56 mass for the oily phase in the pine chips to more than 36.8 mass % for the aqueous phase. The content of volatile compounds as determined by this method in general can be used as an estimate compounds with boiling point lower than 150^{o}C as such must also contain important amount of low molecular weigh furans and phenols.

Viscosity and calorific value of studied oils are presented in Table 1.6. The oils obtained from the decanted oil have higher calorific value than the ones obtained from the aqueous phase.

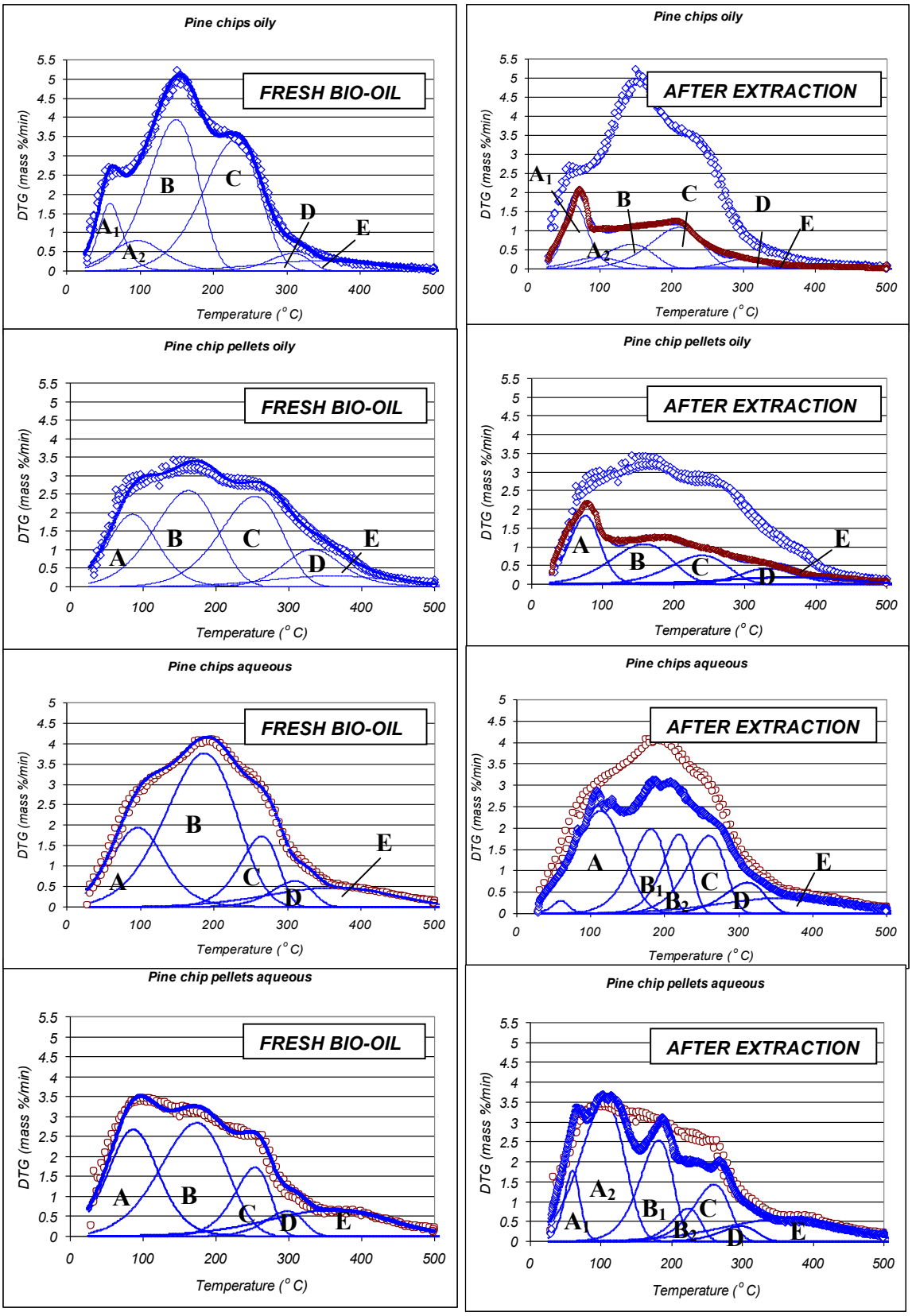

Figure 1.3. DTG curves of Bio-oils before and after extraction.

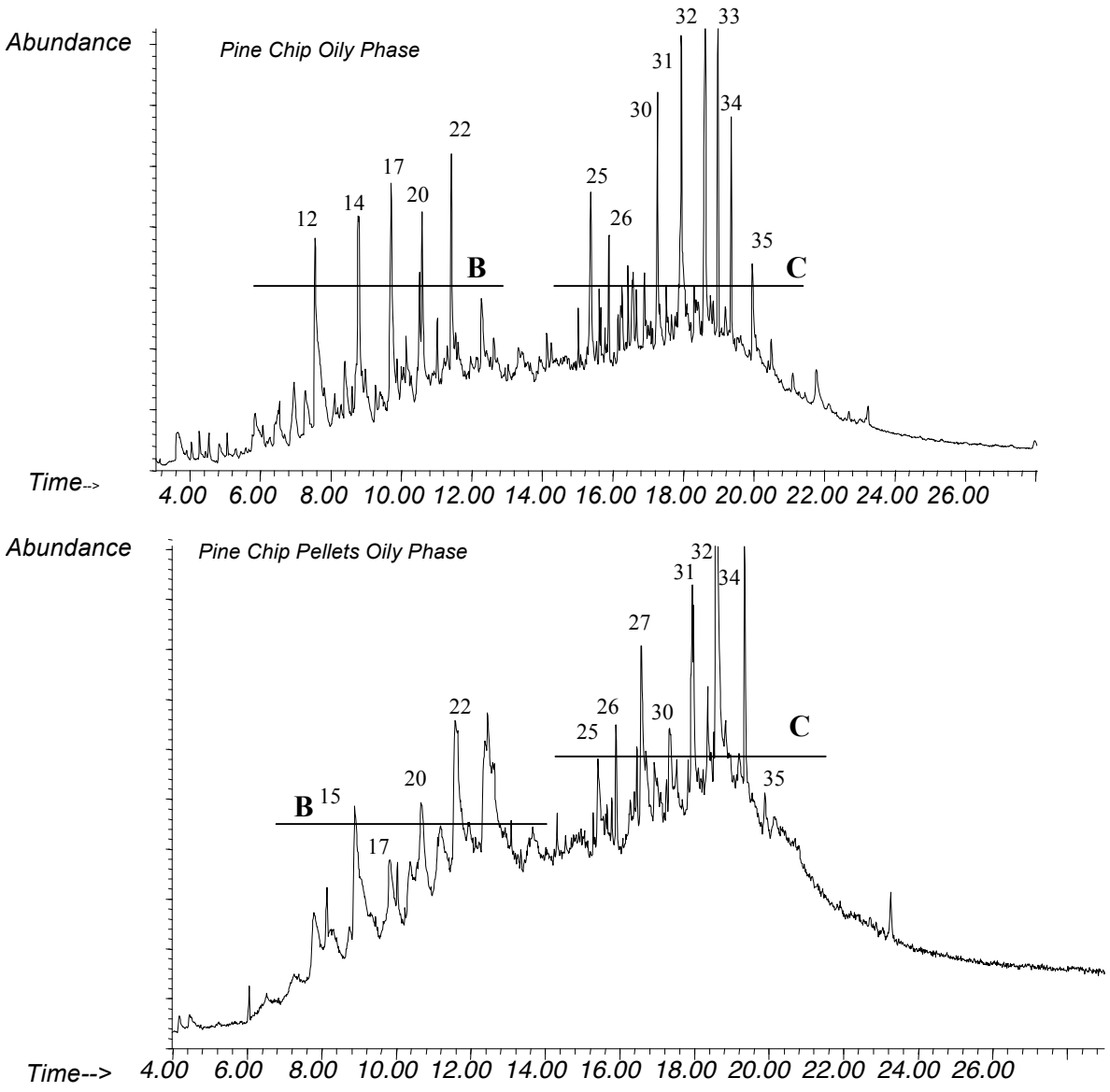

Figure 1.4. GC/MS analysis of oily phases

Table 1.4. GC/MS tests of oily phases

Number	Residence Time	Compound name	Pine chip	Pine chip pellets
1	3,648	2,5 methyl, furan	X	
2	4,037	p-xylene	X	
3	4,272	tetrahydro-2,5 dimethoxy, furan,	X	
5	4,819	1-one, 2-methyl-2-cyclopentent-	X	
6	5,053	alpha.-pinene	X	
7	5,847	5-methyl-2-furancarboxaldehyde,	X	
8	6,068	5-methyl-2-furancarboxaldehyde,	X	
9	6,528	Phenol	X	
10	6,942	3-methyl-1,2-cyclopentanedione	X	
11	7,28	2-methyl-phenol	X	
12	7,567	2-methoxy-phenol,	X	X
13	8,389	2,4-dimethyl-phenol,	X	
14	8,597	2-methoxy-4-methyl-phenol,	X	
15	8,793	2-methoxy-4-methyl-phenol,	X	X
16	9,263	2,6-dimethoxy-toluene	X	
17	9,694	4-ethyl-2-methoxy-phenol,	X	X
18	10,126	1-(2-hydroxy-5-methylphenyl)-ethanone,	X	
19	10,506	Eugenol	X	
20	10,584	2-methoxy-4-propenyl-phenol,	X	X
21	11,016	Eugenol	X	X
22	11,409	2-methoxy-4-(1-propenyl)-phenol,	X	X
23	12,263	1-(4-hydroxy-3-methoxyphenyl)-2-Propanone,	X	
24	15,013	methyl ester hexadecanoic acid	X	
25	15,369	Hexadanoic acid	X	X
26	15,87	2,2-dimethyl-3-bromo-1-oxa-2-sila-1,2-dihydro – naphthalene	X	X
27	16,562	9-Hexadecenoic acid	X	X
28	16,662	3,5-dihydroxy-4,4-dimethyl-2-(1-oxopentyl)-2,5-cyclohexadien-1-one	X	
29	16,887	2,3,5-trimethyl-phenanthrene,	X	
30	17,256	1-methyl-7-(1-methylethyl)-phenanthrene,	X	X
31	17,945	1, 2, 3, 4, 4a, 9,10,10a, -octahydro-1,4a-dimethyl -7-(1-methylethyl) , methyl ester 1-	X	X

		phenanthrenecarboxlic acid,		
32	18,619	, 1, 2, 3, 4, 4a, 9, 10, 10a,-octahydro- 1,4a-dimethyl -7-(1-methylethyl)-1-Phenanthrenecarboxlic acid	X	X
33	18,964	Phthalic aid, di-isooctyl ester	X	
34	19,353	1,5-diphenyl-2H-1,2,4-triazoline-3-thione	X	X
35	19,945	4H-1-Benzopyran-4-one, 5-hydroxy-7-methoxy-2-(4-methoxyphenyl)-	X	
36	20,489	1H-Naphtho(2,1-b)pyran-1-one, 3-acetyl-7,8-dimethoxy-2-methyl	X	
37	21,749	2(3H)-Furanone, dihydro-3,4-bis(4-hydroxy-3-methoxyphenyl)methyl)-, (3R-trans)-	X	
38	23,236	Ergosta-4, 6, 22-trien-3.beta.-ol	X	

Table 1.5. Content of different fractions of produced Bio-oils (mass %)

	Pine chips		Pine chip pellets	
	Aqueous	Oily	Aqueous	Oily
Water	8.3	11.1	14.5	16.8
Toluene soluble	6.6	58.5	2.2	45.3
Methanol insoluble (char)	0.5	0.24	0.4	0.44
Water soluble	52.3	18.5	41.7	11.7
Water insoluble	2.4	4.1	2.9	1.3
CH_2Cl_2 sol.	2.1	2.1	0.3	1.1
CH_2Cl_2 insol.	1.6	0.1	1.2	0.2
Others (volatile)	29.9	7.56	36.8	24.5

Table 1.6. Fuel properties of obtained oils**.**

Properties	Pine chips		Pine chip pellets		Bio-diesel
	Bottom / Oily phase	Aqueous phase	Bottom / Oily Phase	Aqueous phase	
Dynamic viscosity @ 25^{o}C, 3rpm (cP)	140.2	125.6	76.8	44.8	6.4
Calorific Value	23.84	17.91	24.75	19.46	39.02

(MJ/kg)					
pH	2.4267	2.5667	2.5633	2.6733	4.1500
Density (kg/dm^3)	1.0880	1.1830	1.1337	1.2362	0.8572

Enhancing the use of BioOil as a fuel by blending with Biodiesel

In addition to fractionated BioOil and whole BioOil properties we measured earlier, we wanted to develop a fuel additive that would be usable in diesel engines directly. This was achieved by the preparation of mixtures o BioOil and Biodiesel (which served as an emulsifier). Several blends were prepared using biodiesel/bio-oil ratios of 1, 1.5, 4 and 9. The relationship between the ratio used in the preparation and the Biodiesel rich / Bio-oil rich phases equilibrium ratio obtained after separating the blend at 25 ^{o}C is presented in Figure 1.5. The slop of the resulting straight lines can be used as a good indicator of the solubility of studied bio-oils in biodiesel.

The decanted oils were considerably more soluble in the biodiesel than the oils obtained from the aqueous phase. The oils from pine chip obtained in the batch reactor were more soluble than the oils obtained from the pine chip pellets in the continuous reactor. The slop of resulting experimental lines (Figure 1.5) can be used to calculate the concentration of bio-oil compounds in the biodiesel rich phase knowing the initial biodiesel / bio-oil ratio.

The concentrations of bio-oils in the bio-diesel rich phases for each of the studied blends can be observed in Figure 6. Biodiesel rich phases with loads of up to 34 mass % of biooils were obtained when blending equal amounts of pine chip bottom layer bio-oils with biodiesel.

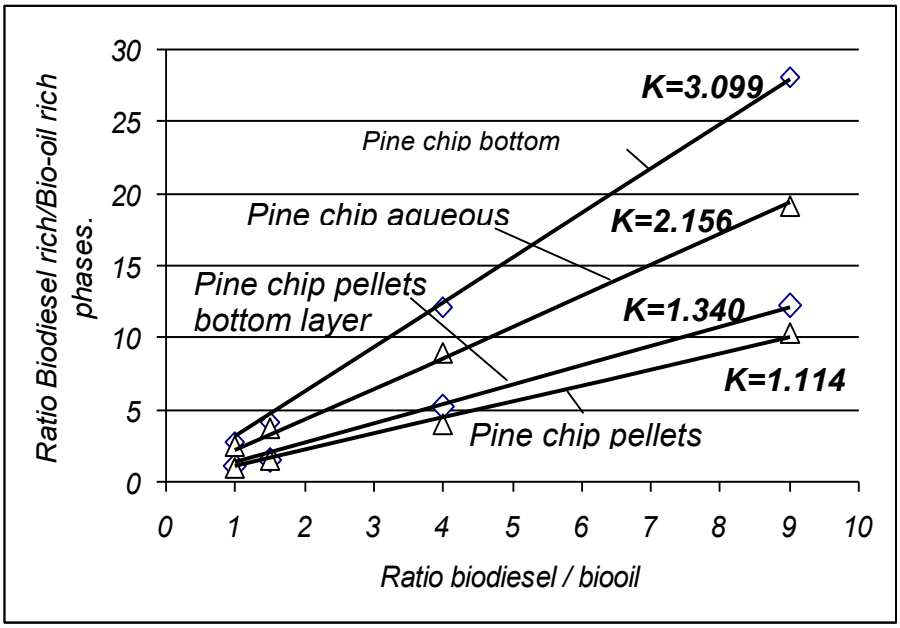

Figure 1.5. Yields of Bio-diesel and Bio-oil rich phases

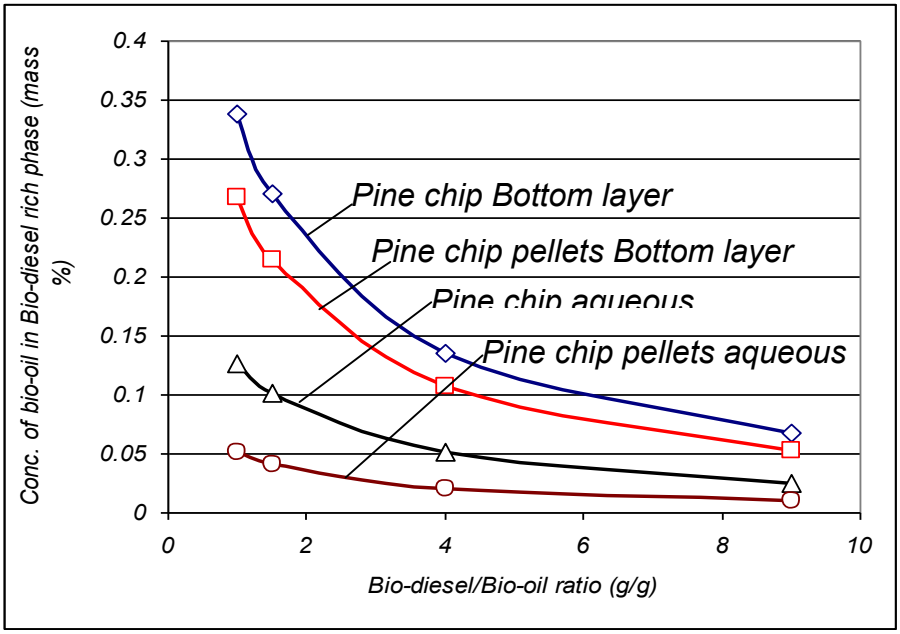

Figure 1.6. Bio-oil concentrations in the Bio-diesel rich phase.

Analysis of Bio-oil and Biodiesel Rich Phases

The right side of Figure 1.3 shows the DTG curve of bio-oil rich phases multiplied by the yield corresponding to the bio-oil rich phases. Fractions B and C from the bottom layers were the most soluble fractions in biodiesel. The mono-phenols and furans as well as dimmers are likely to be the main compounds in these fractions. These compounds have boiling point in the range of gasoline and Diesel being the most promising fractions for fuel applications.

The low molar mass compounds and the water (family A) were poorly soluble in bio-Diesel. This is a good result since this fraction is responsible for many of the undesirable fuel properties observed in bio-oils.

Small amount of oligomers (family D and E) were also soluble in bio-Diesel. Special attention must be paid to these compounds since they may increase the tendency of biodiesel to form carbonaceous residues in the injectors.

The change in the density of biodiesel rich phase upon the addition of bio-oils is presented in Figure 1.7. The results obtained suggest an increase in 0.00235 g/ml per mass % of bio-oil added. Figure 8 shows the change in the viscosity of biodiesel rich phases at different concentrations of bio-oils. The addition of pine chip decanted oils seems to cause a larger increase in viscosity than the pine chip pellets derived oils.

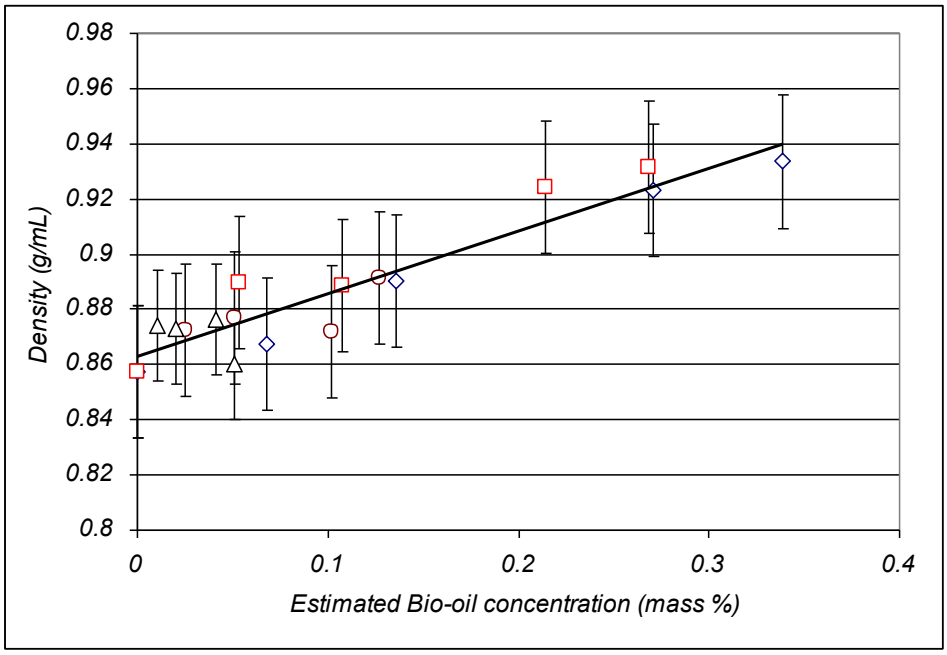

Figure 1.7. Density of Bio-diesel bio-oil blends (25◇C) Pine chip c◯y, Aqueous□, Pine chi△pellet Oily , Aqueous.

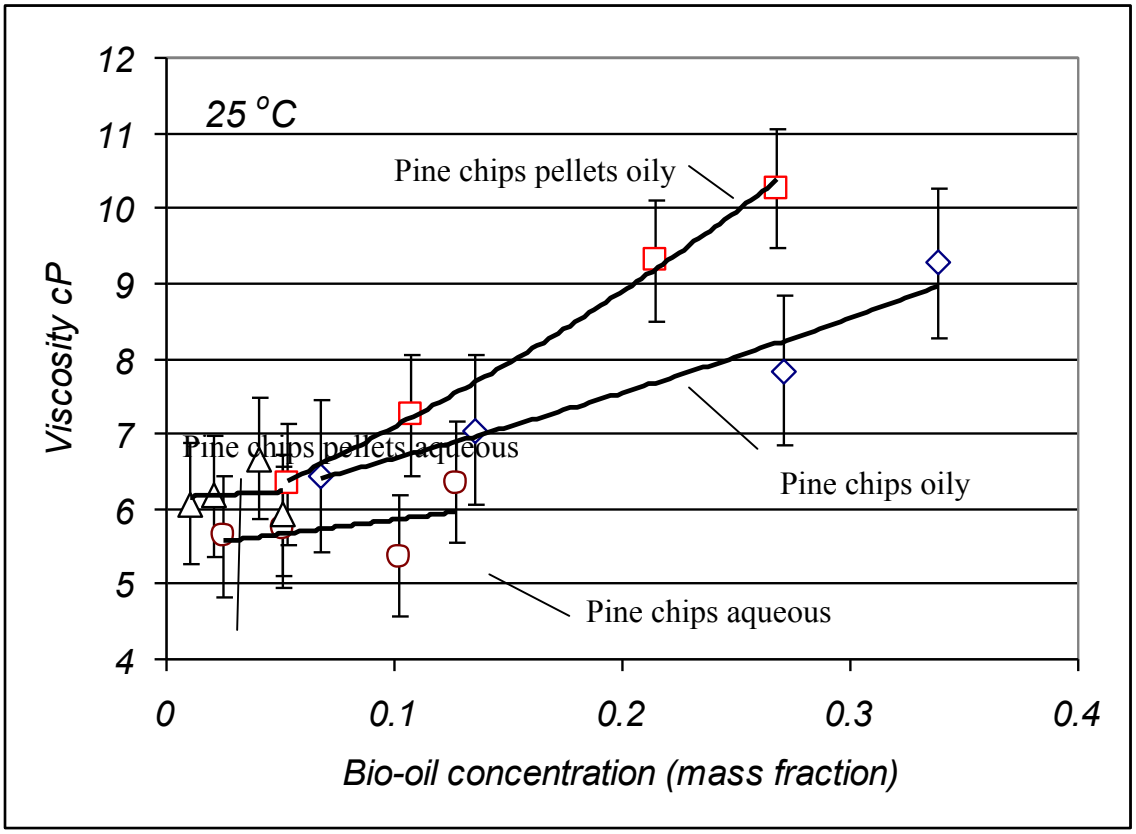

Figure 1.8. Viscosity of Bio-diesel bio-oil blends (25 °C).

Addition of bio-oils to the bio-diesel does not seem to affect the calorific value of the resulting blend (Table 1.7). The water content in the bio-oil-biodiesel blends increases upon the addition of bio-oil derived compounds reaching 1.65 mass % of water in blends prepared with 50 mass % of bio-oil (Table 1.8). Table 1.9 shows a reduction in the pH of the blends is observed when the bio-oil is added to the biodiesel. This reduction in pH could be attributed to the solubilization of some acids in the biodiesel. The impact of this reduction of pH in the corrosiveness of the biodiesel rich phase needs to be studied in the future.

Table 1.7. Calorific value of bio-diesel rich phase (MJ/kg) (bio-diesel = 39.02 MJ/kg)

Bio-oil/Bio-diesel mixtures (mass % Bio-diesel)	*Pine chips*		*Pine chip pellets*	
	Bottom / Oily phase	Aqueous phase	Bottom / Oily phase	Aqueous phase
10	38.50	37.00	35.52	36.16
20	37.52	35.81	35.44	38.02
40	35.99	35.63	36.68	38.47
50	38.99	36.09	35.58	37.61

Table 1.8. Water content (mass %) of Bio-diesel rich phase (Biodiesel = 0.1730 mass % water)

BioOil-Biodiesel mix, mass % Bio-diesel	*Pine chips*		*Pine chip pellets*	
	Bottom / Oily phase	Aqueous phase	Bottom / Oily phase	Aqueous phase
10	0.29	0.17	0.36	0.22
20	0.47	0.21	0.36	0.14
40	0.95	0.25	0.60	0.16
50	1.65	0.38	0.83	0.78

Table 1.9. pH of Bio-diesel rich phase (pH biodiesel = 4.15)

BioOil-Biodiesel mix, mass % Bio-diesel)	*Pine chips*		*Pine chip pellets*	
	Bottom / Oily phase	Aqueous phase	Bottom / Oily phase	Aqueous phase
10	2.66	2.47	2.77	2.74

20	2.68	2.64	3.28	3.29
40	1.88	2.62	3.22	3.06
50	2.67	2.54	3.20	2.70

Fuels stability is a major issue for engine and fuel system manufacturers. Stability is abroad term that really refers to two issues for fuels: long-tem storage stability or aging (oxidation stability) and stability at elevated temperature and/or pressures as the fuel is recalculated through an engine's fuel system (thermal stability).

In biodiesel, fuel ageing and oxidation can lead to high viscosity and the formation of gums and sediments that clog filters. Biodiesel with high oxidation stability, usually rich in saturated compounds, will take longer to each an out of specification condition, while bio-Diesel with low stability will take less time in storage to reach an out of specification condition.

The thermal stability of biodiesel rich phase was determined using by DSC method using a dynamic method under oxygen. Figure 1.9 shows some of the results obtained for some pine chip bottom layer – biodiesel blends. The increase in the onset temperature with the bio-oil concentration is clear. Figure 1.10 shows how the onset temperature changes as a function of bio-oil concentration for all the prepared blends. The obtained results seem to suggest that the bio-oils could act as biodiesel anti-oxidants.

The auto-oxidation of many liquid and solid hydrocarbons systems such as fuels, lubricants and polymers can be represented by a series of free-radical reactions involving O_2.[14] Hindered phenol antioxidants, used in polymers, lubricants and fuels, are probably the most important class of commercial anti-oxidants. Hindered phenols act by interrupting the reaction of propagation. In the absence of antioxidant, a peroxyl radical (ROO.) will abstract a proton from polymer (RH) by reaction. This is the rate-limiting step of the autooxidation. However, when a hindered phenol is added, it provides a more easily removable proton than those of the hydrocarbon, thus providing a more favorable reaction. The phenoxyl radical formed is sterically hindered and this makes it relatively stable so that it does not contribute to further polymerization.[15]

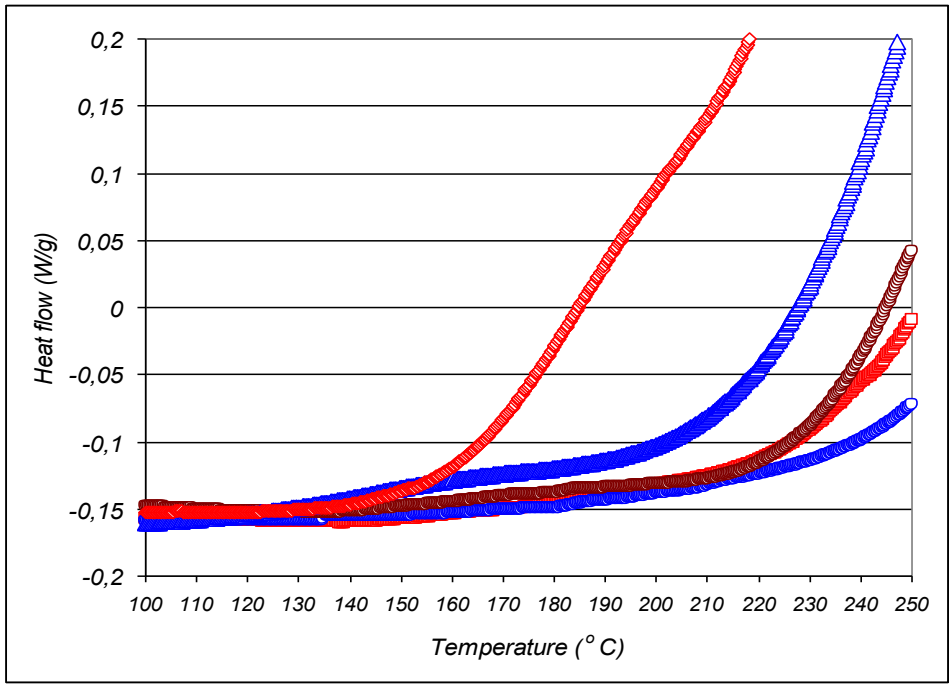

Figure 1.9. Heat evolution during the oxidation tests

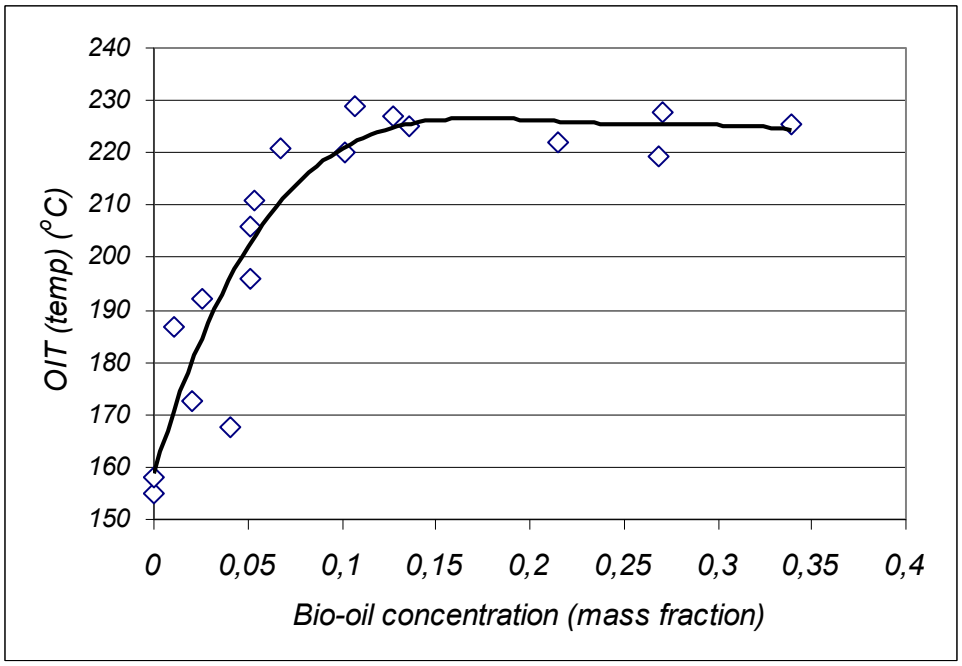

Figure 1.10. OIT versus concentration of bio-oils in bio-diesel rich phase

Bio-oils are very rich in phenols especially as part of family B and C. The results presented in this paper can only be considered as preliminary indications of the potential antioxidant character of some bio-oil compounds soluble in biodiesel. Further studies using other anti-oxidation standards tests like ASTM D4625, D6468, D2274, D5483, D3241 EN 14112 (the Rancimat), modified IP 306 are needed to confirm the anti-oxidant character of these fractions.

Milestone 1: BioOil testing and characterization from two biomass sources were completed in the laboratory.

Go/No Go: We conclude with the improved miscibility with BioOil – Biodiesel blending that an improved fuel was produced. This was a "go" result and we proceeded with producing larger quantities and further testing.

Production of larger quantities of BioOil-Biodiesel blends in the continuous reactor and engine testing

Several experiments were conducted using blending studies and rapid cooling with biodiesel mixtures. A photograph of the setup is shown in Figure 1.11. As expected, it was found that capture rates of BioOil components increased with increase in the ratio of Biodiesel to BioOil (Figure 1.12). Higher spray rates capture more of the vapor. A linear relationship was observed with a reasonably good fit.

Figure 1.11. Setup of mixing column for biodiesel and biooil.

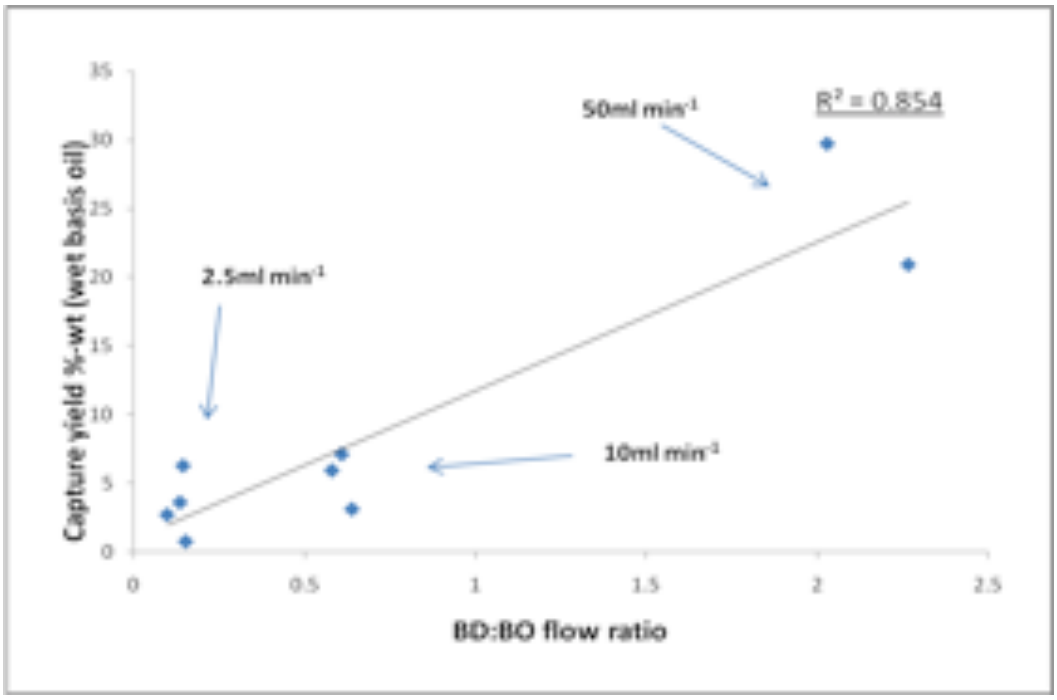

Figure 1.12. Relationship between capture rate of BioOil and amount of biodiesel used.

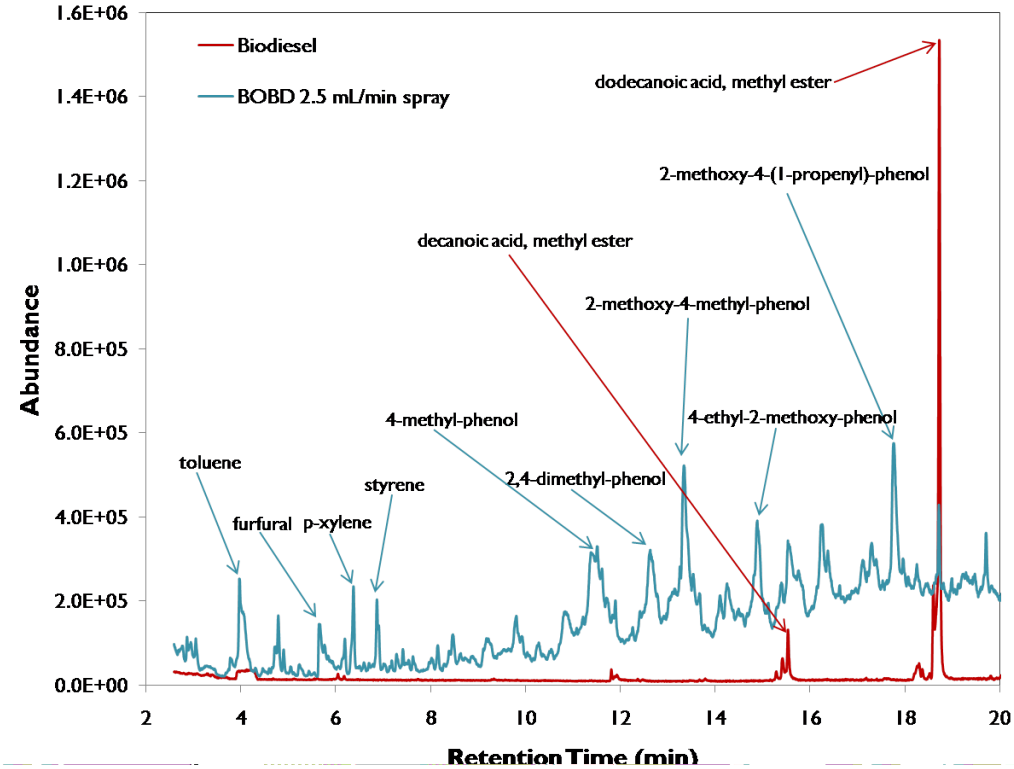

Figure 1.13. Gas chromatograph of the composition of resultant green diesel.

The chemical species present in the resultant compound and the biodiesel used is presented in Figure 1.13. The produced BioOil Biodiesel blends were shipped to an external laboratory for engine testing. The engine testing setup used and results are shown in Figure 1.14 and Table 1.10) and results look promising.

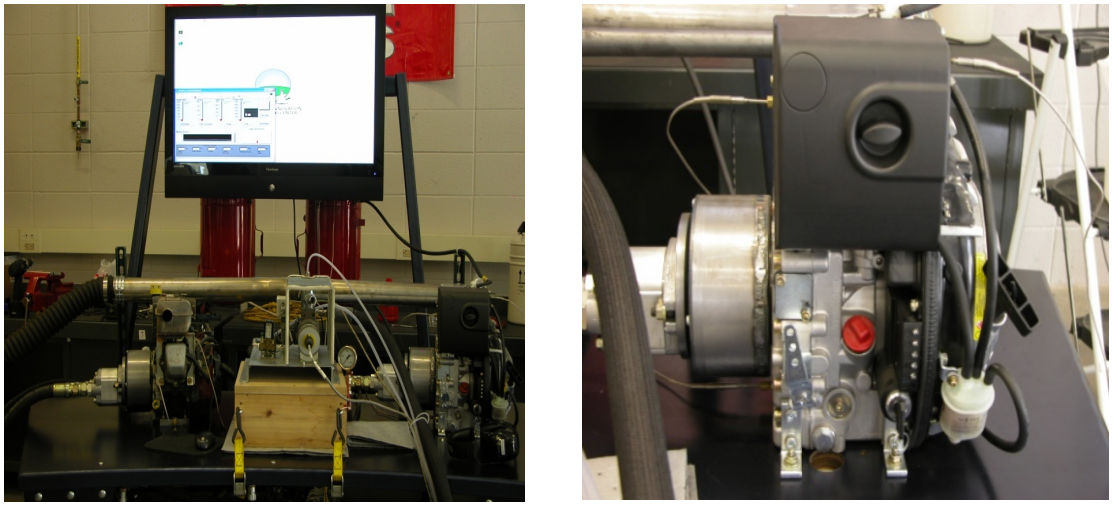

Figure 1.14. Engine test setup used to test BioOil- Biodiesel blends.

Table 1.10. Test results of engine testing of BioOil- Biodiesel blends in a diesel engine.

Fuel	Fuel Consumption	
	lbs/hr	liters/hr
Diesel	1.92	1.06
B10	2.31	1.26
B50	1.86	0.99
B100	1.43	0.75

Fuel	HORSEPOWER		
	10% load	40% load	80% load
Diesel	0.95	1.56	2.27
B10	0.94	1.54	2.05
B50	0.94	1.51	1.70
B100	0.93	1.40	1.44

Milestone 2: Identification of a BioOil-based fuel and its testing in a diesel engine completed.

Subtask 1.4 Pro forma analysis of most BioOil-based fuel development

Because biodiesel is an easily available fuel that would be used in the development of the above developed fuel, we focused the pro forma analysis on the BioOil production part alone. The pro forma analysis was completed with available information. Information on scaling up was obtained from Farag et al (2002) and calculating for a 440-t/d plant (equivalent to 245 dry ton/d at 45% assumed moisture content for biomass), the estimated capital investment was found to be $14.3 million. Annual costs of O&M and repayment of capital was calculated to be $10.92 million. The resulting cost of BioOil production (assuming 45% BioOil yield and 300 d of operation) would be $1.52/gal.

In our experimental work, we found that on average the amount of BioOil transferred to the BioOil/biodiesel mixture ranged between 5.4 to 7.5%. Using an intermediate value of 6.5%, the diesel supplement generated would cost $23.4/gal. This supplement can be added to petroleum diesel as B20. These results suggest a very high cost relative to present price of diesel. Two avenues are suggested for the future. From a technology perspective, we will have to raise the percentage of BioOil transferred to the diesel supplement from its current value of 6.5% to a higher value in the range of 75 to 100%.

Alternatively, the approach of extracting co-products of higher value to supplement the cost can be pursued. Although that was not the goal of the present research, our pro forma analysis evaluated the opportunity for chemicals of higher value and results are summarized in Table 1.11. These results appear much more attractive, however it must be noted that they are theoretical at present and their technical feasibility have to be further evaluated.

Table 1.11. Summary of facility costs and revenues.

SUMMARY TABLE OF CASH FLOWS		440 tpd Facility	220 tpd Facility
		$/yr	$/yr
Total cost of the Biomass Pyrolysis Operation[1, 2]		12,086,414	6,732,863
Cost of processing BioOil to chemicals for Product 3[3]		5,174,934	2,587,467
TOTAL of cash OUTFLOW		**17,261,348**	**9,320,330**
Product revenues:			
Product 1	Char use as soil fertilizer	3,633,630	1,816,815
Product 2	Carbon sequestration credit	188,869	94,434
Product 3	BioOil conversion to chemicals	10,349,867	5,174,934

Product 4	Residual BioOil for energy ($147.97/ton)	4,133,280	2,066,640
Product 5	Gas for energy ($98.65/ton)	2,363,457	1,181,728
TOTAL of cash INFLOW through product revenue		**20,669,103**	**10,334,552**
Net profit		3,407,755	1,014,222
Total capital investment		14,300,000	8,800,000
Annual return after expensing cost of capital, %		23.8	11.5

[1] Total costs obtained from Farag et al. (2002) - includes capital repayment over 10 yr at 8% interest; [2] Annual operation is considered to be 330 days, 24 hr/day; [3] Cost of processing is assumed to be 50% of the final recoverable value of products.

Subtask 1.5 Scale up pyrolyzer capacity

Modification of plans: Our original proposed plan was to build a larger scale pyrolysis system to produce larger quantities of BioOil to develop fuels that could be more extensively tested. Because of time constrains, and the fact that our pro forma analysis indicated excessive costs in a BioOil only production facility, we did not pursue this task of building a pilot facility.

Task 2.0 Laboratory Developments of Fuels and Chemicals

Two extraction pretreatment steps were investigated to evaluate the economic potential to produce products from biomass. The goal was focused on developing further the biorefinery, so that value added products could overall reduce the cost of production of fuels. The specific pathways explored were: [1] hot water extraction of biomass to produce sugars that could subsequently be converted to ethanol-fuel, and [2] production of levoglucosan (LG) from pyrolysis of biomass.

Subtask 2.1 Develop a pre-treatment extraction system: Part A – Hot-water extraction

Methodology and results described and summarized below have independently been reported in the following peer-reviewed publications:

1. *Brandon, S.K., M.A. Eiteman, K. Patel, M.M. Richboug, D.J. Miller, W.F. Anderson, and J. Doran Peterson. 2008. Hydrolysis of Tifton 85 bermudagrass in a pressurized batch hot water reactor. Journal of Chemical Technology and Biotechnology, 83(4):505-512*

A pressurized batch hot water (PBHW) reactor was built based on the schematic shown in Figure 2.1. PBHW hydrolysis was conducted in a 2-liter pressure vessel (Model 4600 Parr Instrument Co., Moline, IL) surrounded by retractable ceramic heaters. Native grass (or other biomass as needed) was placed in a 500μm (35 mesh) or a 100μm stainless steel basket (depending on biomass particle size) and then immersed in 1000 to 1500 mL of deionized water in the vessel, depending on the

mass of the solids being treated and the final solids concentration desired. Prior to reaction cycles, the head plate was secured and the headspace purged with nitrogen via two ports. The vessel was then filled with nitrogen at room temperature to achieve a target pressure at the set point temperature. Heating, release of vessel contents and collection of time, temperature and pressure data were measured via a datalogger and associated software (Model 21X micrologger, Campbell Scientific, Inc., Logan UT).

A reaction cycle begins by heating the vessel to a set point temperature. The *reaction time* is the time set to elapse from the moment the contents of the reactor first reached the set point temperature to the moment the outlet valve automatically opened. The *reaction temperature* and *reaction pressure* are calculated as the mean of each variable recorded at 15 second intervals during the reaction time. After the reaction time elapsed at this set point temperature, an 80 psi pneumatically actuated ball valve releases the liquid hydrolysate from the pressure vessel to a partially evacuated condenser cooled by tap water. The hot liquid is cooled to less than 50°C and the system depressurized to less than 40 psi in roughly ten seconds. The hydrolyzed solids (wet but no longer pressurized) remain in the basket to cool. As a safety precaution, a low pressure switch at the water inlet required a minimum pressure of 10 psi to actuate the pneumatic valve and to allow the ball valve to release the hydrolysate into the condenser. A manual ball valve to release the condensate and a 50 psi pressure relief valve are located at the outlet of the condenser. The hydrolyzed solids are then removed from the vessel and dried in a conventional oven at 175°F for 1.5 hours. Liquid and dried samples are stored (at -20°C and 4°C, respectively) for subsequent enzyme and fermentation studies. This reactor system was extensively characterized and detailed results are reported in the publication cited above (Brandon et al., 2008).

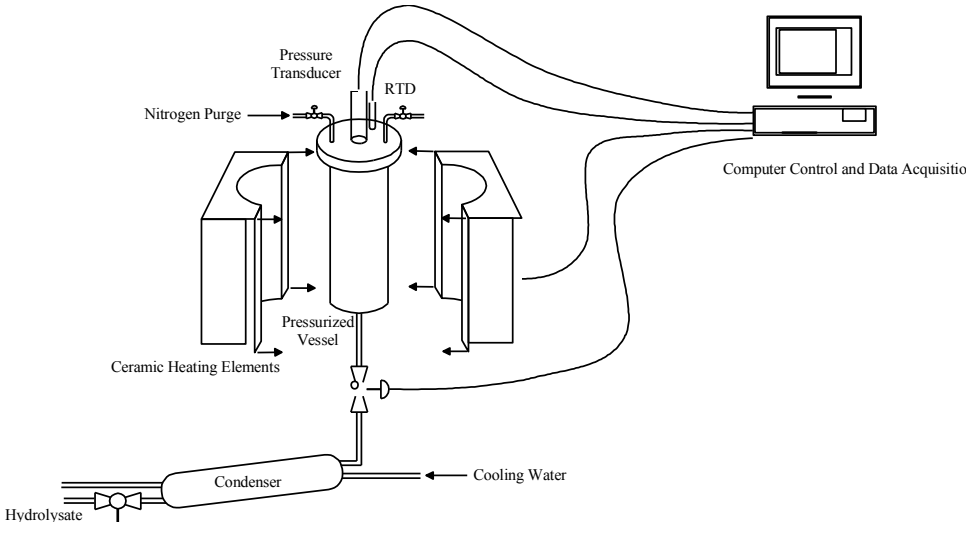

Figure 2.1. Temperature and pressure profile for a typical hydrolysis experiment. For this particular experiment the reaction time was 2 minutes and the set point temperature was 200°C**.**

Of the four hydrolysis dependent variables studied, three quantified the effect of the physical parameters of the reactor (time, temperature, and pressure) on the dissolution of simple sugars in liquid hydrolysate. Pressure did not significantly affect any of the four measured variables. The mass of glucose dissolved over the range of temperature and time studied did not correlate with either of these two factors. However, the mass of xylose and the total mass of reducing sugar both correlated linearly with the time and temperature, increasing as either variable increased, but with the temperature having a slightly greater effect.

The other variable studied was the digestibility of the solid grass which was calculated by determining the sugar yield, defined as the mass of reducing sugar hydrolyzed in the enzymatic reaction after hot water treatment per mass of sample. Both temperature and time significantly affected this sugar yield. Maximum sugar yield within the range studied occurred at the highest temperature (230°C) and lowest time (2 min.), while the minimum occurred at the lowest temperature (200°C) and time (2 min.). This phenomenon for a two-minute hydrolysis time is shown in Figure 2.2.

By combining net weight loss data with the NIR data, the percent dissolution of cellulose, hemicellulose and lignin were estimated. There is a significant increase in the dissolution of hemicellulose for the 230°C pretreatment (54 %) over the 200°C pretreatment (21 %). A modest increase in cellulose dissolution from 6% at 200°C to 11% at 230°C was observed. Lignin dissolution increased from 0% to 5% at the higher temperature.

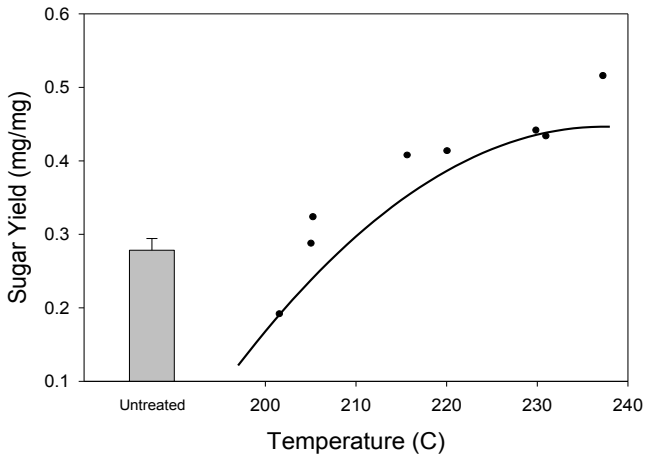

Figure 2.2. Enzyme digestibility of bermudagrass following 2 minute hydrolysis. The curve depicts the model prediction of sugar yield resulting from statistical analysis and the data points represent observed sugar yields as a function of reaction temperature (at a variety of reaction pressures). Values are corrected for contribution of DNS-reactive stabilizers in the enzyme mixtures. The bar represents the sugar yield of a sample of untreated bermudagrass.

To confirm that increase in digestibility would correlate in increased ethanol yield, a series of partial saccharification and co-fermentation experiments (PSCF) were conducted using three conditions: untreated T85, 200˚C (2 min.) treated T85, and 230˚C (2 min.) treated T85. There was no furfural or 5-HMF present in the hydrolysate following the pretreatments (data not shown). Table 2 outlines the profile of sugars released by the PBHW pretreatments as well as by the 24 hour enzymatic hydrolysis. Minimal sugars were released by the PBHW pretreatment alone. More arabinose and xylose were released from the 230°C treated solids than the 200°C or untreated solids which corresponded well with the increased dissolution of hemicellulose that occurred in the 230°C treated grass (Table 2.1). At time zero there is more glucose liberated in the untreated grass, perhaps because autoclaving liberated the easily released sugars and these sugars had already been released in the PBHW pretreated samples. However, after 24h of enzymatic hydrolysis, the glucose released from either pretreatment of the grass solids is very similar and higher than the untreated grass, presumably due to enhanced accessibility of the cellulose. Ethanol production and reducing sugar levels over the course of the fermentations are shown in Figure 2.3. As expected from the preliminary reducing sugar analyses, the 230°C pretreated grass resulted in an increase in ethanol production of roughly 4.5 g/L over the 200°C pretreated grass. Untreated grass produced the least amount of ethanol of the experiment (9 g/L). For additional details on methodology and results, please review (Brandon et al., 2008).

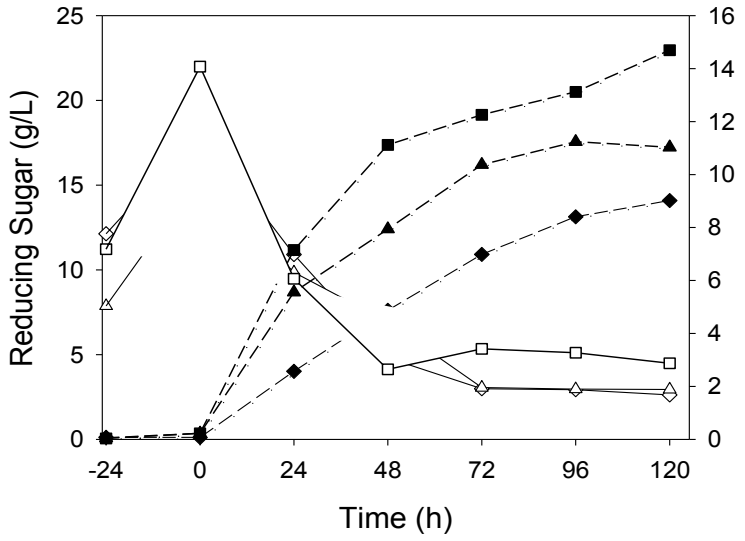

Figure 2.3. Average reducing sugar concentration and ethanol production over the course of fermentations of untreated, 200°C, and 230°C treated T85. Solid symbols are ethanol and open symbols are sugar concentrations. Symbols are as follows: diamond, untreated; triangle, 200°C; square, 230°C. Fermentations were conducted at 35°C in an immersion circulator for five days at 10% solids. The -24 hour time point corresponds with the beginning of the 24-h enzymatic hydrolysis (at 45°C). Actual

fermentation began (bacterial inoculation) at time 0 h. Reducing sugars are removed at the same rate that ethanol is produced.

Table 2.1. Sugars released from treated and untreated Tifton 85 bermudagrass by 24 hour enzymatic hydrolysis.

Treatment	Arabinose (mg/g grass)			Xylose (mg/g grass)			Glucose (mg/g grass)		
	Hydrolysate	0 hrs	24 hrs	Hydrolysate	0 hrs	24 hrs	Hydrolysate	0 hrs	24 hrs
Untreated	n/a	48.91	60.45	n/a	14.79	29.88	n/a	371.69	541.63
200°C Treated	0	56.28	69.23	0	60.03	133.15	0.69	244.09	640.34
230°C Treated	0.25	79.39	76.75	0	129.49	282.36	0.31	209.5	635.32

Subtask 2.1 Develop a pre-treatment extraction system: Part B – Levoglucosan from BioOil

Methodology and results described and summarized below have independently been reported in the following publications:

1. *Ormsby, R.V. 2011. Levoglucosan transformation and kinetics of hemicellulose hydrolysis using carbon supported solid acid catalysts. Unpublished M.S. Thesis, Biological Engineering, The University of Georgia, Athens GA 30602.*

Our goal was to use fast pyrolysis and variations of it to develop levoglucosan (LG) as an intermediate and subsequently develop sugar from hydrolysis of LG. Two forms of fast pyrolysis oil production were used to generate the levoglucosan feedstock: ground pine chip fast pyrolysis (FP) and ground pine pellet in-line-condensation fast pyrolysis (ILC). HPLC analysis was performed on bio-oil samples diluted to 5% with deionized water to identify and quantify the initial compounds found in the oil. Both forms of pyrolysis occurred under bubbling fluidized bed conditions.

Details of procedures are outlined in Ormsby (2011). In brief, the pyrolysis reactor utilized a nitrogen sweep gas with a pyrolysis reactor gas flow rate of 20 L/min with 16-18 L/min of fluidization (Figure 2.4) . The residence time of any solids was approximately 5s at reaction temperatures of 500 ^{o}C. The oil feed rate to a downstream reactive condensation unit was 40-147 g/hr. The ILC bio-oil generation had an additional process that added water vapor at to the oil condenser.

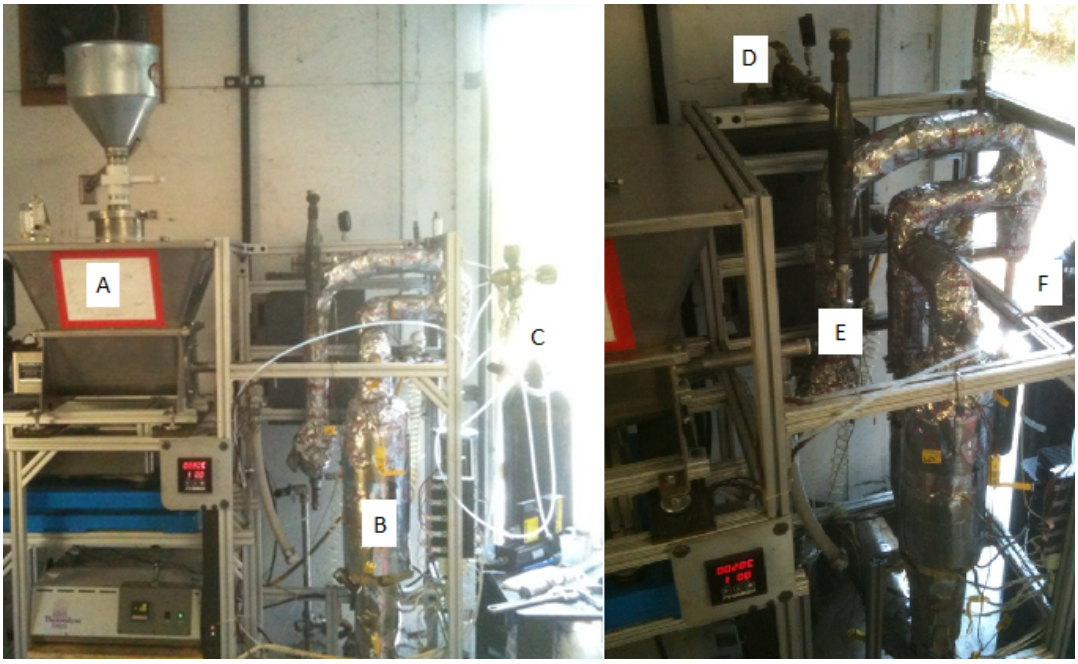

Figure 2.4. Fast pyrolysis reactor: biomass hopper (A), sand bed reactor (B), nitrogen sweep gas (C), hot gas filter (D), condenser inlet (E), and char collector (F).

The water spray rate of the ILC method was 79-102 g/hr via a small bore atomizer. The final oil product of the ILC method was a 50/50 wt. mix of water an oil, which allowed extraction of the aqueous phase bio-oil directly from the reactor.

ILC bio-oil samples had an approximate water/oil ratio of 50%, and had not been filtered before the hydrolysis reaction. Ten mL of the ILC oil was combined with 1 g of catalyst and heated to 120 ^{o}C over time intervals ranging from 1 to 24 hours. A 10 mL sample of ILC oil was prepared without the catalyst as a thermal control. Hydrolysis products were gravity filtered through a coarse glass fiber Whatman filter then diluted to 10% with de-ionized water and re-filtered for HPLC analysis.

HPLC chromatograms were used to determine the concentration of levoglucosan and glucose following levoglucosan hydrolysis. Model compound of levoglucosan was used for the preliminary hydrolysis reaction with PCC. The glucose and levoglucosan peaks were identified given the retention time of 10 g/L glucose and 1 g/L levoglucosan standard. A thermal control was used to verify that hydrolysis did not occur without catalyst. Figure 2.5 shows the matching retention times (approximately 10.8 minutes for glucose and 14.5 minutes for levoglucosan) between the glucose standard (A), levoglucosan standard (B), products following 17 hr. hydrolysis of levoglucosan at 123 ^{o}C (C), and as well as the absence of glucose in the thermal control of 17 hrs at 123 ^{o}C (D). The model compound of levoglucosan was found to almost completely convert to glucose, while the thermal control showed no change in levoglucosan concentration.

Bio-oil samples were collected from both fast pyrolysis (FP) and in-line-condensation fast pyrolysis (ILC) methods. De-ionized water was added to the FP samples to bring the water concentration from approximately 20% wt. to 50% wt. Samples were then centrifuged at 3500g for 15 minutes at room temperature and the

aqueous phase was extracted for HPLC analysis. The aqueous phase of the ILC bio-oil samples was drawn directly from the pyrolysis reactor for HPLC analysis. Initial sugar concentrations for the aqueous phase ILC and FP samples as well as the non aqueous FP oil are shown in table 2.2

Table 2.2. Initial sugar concentrations for aqueous and non aqueous phase FP oil

Oil	Levogluco-san (g/L)	Xylose (g/L)	Glucose (g/L)	Acetate (g/L)	5-HMF (g/L)	Furfural (g/L)	Water (%)
ILC (aq)	169.9	3.8	0.0	79.8	1.9	1.3	50
FP (aq)	165.6	5.9	1.1	80.4	1.7	1.1	50
FP	266.8	10.6	2.0	125.8	3.0	2.0	20

The average levoglucosan concentration for the FP and ILC methods was approximately the same at 165.6 g/L and 169.9 g/L respectively. The ILC method is therefore the more efficient method for producing aqueous phase bio-oil as it removes the separation and extraction step required to obtain the aqueous phase of the FP oil. Additional work relating to hydrolysis of levoglucosan to produce more sugars that could further go into fermentation in reported in subtask 7.1 later in this final report.

Milestone 1: Completed development and demonstration of extraction method for value added products like sugars and sugar precursors.

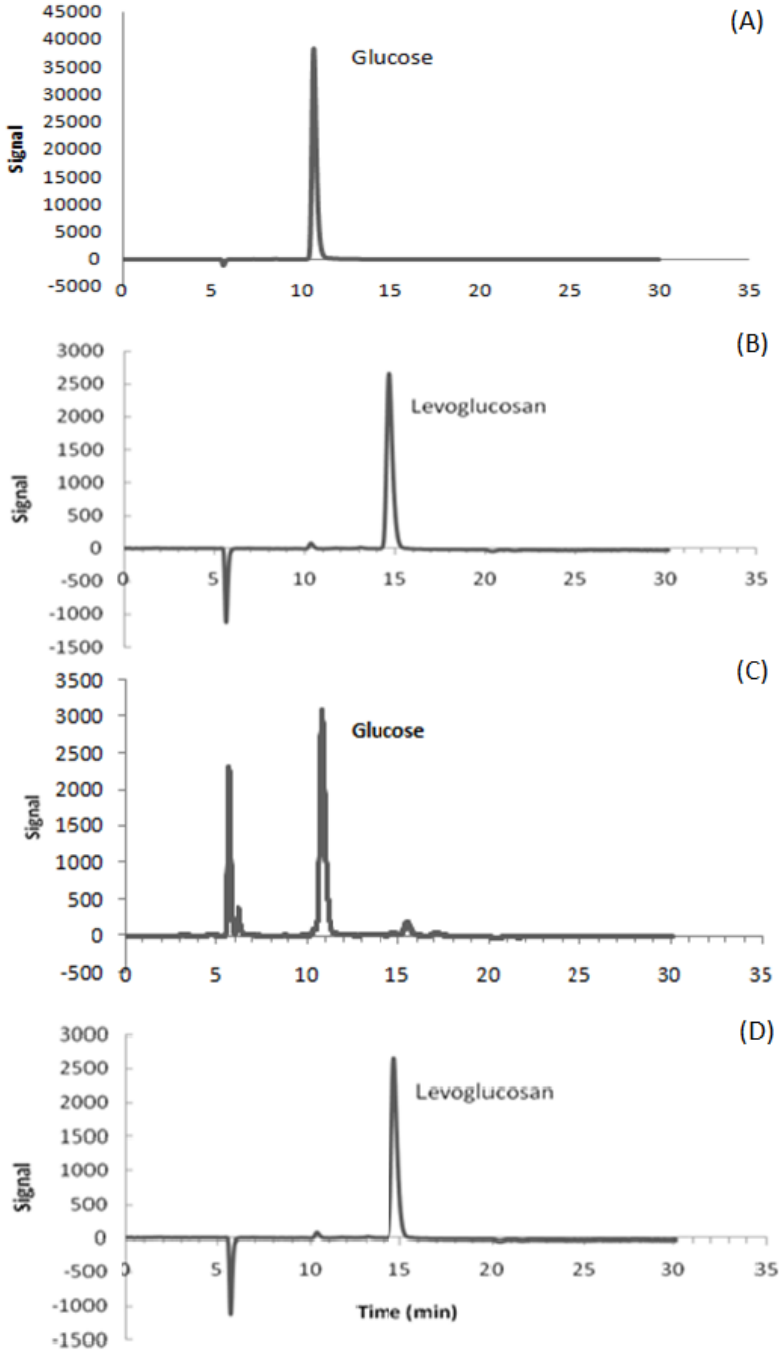

Figure 2.5. HPLC chromatograms of 10 g/L glucose standard (A), 1 g/L levoglucosan standard (B), 17 hr, 123 ^{o}C levoglucosan hydrolysis products (C), and 17 hr, 123 ^{o}C levoglucosan thermal control (D).

Subtask 2.2. Pro forma analysis of methods. This analysis will contribute to the evaluation (indicated above) that will allow prioritization.

Modification of plan: Our plan at the time of writing the proposal was to screen extraction methods and identify a preferred methods that could be brought to a pilot scale in order to determine preliminary economics through a pro forma analysis. However, the extent of work completed in Task 2 was insufficient to pursue realistic economic analysis, therefore this subtask 2.2 was not pursued any further.

Subtask 2.3 Additional literature studies

Levoglucosan can be a significant component of certain pyrolysis BioOils and is an attractive target compounds that could lead to the production of other value added products. Levoglucosan can be hydrolyzed to form glucose, a fermentable monomer, or methyl α-D-glucopyranoside (MGP), an acetal of glucose, depending on the hydrolysis medium. The reaction pathway for the formation of these compounds from levoglucosan is shown in Figure 2.6. Fast pyrolysis bio-oil can be simultaneously esterified to form esters while levoglucosan is hydrolyzed to glucose with acid-catalysts in an alcohol-rich medium. As temperatures increase above approximately 130 ^{o}C glucose and MGP are no longer the primary products. The conversion process continues to generate intermediate oligosugars such as 5-(hydroxymethyl)furfural (HMF) or 2-(dimethoxymethyl)-5-(methoxymethyl)furan (DMMF) and final products such as levulinic acid or methyl levulinate (Hu and Li, 2011). These final products are marketable compounds in the food, diesel fuel, and fragrance industries.

In a water rich medium, however, glucose is easily polymerized into solid humins that diminish the total yield glucose or levulinic acid. Solid acid catalysts combined with esterification agents can be used to stabilize fast pyrolysis oil and reduce polymerization of glucose. Nearly 100% conversion of levoglucosan can be achieved after 1 hour for temperatures greater than 110^{o}C (Hu and Li, 2011).

The Fuels and Energy Technology Institute of Curtin university in Perth, Australia has demonstrated the simultaneous hydrolysis and esterification of fast pyrolysis bio-oil with a solid acid catalyst and methanol over a thermal range of 70 – 170^{o}C. Levoglucosan hydrolysis to glucose became significant at temperatures above 90^{o}C and the reaction rate rose proportionally with the temperature of the reaction (Gunawan et al. 2011). We believe that this path of development holds much promise and will be pursued beyond the scope of this project.

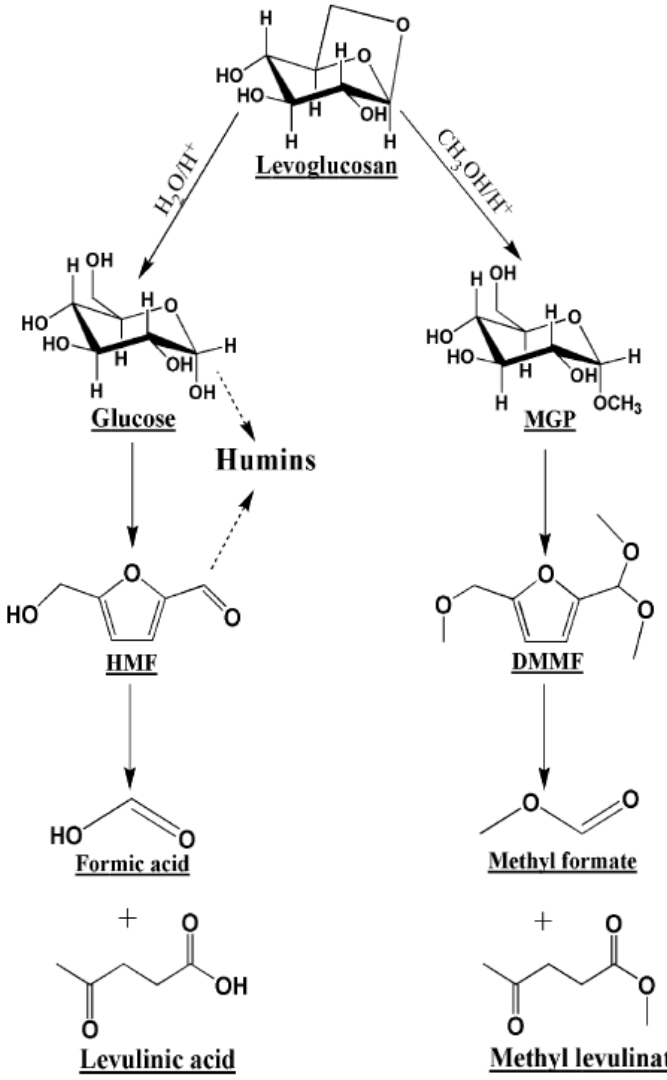

Figure 2.6. Reaction pathways of levoglucosan in water-rich and alcohol-rich mediums (Hu and Li, 2011).

Task 3.0 Production, characterization and uses for pyrolysis-Char.

Pyrolysis Char (Biochar) were be developed under different conditions (different environments, different temperatures and biomass) and characterized for surface properties. The chars were evaluated in applications including as soil amendment and for its use as catalysts.

Subtask 3.1 Development of different types of chars

Methodology and results described and summarized below have independently been reported (all or in part) in the following publications:

1. *Das, K.C., K. Singh, R. Adolphson, B. Hawkins, R. Oglesby, D. Lakly, and D. Day. 2010. Steam pyrolysis and catalytic steam reforming of biomass for hydrogen and biochar production. Applied Engineering in Agriculture, 26(1):137-146.*

Our primary goal was to generate biochar from various available biomass and study their characteristics. Five different woody materials, namely, Pine bark (PB), Pine chips (PC), Pine sawdust (SD), Hardwood with red coloration (HR) and Hardwood with white coloration (HW), were evaluated. The hardwoods, HR and HW, represented biomass from different parts of the tree. These materials were dried to determine moisture content and then steam-pyrolyzed at different temperatures, namely, 360, 380, 400, and 420°C. Each target temperature was reached with an accuracy of ±10°C. Char yield and average biochar pH (acidity level) were measured on each sample. Following pyrolysis the biochars were characterized for C, N, and S and total nutrients. In addition to total nutrients, plant available nutrients were estimated using a Mehlich I extraction procedure.

Each biomass mentioned earlier and included in Table 3.1 was pyrolyzed in a batch pyrolyzer at target temperatures (indicated in Table 3.1) and Char yield and pH were measured. Low temperatures, compared to typically used temperatures in pyrolysis, were chosen in order to enhance the surface properties of the chars. As anticipated, pyrolysis at higher temperatures results in reducing char yield and increasing vapor yields. Between 350 and 450°C, for all the biomass tested, a near linear decline in char yield was observed (Figure 3.1). Although this trend in char yield decrease is commonly seen, the reduction in yields was more than is typically seen in pyrolysis.

The pH data (Table 3.1) shows that all biomass with the exception of hardwood-W (HW) and pine bark (PB) produced chars that had near neutral pH. In addition there appears to be no correlation with changing pyrolysis temperatures (Figure 3.2). The only exception was HW, which appeared to increase in pH with increasing temperatures. Complete analysis as average macro and micronutrient concentrations in chars generated over the whole range of temperatures reported are provided in Tables 2 and 3. The Mehlich I extraction (Table 3.2) is a measure of the amount of extractable nutrients and correlates with what may typically be plant available nutrients.

The woody biomass tested in this study had similar P and K (common nutrients important in agronomic applications) concentrations. However, these values were significantly lower than that present in a char derived from peanut hulls (a nutrient rich biomass) (Figure 3.3). The differences between woody biomass and peanut hull char were more enhanced when considering plant available nutrients (Figure 3.4). Both P and K were about seven times lower than in peanut hull char. The percentage of potassium that is plant available appears to be increasing with higher pyrolysis temperatures (Figure 3.5).

Table 3.1. Pyrolysis data from biochar production batch runs.

Biomass Type	Biomass Avg. Moisture, %	Pyrolysis Char Temp, °C	Char yield % (w/w)	Char Avg. pH
Pine Bark	64.6	358	32.8	-
		382	-	6.71
		399	27.5	6.28
		426	24.2	6.23
Pine Chips	45.4	345	18.4	6.68
		355	23.7	-
		379	15.5	6.56
		401	14.2	6.63
		426	12.7	6.94
Pine sawdust	38.9	350	-	-
		378	14.6	6.95
		399	13.6	6.81
		418	12.5	7.16
Hardwood red	34.5	355	28.4	-
		387	16.1	7.07
		409	18.7	-
		428	17.1	7.07
Hardwood white	-	382	18.2	5.84
		400	-	6.44
		426	14.3	7.05

* Spaces that are blank represent either that data was not measured or was outside of

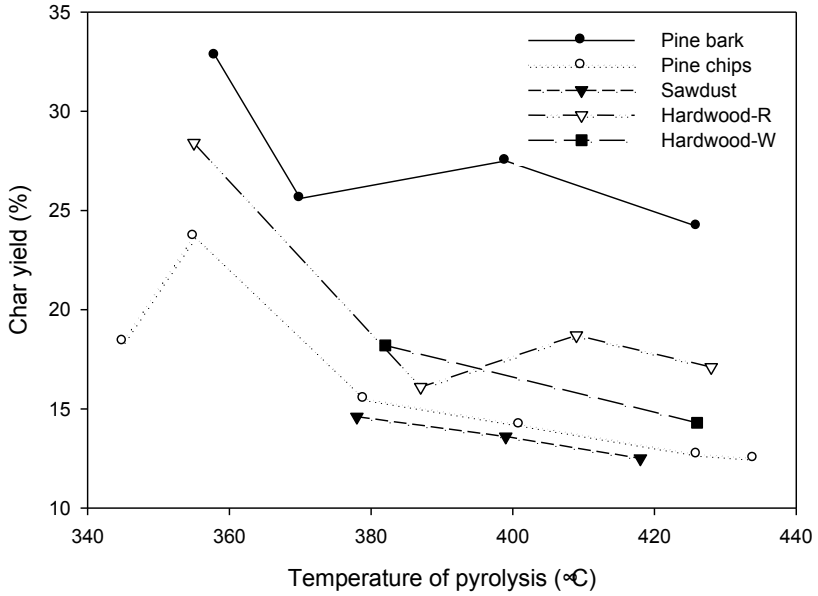

Figure 3.1. Plot of char yield from pyrolysis of different biomass at different temperatures in a batch reactor.

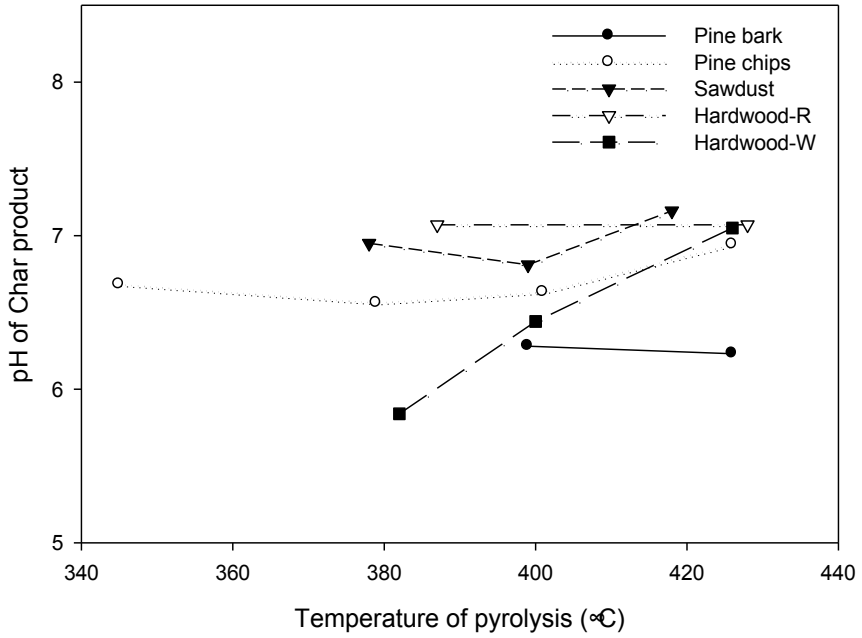

Figure 3.2. Plot of pH changes in char product from pyrolysis of different biomass at different temperatures in a batch reactor.

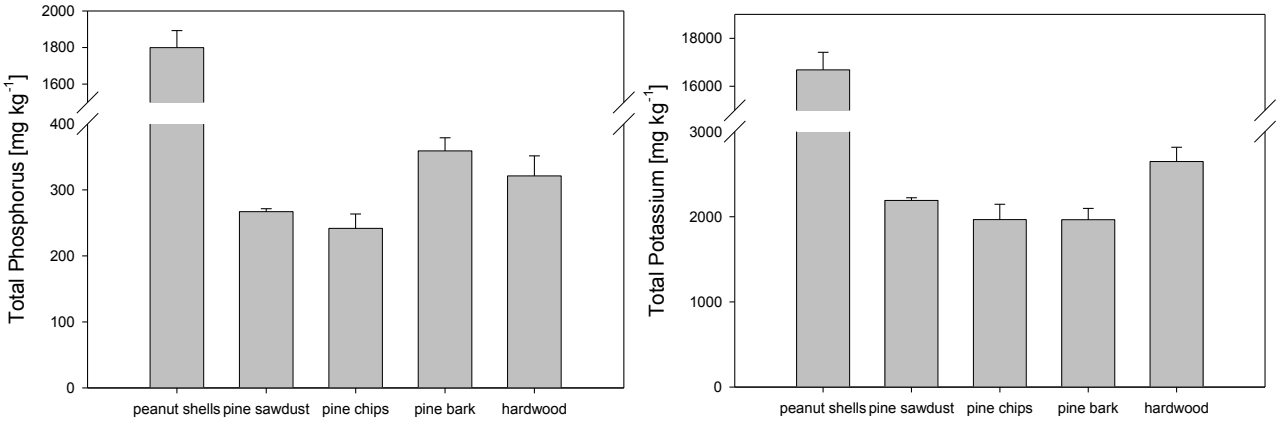

Figure 3.3. Differences in total P and K as a function of biomass. Peanut hull char (a nutrient rich char) is also presented as a comparison.

Table 3.2. Macronutrients and available (Mehlich I extract) micronutrients in char. Values are average in mg/kg followed by standard dev. in column on right. Data are averages of analyses of chars generated over all temperatures tested.

	Pine sawdust	Std. Dev	Pine chips	Std. Dev	Pine bark	Std. Dev	Hardwood – W	Std. Dev	Hardwood-R	Std. Dev
Marco element analysis – values below are in % - Averages for specific treatments followed by standard deviation shown in column on right										
C	70.7	1.2	74.5	1.4	67.8	1.1	71.1	2.1	66.7	1.5
N	0.15	0.01	0.14	0.02	0.31	0.02	0.31	0.04	0.31	0.13
S	0.02	0.01	0.02	0.00	0.04	0.01	0.03	0.01	0.03	0.01
Elemental analysis – all values given below are in mg/kg										
Al	13.5	1.3	10.5	1.2	44.6	13.3	6.0	1.7	5.6	3.2
B	0.90	0.11	0.67	0.31	0.87	0.34	0.57	0.20	0.89	0.19
Ca	594.5	72.1	405.4	83.0	839.8	252.7	499.8	94.5	1941.1	787.8
Cu	10.0	4.0	10.9	11.4	3.7	1.2	3.6	1.4	4.0	0.3
Fe	20.6	9.4	12.7	1.3	41.5	3.2	12.8	6.0	37.4	31.0
K	847.9	241.1	674.5	432.3	586.6	232.8	735.7	373.0	821.1	168.1
Mg	144.0	21.2	96.3	24.1	89.3	26.6	76.7	17.8	153.1	152.9
Mn	64.3	8.8	46.8	11.6	19.8	5.5	14.7	3.3	39.9	10.5
Mo	0.23	0.07	0.18	0.10	0.15	0.04	nd	nd	0.10	0.01

Na	247.3	28.8	201.6	30.1	176.2	11.5	198.0	11.2	130.3	19.0
P	94.1	13.4	93.5	19.6	78.1	20.9	93.7	26.1	75.2	62.3
Pb	4.5	1.3	2.8	0.7	4.1	1.9	2.1	0.8	2.1	1.9
Zn	34.6	5.6	27.7	4.7	25.3	0.1	24.4	1.6	16.2	3.4

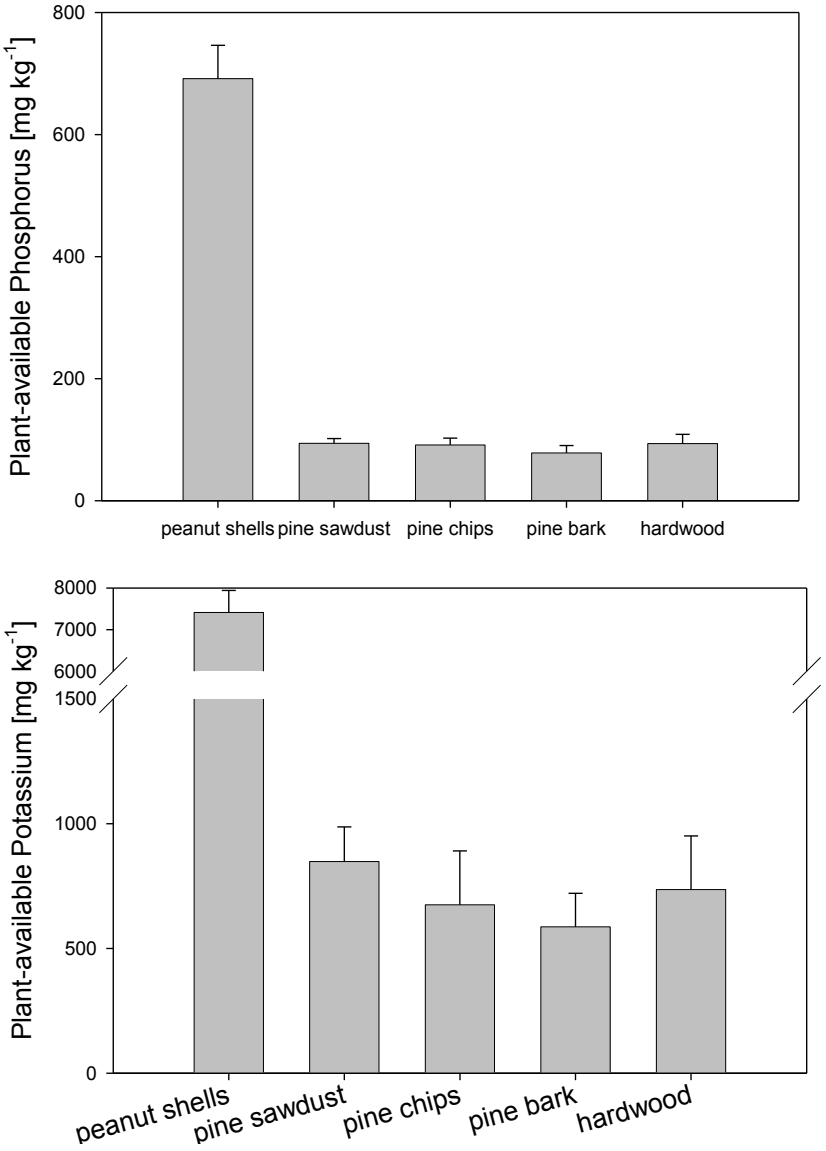

Figure 3.4. Differences in plant-available P and K as a function of biomass. Peanut hull char (a nutrient rich char) is also presented as a comparison.

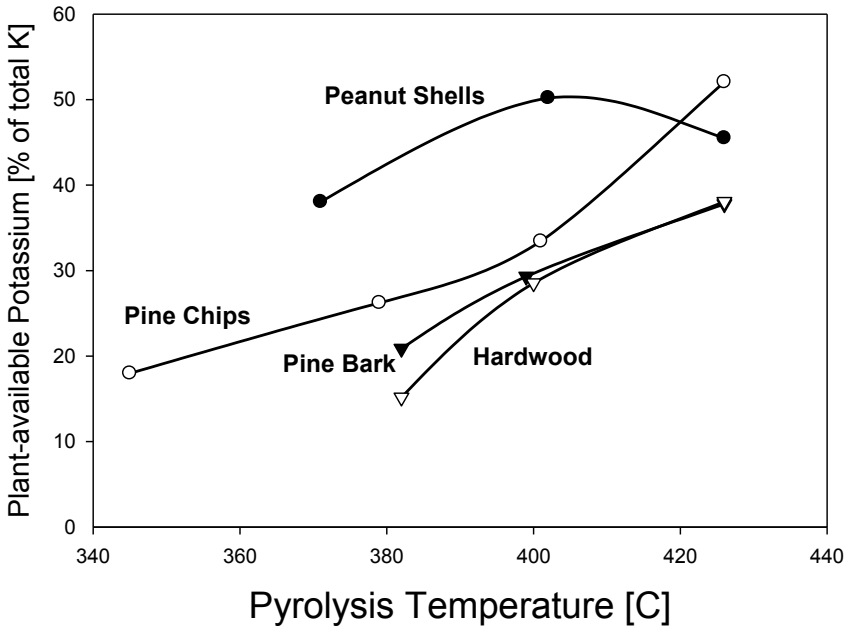

Figure 3.5. Relationship between percentage of plant available potassium and pyrolysis temperatures for different biomass.

Milestone 1: Completed milestone of development and characterization biochar. Additional testing with biochar as catalysts, soil conditioner applications and adsorbent applications are discussed in other tasks in this report.

Subtask 3.2 Field and green house testing of char as nutrient source/soil amendment and carbon sequestering agent

Our goal was to pursue the use of pyrolysis co-product, biochar, in an application in agricultural soils. We produced and characterize char for agricultural use and carbon sequestration. Tests included available nutrients, nitrogen and carbon mineralization, cation exchange capacity, phosphorus adsorption, and moisture retention capacity.

Total and available (Mehlich I) minerals were analyzed for peanut hull (PN), sawdust (SD), pine chip (PC), pine bark (PB), and hardwood (HW) feedstocks pyrolyzed at different temperatures and their characteristics have been reported earlier (Task 3.1). It was found that Pyrolysis temperature had an effect on the availability of several minerals. Averaging feedstocks across temperature showed an increased availability for Al, Ca, Fe, K, Mg, and P as temperature rose. B, Cu, and Zn showed no pattern.

The pH of the char varied with feedstock. PN had the highest pH (10.52), which is due to the higher concentrations of basic cations such as Ca, Mg, and K. The presence of available cations should increase acidic soil pH and may serve as a minor

nutrient source. PN char has the highest potential to affect soil pH and supply P, K, and Ca.

Nitrogen mineralization testing

A Tifton loamy sand soil amended with PN, PC, PB and HW chars pyrolyzed at 420^{o}C at 22 Mg ha^{-1} equivalent rate was incubated for 24-days. N mineralization was low (NH_4-N – 1.32 to 1.40 mg/kg; NO_3-N - 5.22 to 6.88 mg/kg). There was no statistical difference in NH_4-N concentrations between char-amended soils and the control. The PN char amended soils did have statistically different NO_3-N concentrations compared to the control. However, the average PN nitrogen mineralized of 6.88 mg/kg would be equivalent to 0.16 kg N ha^{-1} at a 22 Mg ha^{-1} application rate.

A second incubation of Tifton soils amended with PN and PC chars at 11 and 22 Mg ha^{-1} equivalent rate was conducted. These application rates applied 213 kg total N ha^{-1} – PN 11 Mg ha^{-1} and 19 kg total N ha^{-1} – PC 11 Mg ha^{-1}. Nitrogen mineralization was very low (NH_4-N – 0.38 to 0.59 mg/kg; NO_3-N – 1.31 to 2.21 mg/kg). This is equivalent to less than 2% of the total N. There was no statistical difference in NH_4-N concentrations between the control and char amended soils ($p=0.05$). There was a trend for higher NO_3-N concentrations in the PN amended soils. Only the PN amended soils at the 11 Mg ha^{-1} rate were statistically different from the control.

The data indicates char does not contain N that is readily available to microorganisms in the short–term (24-days). The C:N ratio of the charcoal for several feedstocks was high and could serve as a potential sink for available N, which could cause N deficiency in plants grown in char-amended soils.

Carbon mineralization

Carbon dioxide was measured as part of the N mineralization incubations to evaluate C mineralization. Tifton soil was amended with PN, PC, PB and HW chars pyrolyzed at 420^{o}C at 22 Mg ha^{-1} equivalent rate. Carbon mineralization was measured through CO_2 traps at 3-days, 10 days, and 24 days. Cumulative C mineralization rates were low with total C mineralized ranging from 54.2 mg C/kg oven dry (OD) soil in the control to 72.9 mg C/kg OD soil for the PN amended soil. Carbon mineralization in the char amended soils was only statistically different from the control for the 3-day respiration period.

Similar results were obtained in the second incubation of Tifton soils amended with PN and PC chars at 11 and 22 Mg ha^{-1} equivalent rate. Cumulative C mineralization rates were low ranging from 51.3 mg C/kg OD soil in the PC at 11 Mg ha^{-1} to 124.5 mg C/kg OD soil in the PN at 22 Mg ha^{-1}. The PN amended soil at 22 Mg ha^{-1} was statistically different from the control and PC at 11 Mg ha^{-1} at the 3 and 10-day measurement periods. These were not statistically different to 24-days.

Similar to the results of the N mineralization, short-term lab incubations indicate char does not contain much of a C fraction that is available for microbial growth. There is a small short-term response to the addition of char to Tifton soils, but by 24-days char-amended soils are similar to the control. At the 22 Mg ha^{-1} rate, about

1.5% of C added in the PN amended soils was mineralized; PC amended soils had 0.88%. Because there is a greater response in PN amended soils than PC amended soils, the microbial response may be due to nutrient additions.

Field studies on plant growth with biochar

Methodology and results described and summarized below have independently been reported (all or in part) in the following publications:

1. *Gaskin, J.W., C. Steiner, K. Harris, K.C. Das, and B. Bibens. 2008. Effect of low temperature pyrolysis conditions on biochar for agricultural use. Transactions of the ASABE, 51(6):2061-2069.*

A multi-year field study was established at the University of Georgia Coastal Plain Experiment Station near Tifton, GA. Field plots were in a 0.04-ha section of a 0.20-ha field (Figure 3.6). Tifton loamy sand soil (fine-loamy, kaolinitic, thermic Plinthic Kandiudult) is typical of the Lower Coastal Plain (Table 3.3). Before plot establishment, the field was disk harrowed to a depth of approximately 15 cm and fertilized with 26 kg N ha^{-1} as well as 122 kg P_2O_5 ha^{-1}, and 167 kg K_2O ha^{-1} based on soil test results from the previous fall. Each plot, 2.2 by 1.8 m in size, was delineated by stakes. A wooden frame was placed around each biochar plot during application. The plot size was relatively small compared to typical agronomic plot sizes due to the limited amount of biochar available. Much of the previous work with biochar has been conducted in greenhouses; this mesocosm scale field evaluation of pyrolysis biochar provides a real world evaluation and is, we believe, the first field study of crop response to biochar in the United States.

Figure 3.2. Field study on the use of biochar in agriculture.

Biochar was produced by EPRIDA Inc. (Athens, GA) from pelletized peanut hull and pine chip feedstocks in a pyrolysis reactor at 400°C with steam. Biochars from these two feedstocks represented a range in nutrient characteristics (Table 3.3), and

were applied at three rates (0, 11.2, 22.4 Mg ha^{-1}) with and without N fertilizer in a factorial set of six treatments within a completely randomized design. Nitrogen fertilization rates were based on standard agronomic practice to achieve grain yields of 12.5 Mg ha^{-1}. Each treatment combination was replicated four times (24 plots for each biochar feedstock).

Table 3.3. Initial Tifton soil concentrations (0–15 cm), biochar concentrations, and carbon and nutrient load when biochar was applied at 11 Mg ha^{-1}.

	Soil	Peanut hull		Pine Chip	
		Concentration	Load	Concentration	Load
	–mg kg^{-1}–		–kg ha^{-1}–	–mg kg^{-1}–	–kg ha^{-1}–
C	4,354	728,470	8013	769,930	8,469
N	191	19,000	209	1,700	19
P	21	2,177	24	577	6
K	51	19,311	212	2,822	31
S	83	852	9	350	4
Ca	266	5,414	60	4,028	44
Mg	23	2,716	30	1,228	14
pH	5.59	10.12		7.54	
C/N Ratio	23	38		453	

Biochar was applied by hand and tilled into the soil to a depth of 15 cm with a rotovator. Corn (Pioneer Hybrid 33M53) was planted, fertilized, and harvested using standard agronomic practices. A second year of similar activity was conducted in the subsequent year. Initial soil samples were collected after treatment applications to establish baseline C and nutrient content for each plot. Soil samples were collected again after harvest in year 1 and 2. Soil samples were collected within the zone of incorporation (0–15 cm) and below the zone of incorporation (15–30 cm), using a 1.75-cm diam. push probe. Five subsamples were taken from the plot, composited, air dried, and sieved to < 2 mm. Total C, N, and S were analyzed by combustion (LECO CNS-2000, St. Joseph, MI, USA). Plant available Ca, Mg, P, and K were extracted with a Mehlich I solution (Mehlich, 1953) and measured by inductively coupled plasma spectrometry (ICP, Thermo Jarrell-Ash model 61E,Thermo Fisher Scientific, Waltham, MA).

At plant growth stage R1 (silking), an earleaf was collected from six plants within each plot. The earleaf samples were composited by plot and oven-dried at 60°C for 4 d. Samples were ground, digested with nitric acid, USEPA Method 3050 (USEPA, 1994), and analyzed by inductively-coupled plasma spectrophotometer (ICP, Thermo Jarrell-Ash model 61E,Thermo Fisher Scientific, Waltham, MA). At the time of analysis, percent moisture was determined by weighing the samples, oven-drying at 60°C overnight and reweighing the samples. All results are presented on a dry-weight basis. Corn ears from each plot were removed from their shucks, bagged, and dried for 6 d at 49°C in a forced-air drying shed. After drying, ears were mechanically

shelled, and cob and kernel biomass were determined for each plot. Grain moisture content was determined using a 2100 Grain Analysis Computer (Dickey-John Corp., Auburn, IL). Kernel and grain yield were standardized at 15.5% moisture. After grain harvest, all corn plants within the plot were cut at 30 cm aboveground surface. The stalks and leaves were dried for 6 d at 49°C in a forced-air drying shed. After drying, the stover biomass was determined by weighing stalks and leaves from each plot, and then adding in the dried cob weight. Plant growth response and yields are reported here. Additional details on dates of fertilizer addition, harvest, statistical analysis and influence of biochar on the soil nutrient status please refer Gaskin et al (2008) listed above.

Peanut Hull Biochar Experiment

Peanut hull biochar affected corn biomass production and yield (Table 3.4). The response of grain yield to biochar was nonlinear and was influenced by fertilizer. Corn yield declined with application of 22 Mg ha^{-1} peanut hull biochar compared to the 11 Mg ha^{-1} rate in the fertilized treatment. In contrast, in the unfertilized treatments, corn yield was decreased at the 11 Mg ha^{-1} application rate, but not at the 22 Mg ha^{-1} rate. The response of corn stover to peanut hull biochar application was linear but included a significant year interaction because yields were greater and the biochar effect more pronounced in the first year (data not shown). The main effect of fertilizer was reflected in increases in both grain yield and stover. There was also a significant effect of year with decreased yields and stover in 2007 compared to 2006. For additional details, please refer Gaskin et al (2008).

Table 3.4. Mean grain yield (kg/ha) and stover biomass (Mg/ha) of corn amended with peanut hull biochar at three rates for two growing seasons at Tifton, GA.

Biochar rate	Fert	Grain		Stover	
		2006	2007	2006	2007
0	No	4,703	917	4.24	1.37
11	No	3,049	925	4.78	1.56
22	No	6,073	1,359	6.18	1.82
0	Yes	13,004	8,608	7.03	4.54
11	Yes	13,422	8,553	8.42	4.75
22	Yes	11,679	8,092	7.11	3.93

Pine Chip Biochar Experiment

Pine chip biochar had a significant effect on corn grain yield but not on corn stover (Table 3.5). The effect of pine chip biochar application rate on corn grain yield was different between the 2 yr. In 2006, corn grain yield decreased with increasing pine chip biochar application rate; however in 2007, the linear effect was reversed. A significant response to both fertilizer for grain yield and stover in the pine chip biochar study was observed. Similar to the peanut hull study, both grain yield and stover biomass were decreased in 2007 compared to 2006 due to growing conditions.

Our results indicate the influence of biochar on corn yield in a field setting is not simple. Biochar without the addition of other fertilizers increased yields over the unamended controls, but the yields were relatively low and would produce limited economic return. Our grain yield and stover results should be interpreted with caution due to low rainfall during the two years of this study.

Table 3.5. Mean grain yield (kg/ha) and stover biomass (Mg/ha) of corn amended with pine chip biochar at three rates for two growing seasons at Tifton, GA.

Biochar rate	Fert	Grain		Stover	
		2006	2007	2006	2007
0	No	4,449	521	5.27	1.54
11	No	3,414	740	4.94	1.54
22	No	3,126	807	5.50	1.14
0	Yes	15,127	8,697	8.32	4.35
11	Yes	14,523	10,691	8.32	5.70
22	Yes	13,645	8,868	8.18	4.35

Milestone 1: Evaluation of data from corn growth in field trials completed.

Subtask 3.3 Development of char as ammonia adsorbent in poultry applications

Methodology and results described and summarized below have independently been reported (all or in part) in the following publications:

1. *Doydora, S.A., M.L. Cabrera, K.C. Das, J.W. Gaskin, L.S. Sonon, and W.P. Miller. 2011. Release of nitrogen and phosphorus from poultry litter amended with acidified biochar. International Journal of Environmental Research and Public Health, 8, 1491-1502.*

We conducted tests with biochars blended with poultry litter to determine adsorption benefits generated by biochar. Biochars were produced from pine chips and pelletized peanut hull residues by slow pyrolysis up to 400 and 600°C. These were ground, sieved and acidified (25 g char with 250 mL of 0.5 N HCl and shaking it for 30 min). Soil samples were collected from a previously manure added pasture area in Eatonton, Georgia. Poultry litter samples were taken from a stack of poultry litter applied to the sampled pasture area above in the Spring of 2008. For additional details relating to procedures and treatments, please refer Doydora et al. (2011).

Acid-washed sand and Eatonton soil was packed to 1-cm depth in 7.4-cm diameter funnels with 0.45 μm filter placed at the bottom. To each funnel, three replications of six treatments were randomly assigned. The treatments were as follows: T0 = s; T1 = s + 2.78 g (327.8 g kg^{-1} moisture content) fresh poultry litter (PL); T2 = s + PL + 2.09 g PC400; T3 = s + PL + 2.09 g PC600; T4 = s + PL + 2.09 g PH400; and T5 = s + PL + 2.09 g PH600, where s denotes for the soil-sand mixture, PL denotes for poultry litter, PC for pine chip char and PH for peanut hull char. The

numbers 400 or 600 following after PC and PH are the temperatures up to which the chars were produced.

Treatments were tested in two separated incubation experiments, surface and incorporated incubations. Under surface incubation, the poultry litter was directly applied on the surface of the packed soil. For treatments containing poultry litter and the chars, the two were thoroughly mixed before applying on the surface of the soil. In the case of the incorporated incubation, the poultry litter with or without acidified chars were thoroughly mixed in the soil-sand medium before packing the whole mixture in the funnel. Other than the manner of application of the treatments, the two incubation experiments were done using exactly the same procedure all throughout the incubation period.

Each funnel (experimental unit), was incubated at 20°C for 21 days under a flow-through system with the air flowing through each funnel at a rate of 0.86 L min^{-1}. Meanwhile, on the same day the incubation started, the soil-sand mixture, PL, and the different acidifed chars were extracted with 1 M KCl at a ratio of 1 g : 10 mL. These extracts were characterized for the initial inorganic P, NH_4^+-N, NO_3^--N and inorganic N. Ammonia lost from each treatment was trapped by bubbling the air through 50 mL of 0.1 N H_2SO_4. The acid traps were replaced at 1, 3, 5, 7, 10, 14 and 21 days after incubation. Moisture gained or lost from each treatment was also monitored by weighing each funnel every time the NH_3 traps were replaced and taking the percent difference of moisture gained or lost of the initial moisture at the start of the incubation. Carbon dioxide was measured at 6h, 1, 3, 5, 7, 10, and 14 days after incubation with the use of a CO2 analyzer (LICOR, Inc., Lincoln, NE).

On the 14^{th} day, each funnel was taken out of the incubator and leached with 150 mL of 0.01 M $CaCl_2$, adding 20 mL every hour. After the last addition of 0.01 M $CaCl_2$, 50 mL of N- and P-free solution (66.81 mg L^{-1} Ca, 39.22 mg L^{-1}, Mg, 21.72 mg L^{-1} S, and 119.70 mg L^{-1} K) was added at the same rate. Samples of the leachates were collected and analyzed for TN, NH_4^+-N, NO_3^--N and organic N. After leaching, the funnels were weighed and incubated again at the same temperature and airflow rate. On the 21^{st} day, the funnels were leached again with the same solutions in the same manner. After leaching, the funnel contents were extracted with 645 mL of 1 M KCl. This final KCl extracts were analyzed for inorganic P, NH_4^+-N and NO_3^--N.

All of the ammonia traps, and NH_4-N samples in the leachate and 1 M KCl extracts were analyzed colorimetrically at 667 using a UV spectrophotometer (Shimadzu Corp., Kyoto, Japan), while NO_3^--N analyses was done colorimetrically with an autoanalyzer (Alpkem Corp., College Station, TX) following the standard nitrate reduction method. Carbon dioxide evolved and inorganic N released were reported as the total amounts obtained from each experimental unit (funnel) per g of the sand-amended soil, except for the amount of NH_3 volatilized which was calculated by subtracting the amounts in T0 from the rest of the treatments. Ammonia losses, CO_2 evolved and release of inorganic N in the leachates were statistically analyzed as repeated measures using PROC MIXED in SAS, taking the percent moisture gained or lost from each funnel as a covariable. Inorganic N determined from the final 1 M KCl extractions were analyzed as one-way ANOVA using PROC GLM. All treatment mean comparisons were done based on a set of orthogonal

contrats as follows: T0 vs (T1+T2+T3+T4)/4, T1 vs T2, T3 vs T4, and (T1+T2)/2 vs (T3+T4)/2.

Surface-applied PL volatilized 17 % of its total N while PL amended with acidified biochars lost only 6 to 11 % (Figure 3.7). PC400 performed better than PC600 ($F=20.92$; $p=0.0132$) for reducing NH_3 loss but there was no difference between PH400 and PH600 ($F=2.12$; $p=0.2293$). When PL was incorporated into the soil, the same trends were observed (Figure 3.7). The difference between PC chars may be explained by the lower pH and higher CEC of PC400 compared to that of PC600 (Table 3.6). Volatilization of NH_3 is a highly pH-dependent process. At pH 7, aqueous NH_4^+ could start converting into NH_3 and much more at higher pHs. In this study, the acidified chars had reduced the initial pH of PL from 8.55 to a pH range of 7.16 to 7.65. Similarly, it had brought down the starting pH of the mixture of soil and PL from 6.94 to a pH range of 6.47 to 6.73. However, since these are only initial pH measurements, treatment differences do not necessarily coincide with their trend in reducing the amounts of volatilized NH_3. This is true for PL amended with PH400 versus that with PH600 and also those PL with PCs versus those with PHs particularly under surface incubation.

Aside from lowering the pH of the PL, the chars may have kept the amounts of volatilized NH_3 at lower levels by retaining some of the NH_4^+ on its exchange sites. However, based on the analyzed values their CEC values (Table 3.6), the chars could have only theoretically reduced volatilized NH_3 from poultry litter by 6 to 35%. This is far from the actual reduction which ranges from 36 to 63% that of the unamended PL.

Adding acidified chars to PL depressed CO_2-c evolved under surface incubation ($F=9.24$; $p=0.0083$) by as much as 21% of the unamended PL (Figure 3.8). Conversely, when char-amended PL was mixed with soil, total CO_2-c was greater compared to unamended PL ($F=6.88$; $p=0.0255$) (Figure 3.8) and increased by as much as 37%. Since microorganisms require C to build up tissues, release of respired CO_2-C is also expected to increase. This may have been the reason for the increased CO_2-C released when PL+char mixtures came in good contact with soil under incorporated incubation. However, since chars are known to be relatively refractory against decomposition compared to organic fertilizers (or poultry litter in this case), it is very likely that such a surge of CO_2 evolved may have been largely due to the priming of soil organic carbon by chars. Under incorporated incubation, PL+PC600 and PL+PH600 released more CO_2-C than PL+PC400 ($F=5.86$; $p=0.0360$) and PL+PH600 ($F=6.01$; $p=0.0341$), respectively. Litters amended with PCs were also found to liberate more CO_2-C than those with PHs. This implies that high-temperature chars enhanced microbial activity more than low-temperature chars and that PCs are generally preferred than PHs by the soil microbes.

In terms of N release, surface-applied PL with acidified chars had comparable amounts of inorganic N leached as unamended litter ($F=3.05$; $p=0.1146$) (Figure 3.9) regardless of whether it was on the first or second leaching. For PC-amended litters, s+PL+PC400 had more inorganic N leached than s+PL+PC600 ($F=9.06$; $p=0.0142$). The PC400 reduced NH_3 losses from PL better than PC600. This may have contributed to keeping more of the PL-released NH_4^+ in solution than volatilizing it to

the air. In addition, s+PL+PHs led to greater inorganic N leached compared to s+PL+PCs ($F=6.74$; $p=0.0289$). This could have been due to their difference to cause mineralization of N from PL, soil or combination of both.

Leaching of nitrate was the same for all treatments under surface and mixed incubations (Figures 3.9 and 3.10). Moreover, the amounts of nitrate leached were generally less than that of ammonium particularly during the first leaching. However, extraction of inorganic N at termination of both incubation experiments revealed nitrate dominating over ammonium in exceedingly high amounts (Figure 3.11). Interestingly, under incorporated incubation (Figure 3.11), combining acidified chars with PL had generally greater amounts of inorganic N extracted, mainly in the form of nitrate, than unamended PL ($F=8.47$; $p=0.0173$). In addition, combining PL with PC600 and PH600 had higher amounts of extracted nitrate compared to PL with PC400 ($F=17.35$; $p=0.0024$) and PH400 ($F=28.31$; $p=0.0005$), respectively.

Amending PL with acidified chars reduced NH_3 loss in PL by 63 to 36% with surface incubation and by 60 to 43% under mixed incubation. It also decreased CO_2 evolved from surface-applied PL by as much as 21% but increased it that from incorporated PL by as much as 37%. In terms of nutrient release, it did not affect the release of both leachable and extractable inorganic P from both surface-applied and incorporated poultry litter. Similarly, it did not affect the release of leachable inorganic N from poultry litter under both surface and mixed incubations but yielded greater amounts of inorganic N, primarily in the form of nitrates, extracted from poultry litter under mixed incubation particularly with high-temperature chars. Contrary to the findings from the incubation experiments, the biochars have shown capacity to sorb NH_4-N. However, not a single char were found to sorb any ortho-P at all.

Table 3.6. Selected chemical properties of soil, poultry litter and acidified chars.

Sample	pH	Total C, %	Total P, ug g-1	Total N, ug g-1	CEC, meq 100 g-1
Soil	6.69	2.18	724.20	2027.17	6.44
Poultry litter	8.62	35.33	16237.77	41200.00	-
PC400	2.54	60.77	17.85	1372.00	17.42
PC600	2.63	74.36	109.78	1484.00	3.18
PH400	2.55	62.53	125.95	1835.33	15.74
PH600	2.55	67.78	1293.78	19730.00	5.36

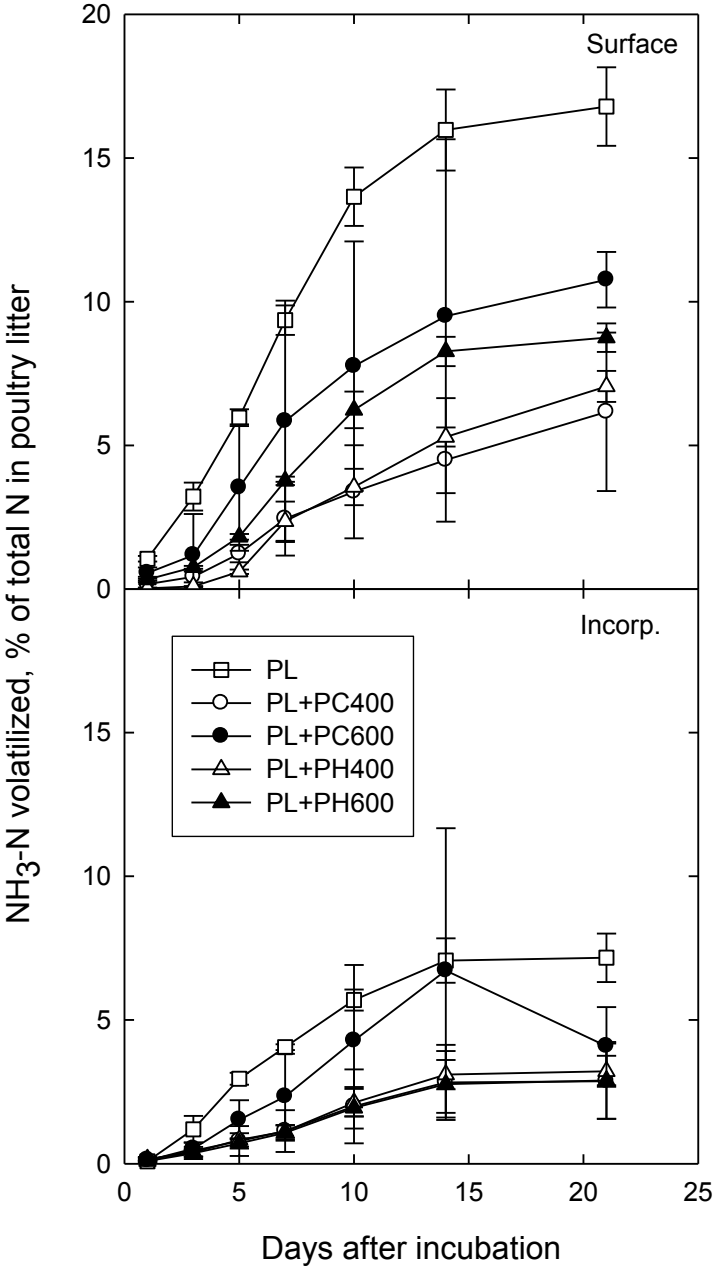

Figure 3.7 Cumulative ammonia nitrogen lost during 21 days incubation of soils and poultry litter with and without acidified chars.

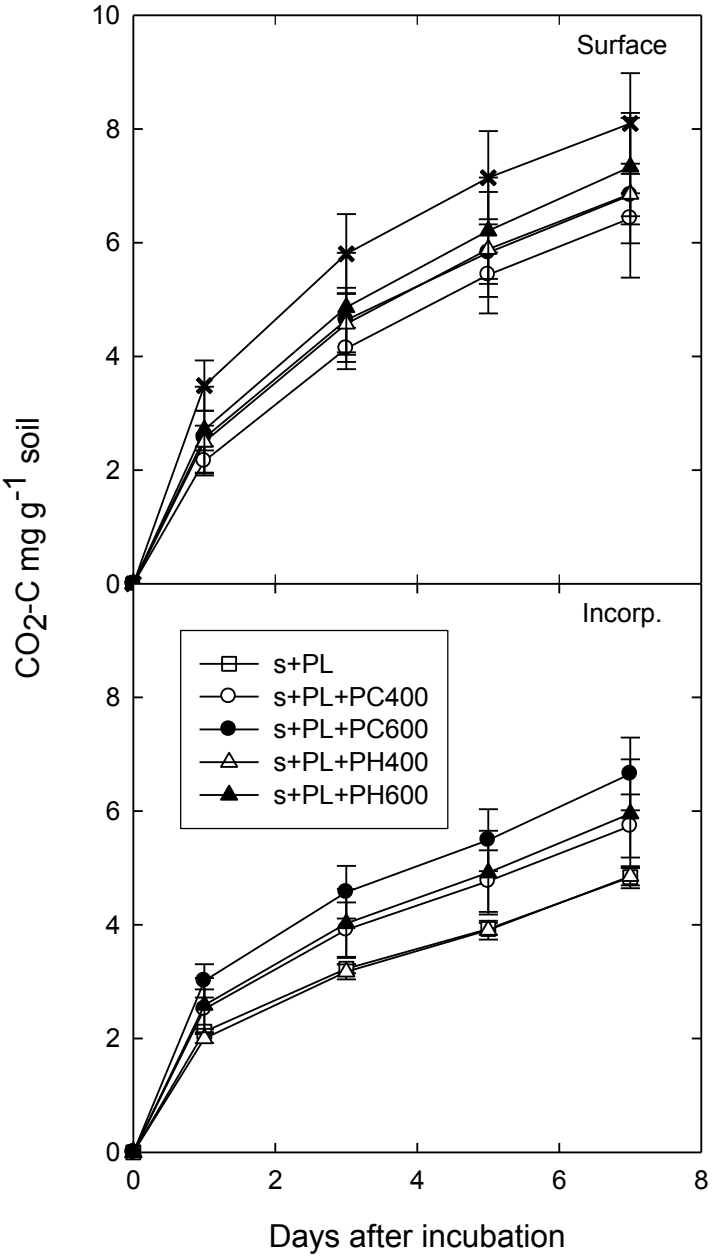

Figure 3.8. Cumulative carbon dioxide lost during 21 days of incubation of soils and poultry litter with or without acidified char.

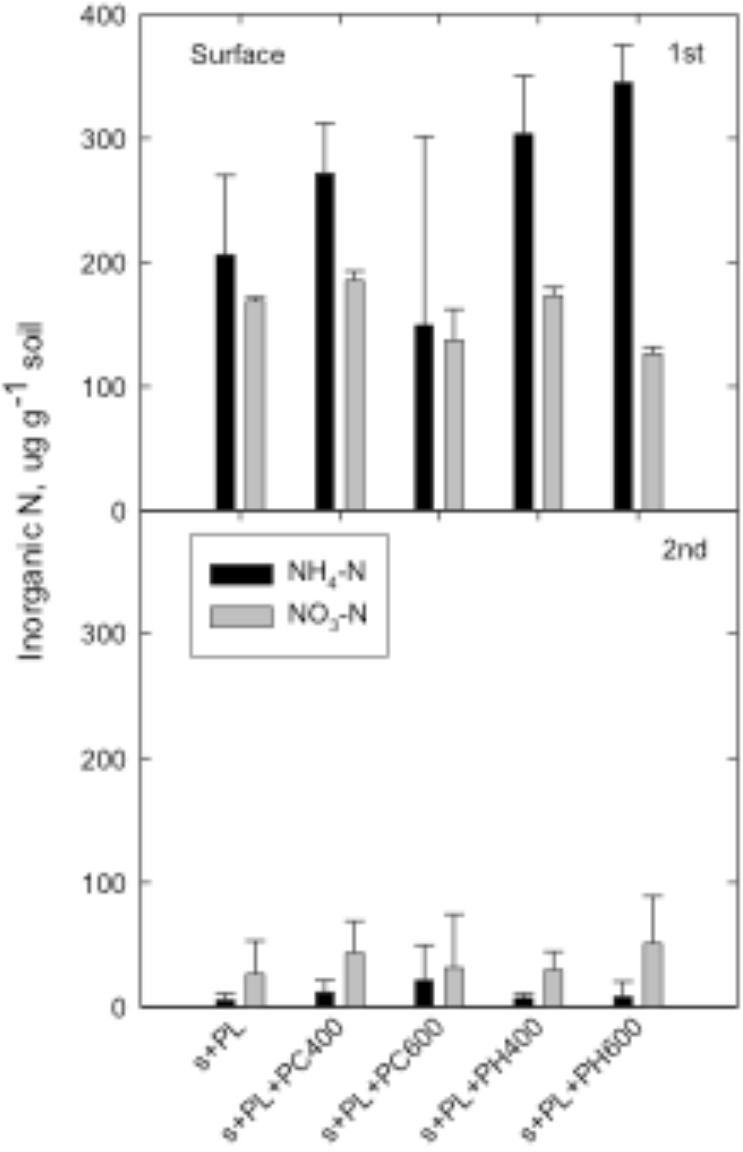

Figure 3.9. Inorganic nitrogen leached from soil and surface applied poultry litter with or without acidified char during the first or second leaching.

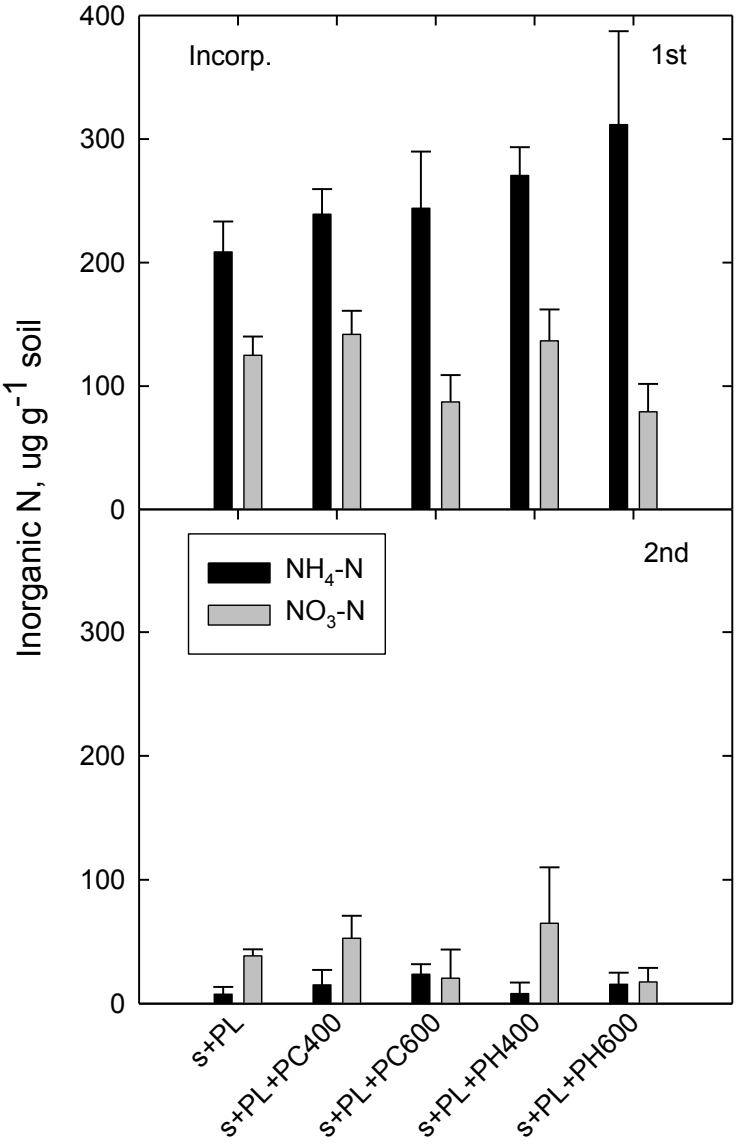

Figure 3.10. Inorganic nitrogen leached from soil and incorporated poultry litter with or without acidified char during the first or second leaching.

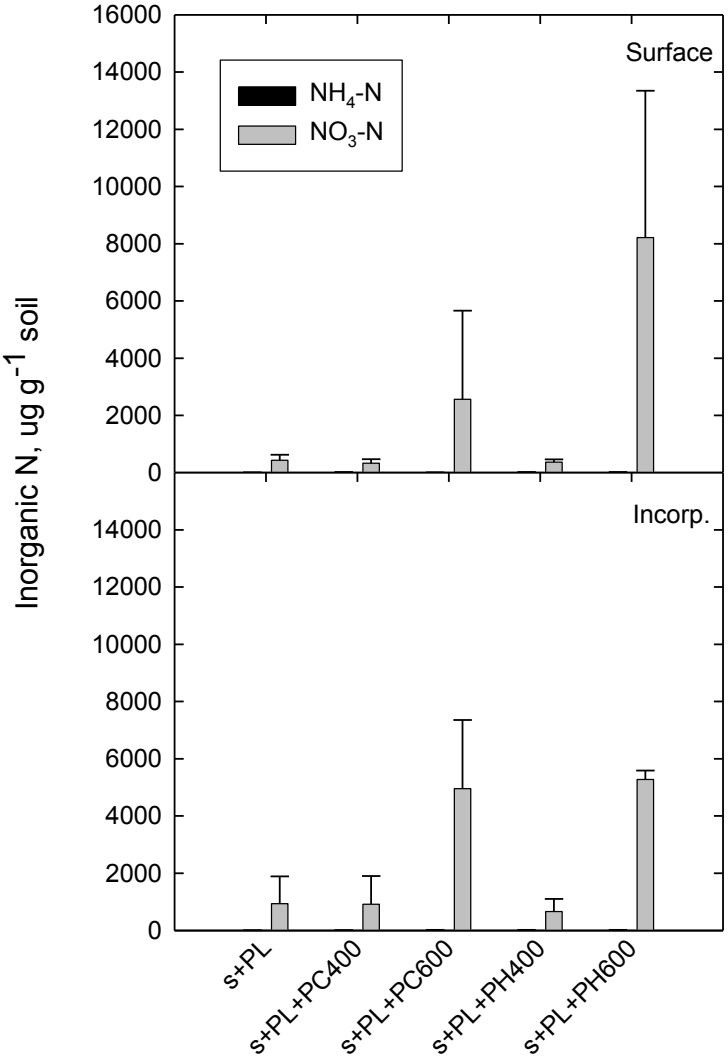

Figure 3.11. Inorganic nitrogen extracted from soil and poultry litter with or without acidified char when surface applied or incorporated.

Milestone 1: Char adsorption tests were completed and it was identified that chars do reduce ammonia releases. Higher performing treatments produced reductions by 60 and 63% which was above our minimum target of 50% above controls.

Task 4.0 Develop Atomic layer epitaxy for fuel cell technology.

The overall goal in this task was to develop methods for deposition of catalytic metals using atomic layer control, a process that has been developed at the University of Georgia and is in further development. The focus will be on controlling the atomic level proximity of metals such as Pt, Ru, Rh, Os, and Pd to create improved catalysts.

Subtask 4.1 Development of metal nanofilms

Methodology and results described and summarized below have independently been reported in the following publications:

1. *Kim, Y-G., J.Y. Kim, D. Vairavapandian, and J.L. Stickney. 2006. J. Phys. Chem. B. 110, 17998-18006.*
2. *Vairavapandian, D. 2009. Formation of platinum thin films by electrochemical ALD and 2nd network of carbon nanotubes for electrochemical applications. PhD Dissertation, The University of Georgia, Department of Chemistry.*

Metal films are important in catalysis, electronics, magnetic data storage, MEMS (Micro Electro Mechanical Systems), and nanodevice construction. Electrodeposition provides a simple, cost effective, room temperature process for their growth. Atomic level control would be an important advantage in the growth of metal films. However, most electrodeposition of metal films results in 3-D growth and surface roughening, the result of nucleation and growth as a deposition mechanism. Interlayer transport of deposited atoms must be rapid to prevent 3D growth. In DMG and SMG, they used either co-deposition of the metal of interest with a reversibly deposited metal or predeposited sub-monolayer of a surfactant metal on top of depositing metal (to make the interlayer transport faster).

Growth of epitaxial films of noble metals like platinum has proven even more difficult to deposit layer by layer because of cluster formation, the result of their high cohesive energy. Others have shown that it is possible to achieve quasi-2-D layer by layer, growth of platinum on Au, by electrochemical reduction of $PtCl_6^{2-}$ complexes. It is known from the literature that atomic level control in the formation of platinum films by using a predeposited Cu UPD layer as a sacrificial layer to subsequently be exchanged for a Pt atomic layer is possible. Copper UPD formed on Au (111) was exchanged for Pt, in a platinum ion solution, at open circuit. This process is referred to as Surface Limited Redox Replacement (SLRR). Subsequent studies have shown that the SLRR can be repeated any number of times, essentially using it in an electrochemical atomic layer deposition (ALD) cycle. Electrochemical ALD cycles have been previously developed for the growth of a number of compound semiconductors. The intent of our work was to report on the formation of platinum nanofilms, by employing SLRR an electrochemical ALD cycle, using Flow cell. In these studies Pb UPD was used as the sacrificial layers.

Experimental methods

Figure 4.1 shows the experimental setup employed in the formation of platinum thin films. It consisted of standard peristaltic pumps (Cole Parmer) and solenoid actuated Teflon valves for solution selection. In order to avoid oxygen problems,

solutions were extensively purged with nitrogen gas. Also, since most tubing is permeable to oxygen, solution delivery tubes along with the valves and solution reservoirs were placed inside a nitrogen purged Plexiglas box. The flow cell consisted of a planar substrate held away from a counter electrode by a 1 mm thick silicone rubber gasket. The deposition area was 3 cm^2. Glass microscope slides coated with 5 nm of titanium, as an adhesion layer, and 300 nm of Au, deposited by vapor deposition, were used as substrates. The glass slides were initially etched in 15% HF for 60 seconds and then rinsed with ultra pure water prior to insertion in the vapor deposition chamber. These substrates were annealed at 400°C for 12 h after deposition. Gold wire was used as the counter electrode and a Ag/AgCl was used as reference electrode. All potentials are reported with respect to this reference electrode. Solutions used include 1mM potassium tetrachloroplatinate in 50mM perchloric acid, 1mM lead perchlorate in 50mM perchloric acid, 50mM sulphuric acid and 1mM potassium iodide in 50mM perchloric acid.

The electrochemical ALD cycle consisted of the following steps: Pb solution pumped through the cell at the open circuit potential (OCP) for 5 seconds (40 ml/min flow rate), at which point the solution was held static in the cell at the chosen deposition potential for 10 sec. The Pt ion solution was then pumped through the cell for 20 sec, at OCP, and then held static in the cell for 3 min, to allow for the replacement. Rinsing with a blank solution of sulfuric acid completed the cycle. The above steps constitute one ALD cycle. The Pb UPD resulted in a coverage of 0.67 monolayer (ML), defined with respect to the number of Au surface atoms on the substrate. Ideally, 100% of the electrons in the Pb would end up in Pt atoms on the surface, or a Pt coverage of 0.67 ML every cycle, as Pt(II) ions were used. As Pb UPD is formed on both gold and platinum, this process can be repeated any number of times to obtain platinum films of desired thickness.

Results and discussions

Pb deposition potentials were determined from Pb cyclic voltammetry on Au. Various deposition potentials from -0.3 to -0.4 V were investigated. Then Pb UPD was replaced using either Pt (II) or Pt (IV) ion solutions.

$$Pb_{UPD} + Pt^{2+} \longrightarrow Pb^{2+} + Pt$$

$$2\,Pb_{UPD} + Pt^{4+} \longrightarrow 2\,Pb^{2+} + Pt$$

The change in OCP was monitored during the exchange, providing an idea of how much time was required for the exchange. The OCP changed from the potential used for Pb deposition, positive to one corresponding to a Pt surface, generally above 0.6V within three minutes, as shown in Figure 4.2. No Pb was expected to be present on the surface at such positive potentials, as based on Pb voltammetry on Au, under those conditions. EPMA was used to determine the deposit composition (Table 4.1) and negligible amounts of lead were present in the platinum films. The films appeared essentially uniform, except for near the flow cell entrance, where the Pt percentage was a little higher. Exchange was observed to be faster (taking about 1 minute) if the Pt solution was constantly flowed during the exchange, at a flow rate of 6 mL/min.

The amount of Pb deposited tended to increase from cycle to cycle. For example, the deposition charge obtained when Pb was deposited at -0.3V (Figure 4.3) indicates an increase in coverage/cycle from 0.7 ML to 3 ML after 30 cycles. This increase in the Pb UPD charge from cycle to cycle was felt to be an indication of an increase in deposit surface area. The Pt surface appeared to roughen, suggesting the growth was not exclusively layer-by-layer. Similar observations are reported in the literature when copper UPD was used as the sacrificial layers. It is known that lead UPD has a tendency to roughen gold surfaces. Roughening of the Au substrate would help explain the increase in surface area for the initial few cycles, but the surface area increased progressively, even after 10 deposition cycles. The high cohesive energy between platinum atoms also contributes to this increased roughening and cluster formation. Cluster formation is evident in the AFM images displayed in Figure 4.4.

In an electrochemical ALD cycle for the formation of a compound semiconductor nanofilm, UPD of one element takes place only on an atomic layer of the other element, forcing layer by layer growth. However, in the present case, the sacrificial Pb UPD layer does for a single complete atomic layer, but during the SLRR, it is not necessary that Pt atoms replace Pb atoms one for one. That is, the electrons from one Pb atom may result in the deposition of a Pt atom at a different spot on the surface, thus accounting for the increase in surface roughness with each cycle.

In order to combat cluster formation, electrochemical annealing (EA), adsorption of iodine atoms has been attempted. EA refers to the tendency of metal surfaces in solution to become smoother with time, dependant on potential, time and the presence of adsorbates. Halides, such as iodide, appear to promote this behavior by increasing surface mobility. Iodine atom layers, however, do not prevent metal deposition. So lead can be deposited on iodine coated platinum or gold. In order to investigate this issue, one more step was added to the electrochemical ALD cycle used for forming platinum films, by rinsing with a solution of KI. The KI solution was passed through the cell after every replacement cycle for 5 sec, and held in the cell for 15 sec. Iodide seemed to make the Pb deposition more difficult. In other words, the presence of an atomic layer of iodine atoms on the surface reduced the amount of lead that was deposited at a given UPD potential. In this work, the presences of the iodine adlayer did not significantly change the tendency for the surface to roughen, at least under the present conditions, the charge for Pb UPD still increased cycle to cycle. For example when Pb was deposited at -0.3 V, the charge increased from 0.4 ML in the first cycle to 3.7ML after the 25^{th} cycle.

Conclusion

Initial studies show that the SLRR Reaction can be used to make platinum films of a desired thickness using the electrochemical flow deposition system. When Pb UPD was used as the sacrificial layer, some 3D growth was encountered. Though atomic level control was achieved, further improvements are needed to obtain real layer-by-layer, 2-D, growth of Pt nanofilms. Use of an iodine adlayer did not appear to improve the surface morphology in the present case.

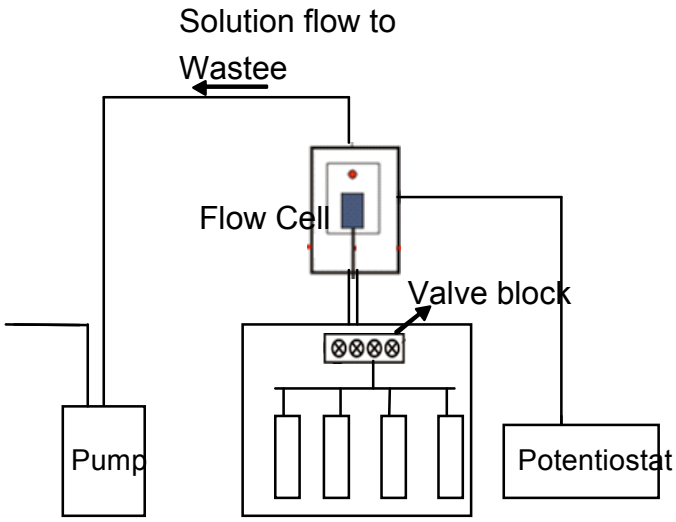

Figure 4.1. Experimental set up used for making Platinum films. Solution bottles and valve are held inside nitrogen purged Plexiglas box. Solutions are sucked through the flow cell and can be changed using different valves.

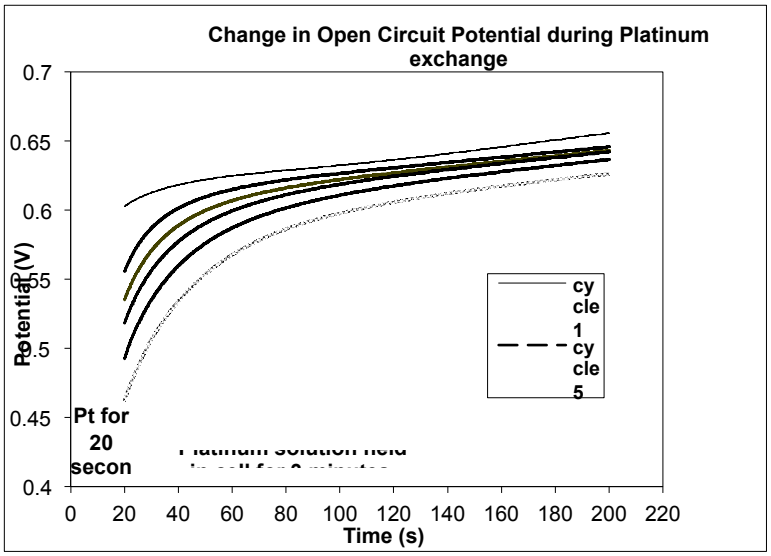

Figure 4.2 shows the change in open circuit potential during Platinum exchange; every fifth cycle .Lead was deposited at -0.3 V for 10 seconds. Platinum solution was flowed for 20 seconds at OCP and then held in cell for 3 minutes during which the OCP was monitored.

Table 4.1. Electron Probe Microanalysis result of the platinum film formed by SLRR Reaction

No.	Pb deposition Potential (V)	Pt atomic%	Pb Atomic %
1.	- 0.36	99.50	2.8
2.	- 0.34	99.95	0.5
3.	- 0.30	100	0

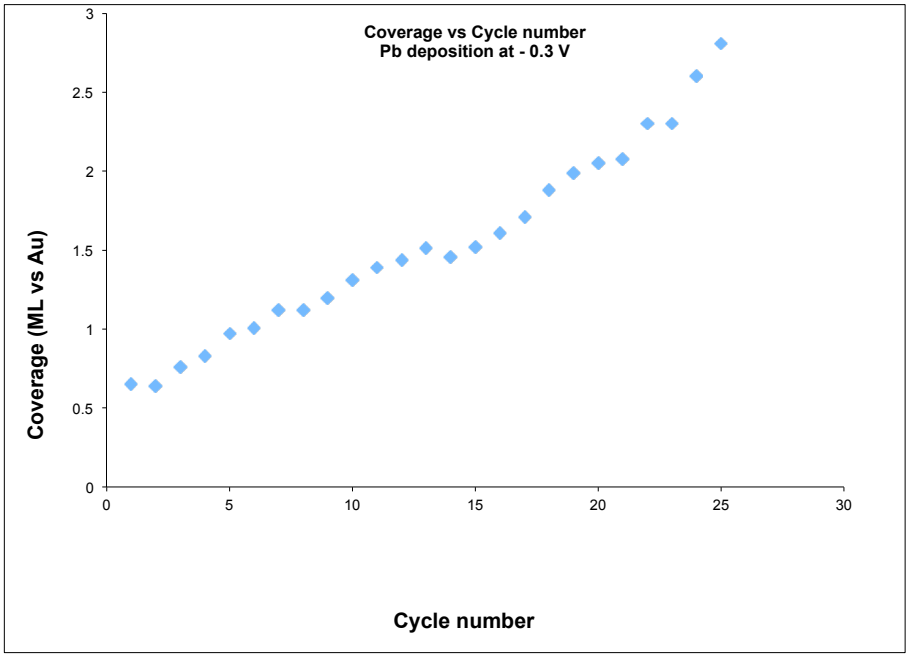

Figure 4.3. Amount of Pb deposited at -0.3 V increased from cycle to cycle indicating increase in surface area.

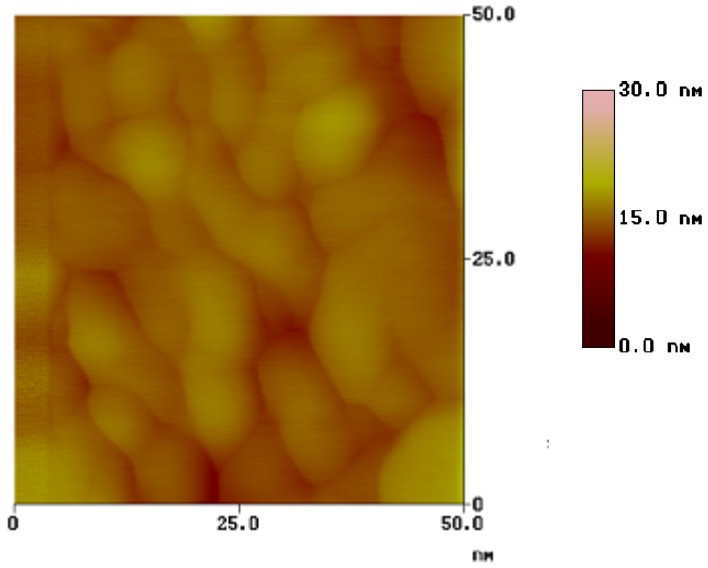

Gold on glass

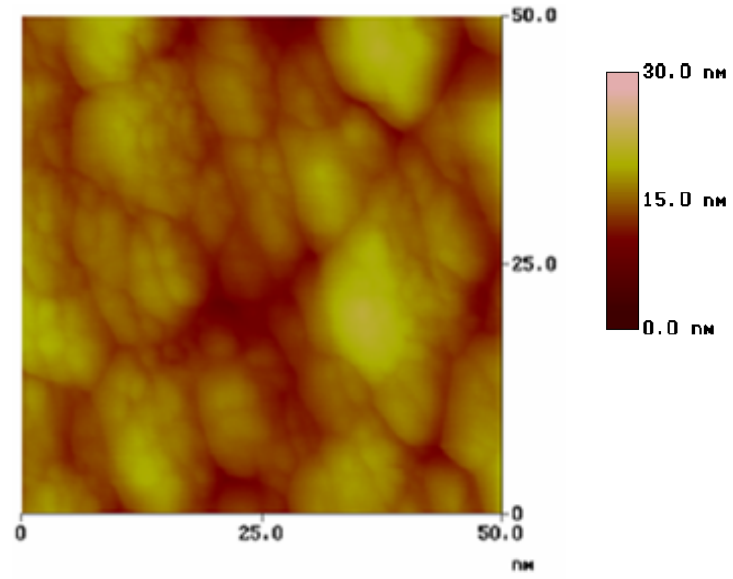

Figure 4.4. Pt film formed by redox replacement of lead deposited at -0.4 V. Clusters suggest the surface is roughening.

Subtask 4.2: Formation of catalytic nanoclusters on carbon substrates

Methodology and results described and summarized below have independently been reported in the following publications:

1. *Kim,J.Y., Kim, Y-G, and J.L. Stickney. 2006. Studies of Cu atomic layer replacement, formed by underpotential deposits, to form Pt nanofilms using electrochemical atomic layer epitaxy. ECS Transactions, 1(3):41-48.*

In the present study iodine atomic layers were used to improve surface mobility of deposited Pt atoms. In previous studies by Adzic (2), Pt atoms deposited using the SLR3 resulted in a surface composed of nanoclusters. The intent here is to promote electrochemical annealing, where the surface atoms increase in mobility by complexing with the halide atoms, and using potentials close to the oxidation potential.

Detailed descriptions of methods are provided in the reference cited above. In brief, the system consisted of a cryopump and ion pump attached to the main chamber. Sorption pumping was used for roughing and Ar ion bombardment was used to clean the Au(111) substrate, and a tungsten wire, used to mount the crystal, was also used for annealing the sample, by passing a current. Electrochemical experiments were performed in the antechamber attached to the main chamber via a gate valve, and solutions were passed to the electrochemical cell and drained to the waste bottle through Teflon tubes. Deposits were transferred to and from the analysis chamber without exposure to air, where they were characterized by AES (Perkin-Elmer) and LEED.

Experimental methods

Ion bombardment was performed by first filling the chamber, with the pumps off, to 10-5 Torr with ultrahigh pure Ar. Ar atoms were then ionized by electron bombardment, and accelerated towards the crystal with an energy of 200 eV. The Ar ions sputtered the Au substrate, removing the last traces of impurities. However, the surface during ion bombardment became roughened, requiring annealing at ~350 ºC, before the clean surface LEED pattern was resolved. A solution of 1 mM $CuSO_4$ and 0.05 M H_2SO_4 was prepared with anhydrous $CuSO_4$ and concentrated H_2SO_4 (Aldrich Co.) in 18 MΩ-cm distilled water. After cleaning the Au substrate, confirming surface cleanliness and order via AES and LEED, the sample was transferred to the ante-chamber. The Au substrate was then modified with an atomic layer of I atoms by exposure to a solution of 0.1 mM KI, and then rinsed in blank solution (1 mM $HClO_4$ solution). The electrochemical cell was then rinsed twice with the Cu solution, and the Au substrate was immersed in the Cu solution at the open circuit. The potential was then scanned negatively from the open circuit potential (OCP) to just after the second Cu UPD peak, where the potential was held, while the sample was emersed (withdrawn) from solution. The resulting I modified Au substrate, with Cu UPD, was then transferred to the analysis chamber. From cyclic voltammetry, the presence of Cu UPD was evident at 0.05 V, which was confirmed with AES and LEED. The resulting deposit was then transferred back, and immersed in the Pt(IV) solution for two minutes at open circuit, where a final OCP of 0.75 V was observed.

The Pt(IV) solution was prepared with H_2PtCl_6 (Fisher Scientific Co.) and $HClO_4$ (Aldrich Co.) in 18 MΩ-cm distilled water.

Results and Conclusions

Detailed results are presented in published manuscripts cited above and related journal articles. In brief, the Au substrate was modified with an I-atom layer, and Cu UPD was formed. This surface was then exposed to a Pt(IV) solution at the open circuit, where the Cu UPD was exchanged for Pt over two minutes. The OCP during the Pt replacement shifted from 0.05 V to 0.75 V. CV in the blank solution after four Pt replacements on Au showed the oxidation of adsorbed I, and the formation of Au and Pt oxides. On the subsequent negative going scan, separate peaks for reduction of Au and Pt oxides were observed. After removal of the I-atom layer by oxidation, hydrogen waves were also observed. Estimation of the Pt coverage, from the Pt reduction peak in the CV suggests that about 0.35 ML of Pt were deposited in each cycle; however, this was just a preliminary study, and 0.35 is a crude approximation.

Studies to better characterize these amounts are underway. The intensity of the I Auger peak suggested that I remained on top of the deposited Pt. While the LEED pattern of the I modified Au showed a (√3°—√3)R30°-I, the LEED patterns after two and four Pt replacement cycles showed diffuse (√3°—√3)R30° and (1 X 1) patterns, respectively.

Subtask 4.3: Testing of produced films/electrode materials

Methodology and results described and summarized below have independently been reported in the following publications:

1. *Kim, Y-G, J.Y. Kim, C. Thambidurai, and J.L. Stickney. 2007. Pb deposition on I coated Au (111), UHV-EC and EC-STM studies. Langmuir, 23, 2539-2545.*

Atomic layer deposited materials were developed and studied using in-situ STM with an electrochemical flow cell, and UHV surface analysis combined directly with electrochemical reactions (UHV-EC). These studies were performed in an in-situ STM flow cell deposition system reported in the literature and using UHV-EC methods. UHV-EC refers to studies where ultra high vacuum (UHV) surface analysis techniques (low energy electron diffraction (LEED) and Auger electron spectroscopy, for instance) are combined directly with electrochemical experiments. In this way, well-defined electrodes were created and characterized in the UHV surface analysis chamber, and transferred to and from the electrochemical cell without exposure to air, in ultra high purity gases.

Here, we describe the Cu nanofilms development using a SLRR in an electrochemical ALD cycle, formation of Pb UPD as a sacrificial atomic layer on the I coated Au(111) substrate. The structures formed on I atom covered Au(111) by Pb UPD are described below. The next step in the cycle would be replacement of the Pb UPD layer at open circuit by the desired element.

Experimental methods

Brief experimental methods are reported here, a detailed methodology can be obtained from the reference cited above. For *in situ* scanning tunneling microscopy experiments (EC-STM), Au single-crystal surfaces were prepared using a variation of the Clavilier method. In both the EC-STM and voltammetry measurements, the supporting electrolyte consisted of 0.1 *M* $HClO_4$ or 0.05 *M* H_2SO_4 prepared from doubly-distilled $HClO_4$ and H_2SO_4 and Milli-Q Plus™ water. Ultrapure-grade $Pb(ClO_4)_2$ and $CuSO_4$ were used. The three-electrode cell included a Au-wire auxiliary electrode and a 3 *M* KCl Ag/AgCl reference electrode (BAS), to which all potentials were reported. EC-STM experiments were performed with a Nanoscope III equipped with W tips, electrochemically etched (15 VAC in 1 *M* KOH) from 0.25-mm wires. The tips were coated with transparent nail polish to minimize Faradaic currents. LEED and Auger electron spectroscopy (AES) optics were contained in the UHV system. This UHV system was equipped to allow sequential electrochemical and surface analytical measurements.

Results and Discussion

Cyclic voltammograms for Pb UPD on a bare Au(111) and an I coated Au(111) single crystal did not reflect pure (111) behavior. Prior to each experiment, the single-crystal was ion bombarded and annealed in UHV, resulting in the (1X1) LEED pattern expected, and an Auger spectrum showing only peaks assignable to Au. This crystal was then immersed into a 1 m*M* KI solution for 30 seconds, and upon emersion (withdrawing) from solution, it displayed a $(\sqrt{3}\times\sqrt{3})R30^{o}$-I pattern (data not shown), and the characteristic I doublet near 500 eV with Auger. The structure responsible for this LEED pattern was composed of 1/3 ML of I atom, as the I^- ions oxidized upon adsorption. One monolayer (ML) of an adsorbate is equivalent to the number of Au surface atoms.

The I coated crystal was then immersed in 0.2 mM Pb^{+2}, and scanned negative to the onset of bulk Pb deposition and back. There were two major peaks, evident in the deposition scan, with a broad hump at higher potentials. This voltammetry, for the bare and I coated Au(111), was essentially identical to that reported previously in the literature for these surfaces in a Pb^{2+} solution. That the two reduction peaks, at −0.2 and −0.3 V, are associated with the formation of two different Pb UPD structures would be a good initial assumption.

Electrochemical and in-situ SPM characterization of Pb UPD on gold has been extensively reported. However, studies in the literature have not decribed the atomic level structures formed by Pb UPD on an I coated Au(111) electrode. For the present in-situ STM studies, after formation of the Au(111)$(\sqrt{3}\times\sqrt{3})R30^{o}$-I structure, a 0.2 m*M* Pb solution containing no I^- was injected into the EC-STM flow cell and the resulting surface was imaged within three minutes. At potentials lower than −0.20 V, a dramatic change from the $(\sqrt{3}\times\sqrt{3})R30^{o}$-I adlayer structure was observed. A wide atomically-flat terrace, supporting a close-packed adsorbed layer, was evident in our results (data not shown). Domain boundaries were clearly visible, each consisting of well-ordered rectangular lattices rotated by 60^{o} or 120°.

To investigate the Pb and I atom configurations in the deposit, and their orientation with respect to the Au(111) surface, EC-STM experiments were performed using increased tunneling currents in an attempt to image the underlying Pb UPD layer. Increasing the current from 20 to 30 nA resulted in an image where the bright spots had shrunk and shifted. Possible reasons for the change in the image include accessing other states, such as those in atoms below the I-layer. Alternatively, the tip may have been lowered into the I atom layer and was moving the I atoms around, allowing imaging of the underlying Pb. Our results seem to indicate that I-atoms were set in four fold Pb atom sites in the (2×√3)-*rect* lattice, suggesting a kind of checkerboard structure.

Our work suggests that for low Pb coverage defects, defects were almost random, and the lines of defects were oriented at an angle to both the substrate atomic rows, and the √3-direction. In deposits with a slightly high Pb coverage, above ¼ ML the defect lines were oriented in the √3-direction, pointing out the possibility of a different origin for defects in the two sets of images.

A greater description of results and interpretations and discussions are provided in the reference cited above.

Conclusions

It was initially expected that the Pb atoms would deposit under the I-atom layer, the I-atoms floating on top and promoting electrochemical annealing. For deposits at potentials as negative as −0.25 V this configuration did exist. The structure formed was a (2×√3)-*rect* lattice, consisting of one Pb and one I atom for each unit cell. The unit cell also contained four Au atoms for Pb and I coverages of ¼ ML. This required loss of I atoms from the initial 1/3 ML from the (√3X√3)R30^{o}-I surface. By increasing the tunneling current it was possible to image the underlying Pb atoms as well as the top layer of I atoms. The (2×√3)-*rect* lattice was composed of I atoms in four fold rectangular sites in the Pb atom layer.

Some defects were evident in the (2×√3)-*rect* lattice, the result of missing Pb atoms, replaced by I atoms. As the potential was shifted more negatively, down to −0.3 V, the Pb coverage increased, and the number of defects increased. In this case the defects were the result of loss of adsorbed I atoms, as the Pb coverage increased. These defects initially manifest as a network of darker lines in the (2×√3)-*rect* structure. Finally, with further increases in the Pb coverage, all I atoms left the surface, leaving a full monolayer of Pb, and a Moiré pattern was formed. This work shows the absences of a strong interaction between I atoms and the Pb surface. As Au sites on the surface were covered up with Pb atoms, I atoms were lost from the surface, finally resulting in the close packed Pb monolayer.

Task 5.0 Develop fermentation based conversion of biomass to fuels and products.

An investigation was done of Tifton Bermuda grass grown in Georgia and the Southeast Region. The task involved obtaining sugars via extraction combined with hydrolysis, followed by development of methods for simultaneous use of multiple sugars.

Subtask 5.1: Extraction of sugars from lignocellulose/ hydrolysis evaluations

The goal was to generate sugars from lignocellulosics to be used for further fermentation for ethanol production. The work overlapped with Task 2.1A, and methods and results are described in complete detail in that section earlier in this report.

Subtask 5.2: Organism selection/engineering – simultaneous use of C5 and C6 and toxin tolerance

The efficient and simultaneous conversion of pentoses and hexoses is a significant hurdle to the economic utilization of biomass hydrolysates. The formation of any fermentation products (ethanol, butanol, succinic acid, lactic acid, pyruvic acid, etc.) from sugar mixtures would be greatly enhanced by designing a process that uses both types of sugars effectively. We have begun work towards demonstrating that the simultaneous consumption of sugar mixtures is feasible using a consortium of organisms that are each "designed" to consume only one sugar. By using this collection of organisms simultaneously, each organism is able to transform the particular sugar into the desired fuel or biochemical product without interference from other organisms. The technology was demonstrated using *Escherichia coli* an organism commonly used in industrial production.

Identification of an E. coli strain that has very fast growth rates

The initial working hypothesis was that various strains of *E. coli* would should vastly different abilities to consume the individual sugars principally found in lignocellulosic hydrolysate: D-(+)-glucose, D-(+)-xylose, L-(+)-arabinose, D-(+)-galactose, D-(+)-mannose. A comparison of specific growth rates was completed by first growing cells at 37°C with agitation of 250 rpm (19 mm pitch) in 250 mL shake flasks containing 30 mL basal medium with 5 g/L of a single sugar. When the OD of this culture reached approximately 1, 5 mL was transferred to a second shake flask containing 45 mL basal medium with 5 g/L of a single sugar from which optical density was measured at 0.5 – 1.0 h intervals to determine growth rates.

The basal medium used in all experiments contained (per L): 13.3 g KH_2PO_4, 4.0 g $(NH_4)_2HPO_4$, 1.2 g $MgSO_4 \cdot 7H_2O$, 13.0 mg $Zn(CH_3COO)_2 \cdot 2H_2O$, 1.5 mg $CuCl_2 \cdot 2H_2O$, 15.0 mg $MnCl_2 \cdot 4H_2O$, 2.5 mg $CoCl_2 \cdot 6H_2O$, 3.0 mg H_3BO_3, 2.5 mg $Na_2MoO_4 \cdot 2H_2O$, 100 mg Fe(III)citrate, 8.4 mg $Na_2EDTA \cdot 2H_2O$, 1.7 g citric acid, 4.5 mg thiamine·HCl, and 5 g sugars (D-(+)-glucose, D-(+)-xylose, L-(+)-arabinose, D-(+)-galactose, D-(+)-mannose). The OD measured at 600 nm using a Beckman DU-650 spectrophotometer to monitor cell growth.

Seven different *E. coli* strains were used to compare their growth rates on each of the five monosaccharides found in lignocellulosic hydrolysates. Generally K-12

derivatives *E. coli* MC4100 and MG1655 showed lower growth rates on monosaccharides than strains W, C and B (Table 5.1). *E. coli* W showed the highest growth rate on glucose or arabinose, while ATCC8739 (C strain) was the fastest growing strain on xylose. In general, this C strain and W were both 'fast growing', and therefore these strains were selected for detailed study. We were surprised that the well-characterized *E. coli* strain MG1655 performed poorly.

Table 5.1. Specific growth rates (h^{-1}) of *E. coli* strains on different carbon sources.

Substrate	W	B	C ATCC8739	C ATCC13706	C CGSC3121	MC4100	MG1655
D-Xylose	0.84	0.78	0.89	0.78	0.73	0.72	0.55
D-Glucose	1.00	0.97	0.96	0.85	0.73	0.88	0.72
L-Arabinose	0.94	0.86	0.93	0.80	0.75	0.67	0.68
D-Mannose	0.46	0.33	0.46	0.51	0.44	0.45	0.26
D-Galactose	0.66	0.79	0.75	0.45	0.25	0.83	0.33

Conclusion and next step

Based on this work, we have compared and identified a preferred species for further studies based only on the growth rate.

Subtask 5.3: Pro forma analysis of successful methods

Modification of plan: Our plan at the time of writing the proposal was to evaluate several pathways and identify preferred methods that could be further studied at larger scale in order to determine preliminary economics through a pro forma analysis. However, the extent of work completed here does not justify pursuit of realistic economic analysis, therefore this subtask was not pursued any further.

Task 6.0 Develop biomass production technologies (e.g. algae).

In this task, our goal was to develop an understanding of algal strains that are robust and can be grown to yield high amounts of lipids using nutrients from waste streams.

Subtask 6.1: Development of algae cultivation methods

Our work encompassed the study of various strains that were grown on standard cultures and municipal wastewaters from an area of the state that was dominant in industrial operations. The municipality's wastewater treatment facility estimated that approximately 85% of the wastewater treated was derived from carpet manufacturing operations that had undergone onsite pretreatment. The remainder 15% was common municipal wastewater.

Methodology and results described and summarized below have independently been reported in the following publications:

1. *Chinnasamy, S., A. Bhatnagar, R.W. Hunt, and K.C. Das. 2010. Microalgal cultivation in a wastewater dominated by carpet mill effluent for biofuel production. Bioresource Technology, 101, 3097-3101.*

Procedures

Wastewaters were collected from treatment plant processing 110-150 million L/d of wastewater. Because of the use of process chemicals in the industrial operations, the wastewater had slightly higher phosphorus (P) levels than typical and this was the opportunity. Algae use large amounts of P for its growth and are known to respond well to waters that have higher then usual P levels. Wastewater samples were collected during different seasons and identification of algal taxa and biovolume assay were carried out using standard protocols reported in the literature.

Briefly, samples were subjected to the blooming process by incubating the samples in a growth chamber at 25±1^{o}C and an irradiance of 75-80 µmol photons/m^{2}/s. Untreated and treated wastewater samples and soil samples collected from the wastewater land application sites were used as the sources for isolating native algal strains. Standard growth media (BG11) was used as the enrichment and isolation medium. Algae were isolated by serial dilution technique. One mL of the culture from bottles showing algal growth in highest dilution bottles was spread plated on BG11 agar plates. The plates were incubated for 2 weeks and after the colony formation, isolated single colonies were picked up and maintained on the BG11 agar slants.

Preliminary screening

Thirteen microalgal strains (Table 6.1) and a consortium of wastewater isolates, were screened for their growth response in terms of chlorophyll *a* content. A consortium of native algal isolates was prepared by mixing equal quantities of 15 wastewater isolates with a biomass concentration of ~ 0.1 g/L each. Preliminary experiments were conducted in test tubes containing 15 mL of filtered and sterilized treated and untreated wastewater as growth medium with standard algal growth medium as control. Incubation conditions were the same as mentioned earlier. Based on the preliminary screening, two freshwater and two marine forms and the consortium were selected for a time-scale batch study to evaluate their biomass and lipid production potential in the wastewaters (treated and untreated wastewater) in comparison with standard growth medium.

Analytical testing and biodiesel production from consortium

After harvesting 10 mL of homogenized algal cells by centrifugation (5000 rpm, 10 min), the algal pellet was exhaustively extracted with hot methanol until it was colourless. Chlorophyll (chl) *a* concentration was spectrophotometrically determined with the extinction coefficients in methanol and calculated. To determine biomass, 4.7 cm Whatman GF/C glass fibre filters were dried at 90 ^{o}C for 4 h, vacuum desiccated to cool to room temperature and weighed. Biomass was determined by filtering 10 mL of culture which was passed through these preweighed filters, washed

with 10 mL of 0.65 M ammonium formate solution to remove excess salts and dried and weighed as above. Lipid content was measured gravimetrically with Ankom XT10 automated extraction system using hexane as solvent.

Nutrient Analysis was done by the University of Georgia's Stable Isotope/Soil Biology Lab and Soil, Plant and Water Lab using the automated cadmium reduction method, ascorbic acid reduction method and the phenate method for the determination of nitrate, phosphate and ammonium, respectively. Total nitrogen and total phosphorus were determined using the persulfate method that employs simultaneous digestion of nitrogen and phosphorus components. Analysis of other parameters for wastewater was done as per the standard procedures prescribed by APHA-AWA-WEF.

Results and Discussion

Treated and untreated wastewaters received from the utility were periodically analyzed for physico-chemical characteristics to monitor the change in nutrient concentration throughout the year. Biochemical Oxygen Demand (BOD), Chemical Oxygen Demand (COD), Total Suspended Solids (TSS), Total Dissolved Solids (TDS), Total Volatile Solids (TVS), Total Solids (TS) and Total Kjeldahl Nitrogen (TKN) showed remarkable reduction in the treated wastewater (Table 6.2).

Amounts of P appeared sufficient to support algal growth in both untreated as well as treated wastewaters. It is known that for a medium with balanced supply of N and P, an optimal mass ratio of C: N: P 46.1: 7.7: 1 would be required for benthic microalgae, which is slightly higher than the Redfiled ratio (41.1: 7.2:1). In our work, both untreated and treated wastewater used in this experiment showed an N: P ratio of 4.06: 1 and 0.83: 1 which indicated N limitation (Table 2). Total nitrogen was found to be less in treated wastewater but appeared sufficient (32.6-45.9 mg L^{-1}) to support the growth of microalgae in untreated wastewater (Table 6.2).

Diversity and community composition of microalgae in carpet industry wastewater

The microalgal community of wastewater treatment systems primarily treating industrial wastewaters are continuously exposed to pollutants. There is little data available on the structure and seasonal variation of microalgal community in wastewater, which indicates their robustness. The composition of algal communities was assessed in the target wastewaters for all 4 seasons. About 27 species of green algae, 20 species of cyanobacteria and 8 species of diatoms were observed in both treated and untreated wastewaters (Table 6.3). Green algae dominated untreated wastewater in all seasons and treated wastewater during cooler weather. In contrast, cyanobacteria dominated treated wastewater in summer and fall (Table 6.3).

Scenedesmus was the dominant species, represented by 14 species (Table 6.3). Cyanophyta dominated during summer and fall in treated wastewater. During spring cyanophyta had a slight domination over chlorophyta in treated wastewater; however, the presence of diatoms (Bacillariophyta) was also significant. Chlorophyta dominated untreated wastewater in all seasons.

Strain isolation and development of consortium

Fifteen isolates were obtained from the wastewaters and soil and analysed for their lipid content. Isolates were mostly green algal species such as *Chlorella, Chlamydomonas, Scenedesmus and Gloeocystis* and cyanobacterial species such as *Anabaena* and *Limnothrix*. Maximum lipid (16 and 13%) content was found in two strains of *Gloeocystis* (Data not shown). The remaining species contained less than 9% lipids. All isolates were grown in pure cultures and mixed together in equal quantities to form a consortium for further experiments

Thirteen strains of algae namely *Botryococcus braunii* UTEX 572, *Chlorella protothecoides* UTEX 25, *C. saccharophila* var. *saccharophila* UTEX 2469, *C. vulgaris* UTEX 2714, *Cricosphaera carterae* UTEX LB1014, *Dunaliella tertiolecta* UTEX LB999, *Nannochloris oculata* UTEX LB1998, *Spirulina platensis* UTEX LB1926, *S. maxima* UTEX LB2342, *Tetraselmis suecica* UTEX LB2286, *T. chuii* UTEX LB232, *Phaeodactylum tricornutum* UTEX 646 and *Pleurochrysis carterae* CCMP 647 were evaluated along with the consortium for their growth response in treated and untreated wastewater in comparison with standard growth medium (Table 6.1). Growth after 10 days was estimated in terms of chlorophyll *a* content. Among all the algal strains tested, *P. Carterae* (3.4 µg m/L)*, B. braunii* (0.9 µg m/L) and *C. saccharophila* (1.8 µg m/L) recorded 56, 26 and 23% increase in chl *a* content in treated wastewater, respectively over the standard BG11 medium. The consortium of native isolates from wastewaters recorded highest chl *a* content of 11.9 µg mL^{-1} in the standard medium when compared to all other algal cultures and treatments. However, the consortium recorded chl *a* content of only 2.1 and 2.9 µg mL^{-1} in treated and untreated wastewaters, respectively.

Biomass and lipid production potential of selected cultures

Based on the preliminary screening we selected *B. braunii*, *C. saccharophila*, *D. tertiolecta*, *P. carterae* and the consortium for a time-scale study to evaluate biomass and lipid production potential in comparison with BG11 standard (Table 6.4). Except *Chlorella saccharophila* all others showed their best growth in treated wastewater than in standard growth medium. In untreated wastewater however, it was *Dunaliella tertiolecta* that could not perform better than modified BG 11 medium. This study showed that in comparison to all unialgal cultures, consortium performed the best in treated wastewater. It was the most potent candidate that might generate 29.3 tons of biomass and ~4,060 L of oil ha^{-1} $year^{-1}$ (Table 6.4).

Table 6.1. Strains used in the preliminary screening

Strain	Form	Standard Growth Medium
Botryococcus braunii UTEX 572	Fresh water	BG11
Chlorella protothecoides UTEX 25	Fresh water	BG11
Chlorella saccharophila var. *saccharophila UTEX 2469*	Fresh water	BG11
Chlorella vulgaris UTEX 2714	Fresh water	BG11

Cricosphaera carterae UTEX LB1014	Marine	Modified BG11
Dunaliella tertiolecta UTEX LB999	Marine	Modified BG11
Nannochloris oculata UTEX LB1998	Marine	Modified BG11
Spirulina platensis UTEX LB1926	Marine	Modified BG11
Spirulina maxima UTEX LB2342	Fresh water	Modified CFTRI
Tetraselmis suecica UTEX LB2286	Marine	Modified BG11
Tetraselmis chuii UTEX LB232	Marine	Modified BG11
Phaeodactylum tricornutum UTEX 646	Marine	Modified BG11
Pleurochrysis carterae CCMP 647	Marine	Modified BG11
Consortium of wastewater isolates	Fresh water	BG11

Table 6.2. Physicochemical characteristics of wastewater

Parameter	Units	Untreated	Treated
pH	ppm	6.54 - 7.18	6.88 - 8.04
Conductivity	$mS.cm^{-1}$	682 -1073	654 - 1067
Hardness	ppm	182.40	140.7
Biochemical Oxygen Demand	ppm	331 -487	2 -21
Chemical Oxygen Demand	ppm	1412	106-183
Total Suspended Solids	ppm	81- 268	4-27
Total Dissolved Solids	ppm	810	664
Total Solids	ppm	1416	780
Total Volatile Solids	ppm	840	188
Alkalinity	ppm	166	107
Acidity	ppm	38	4
TKN	ppm	32.6 - 45.9	3.97 - 5.53
NH_4-N	ppm	17.58 - 25.85	0.57 - 3.61
NO_3-N	ppm	0.21 - 28.13	1.39 - 3.91

P	ppm	5.47 - 13.83	3.47 - 7.89
PO_4	ppm	20.31 - 35.10	17.59 - 21.95
Na	ppm	112.1 -133.4	117.8 - 151.50
K	ppm	7.75 - 10.32	9.74 - 10.17
Ca	ppm	29.06 - 38.90	34.65 - 37.01
Fe	ppm	0.39 - 0.48	0.43 - 0.51
Mg	ppm	13.82 - 20.78	11.28 - 13.21
Mn	ppm	0.02 - 0.04	0.01 - 0.02
Mo	ppm	0.005 - 0.07	<0.005
Zn	ppm	0.03 - 0.13	0.17 - 0.18
S	ppm	46.46	51.76
SO_4	ppm	86.96 - 142.80	128.26 - 182.10

Table 6.3. Seasonal variations in the microalgal diversity and community composition in treated (T) and untreated (U) wastewaters (in % biovolume).

Genus	Summer		Fall		Winter		Spring	
	T	U	T	U	T	U	T	U
Chlorophyta								
Chlamydomonas sp.	-	-	0.89	88.83	1.57	-	-	-
Chlorella vulgaris	-	-	4.11	-	0.35	-	-	-
Chlorococcaceae sp.	-	-	-	-	-	-	12.79	0.72
Chlorococcum humicola	0.11	77.59	4.23	5.5	-	83.95	-	-
Coelastrum microporum	-	-	1.3	-	-	-	5.62	-
Gloeocystis vesiculosa	1.46	-	5.19	-	-	-	-	-
Kirchneriella contorta	-	-	-	-	-	-	-	-
Monoraphidium mirabile	-	-	7.97	-	-	-	-	-
Oedogonium sp.	-	-	-	-	-	-	0.23	-
Oocystis lacustris	-	-	7.75	1.21	-	-	-	-
Scenedesmus abundans	-	-	-	-	-	-	0.09	-
Scenedesmus acuminatus	-	-	-	-	-	-	2.61	-

Scenedesmus acutus	-	-	-	-	-	-	3.42	11.84
Scenedesmus acutus alternans	-	-	-	-	-	-	0.75	-
Scenedesmus bicaudatus	-	-	-	-	-	-	0.16	-
Scenedesmus bijuga	-	-	2.11	0.42	-		1.59	-
Scenedesmus bijuga alternans	-	-	-	-	-	-	0.23	-
Scenedesmus denticulatus	-	-	-	-		-	0.13	-
Scenedesmus dimorphus	-	-	-	-	92.97	1.61	1.87	-
Scenedesmus incrassatulus	-	-	-	-	1.3	-	-	-
Scenedesmus obliquus	-	-	-	-	-	-	0.67	0.06
Scenedesmus quadricauda	-	-	2.17		1.48	-	1.29	-
Scenedesmus quadrispina	-	-	-	-	-	-	3.54	-
Scenedesmus serratus	-	-	-	-	-	-	0.09	-
Stigeoclonium sp.	-	-	-	-	-	-	-	38.84
Ulothrix variabilis	0.03	-	-	-	-	-	-	-
Uroglena sp.	-	-	-	-	-	-	-	46.49
Chlorophyta contrib.	*1.6*	*77.59*	*35.72*	*95.96*	*97.67*	*85.56*	*35.08*	*97.95*
Cyanophyta								
Anabaena sp	54.09	-	-	-	-	-	-	-
Aphanocapsa delicatissima	-	-	-	-	-	-	-	0.02
Aphanocapsa hyalina	0.02	-	-	-	-	-	-	-
Aphanothece sp.	-	-	-	-	-	-	-	0.12
Calothrix braunii	2.06	-	-	-	-	-	-	-
Chroococcaceae sp.	-	-	-	-	-	-	0.02	0.81
Chroococcus minutus	-	-	-	-	-	-	0.05	-
Cylindrospermopsis sp	4.65	-	-	-	-	-	-	-
Leibleinia kryloviana	-	-	-	0.47	-	7.93	-	-

Limnothrix sp.	-	0.04	-	-	-	-	-	
Limnothrix redekei	-	-	-	2.8	1.03	6.51	-	-
Lyngbya sp.	-	-	-	-	-	-	36.74	-
Nostoc sp.	5.86	-	-	-	-	-	-	-
Oscillatoria sp.	20.34	-	-	-	-	-	-	-
Oscillatoria tenuis	-	22.37	-	-	-	-	1.59	-
Planktolyngbya limnetica	11.09	-	-	-	-	-	-	-
Raphidiopsis curvata	-	-	64.28	0.76	-	-	-	-
Synechococcus elongatus	-	-	-	-	-	-	-	0.11
Synechococcus sp.	-	-	-	-	-	-	0.06	0.35
Synechocystis sp.	-	-	-	-	-	-	-	0.17
Cyanophyta contrib.	*98.11*	*22.41*	*64.28*	*4.04*	*1.03*	*14.44*	*38.46*	*1.72*
Bacillariophyta								
Eunotia sp.	-	-	-	-	-	-	1.49	-
Navicula pelliculosa	-	-	-	-	-	-	3.12	-
Navicula sp.	-	-	-	-	1.3	-	-	-
Nitzschia palea	-	-	-	-	-	-	21.85	0.33
Nitzschia amphibia	0.09	-	-	-	-	-	-	-
Nitzschia pura	0.02	-	-	-	-	-	-	-
Gomphonema parvulum	0.02	-	-	-	-	-	-	-
Gomphonema gracile	0.01	-	-	-	-	-	-	-
Bacillariophyta contri.	*0.14*	*0*	*0*	*0*	*1.3*	*0*	*26.46*	*0.33*
Cryptophyta								
Rhodomonas sp.	0.15	-	-	-	-	-	-	-
Cryptophyta contrib.	*0.15*	*0*	*0*	*0*	*0*	*0*	*0*	*0*

Table 6.4. Biomass and oil production potential of *B. braunii*, *C. saccharophila*, *D. tertiolecta*, *P. carterae* and consortium in (treated and untreated) wastewaters

Culture	Medium	Biomass ($g\ L^{-1}\ d^{-1}$)	Lipids (%)	Estimated biomass productivity ($t\ ha^{-1}\ year^{-1}$)	Estimated oil yield ($L\ ha^{-1}\ year^{-1}$)
Botryococcus braunii	BG11	0.019	13.50	13.7	2109
	Treated	0.037	9.50	26.3	2839
	Untreated	0.034	13.20	24.5	3675
Chlorella saccharophila	BG11	0.018	12.90	12.7	1869
	Treated	0.016	17.00	11.4	2194
	Untreated	0.023	18.10	16.1	3319
Dunaliella tertiolecta	Modified BG11	0.031	12.80	22.1	3216
	Treated	0.038	12.20	26.9	3728
	Untreated	0.028	15.20	20.3	3510
Pleurochrysis carterae	Modified BG11	0.028	9.70	20.3	2240
	Treated	0.037	11.80	26.3	3526
	Untreated	0.033	12.00	23.9	3260
Consortium	BG11	0.027	10.90	19.1	2369
	Treated	0.041	12.20	29.3	4060
	Untreated	0.039	12.00	28.1	3830

Milestone 1: Identification at the bench scale of robust species (from around 30 screened) that can produce lipids is completed. This completes the milestone on the technical feasibility of cultivation/production method for a robust organism (or consortium). The broader goal of economic feasibility remains to be evaluated.

Subtask 6.2: Develop harvesting, extraction, and conversion methods for algae used in biodiesel production

Procedures

Algal biomass production in raceway ponds and lipid extraction

To assess the feasibility of producing biodiesel from mixed/wild native isolates of microalgae, the consortium was cultivated in treated wastewater in 4 raceway ponds of 950 L capacity each supplemented with ~250 mg/L nitrogen as sodium nitrate and 5-6% CO_2 air mixture bubbled through 2 air stones at a rate of 10 L/min. After 10 days, the biomass was harvested using a centrifuge (AML Industries Inc. Model 12-413V) with an inlet flow rate of 230 L/h. Harvested algae with ~15% solids were dried at 60^{o}C for 24 h for extraction of lipids and biomass analysis. Lipids were extracted with hexane in a Soxhlet apparatus.

Analytical testing and biodiesel production from consortium

Biodiesel from crude microalgae oil was obtained by a two-step process, an acid transesterification followed by a base transesterification due to the high acid value of crude algal oil. The free fatty acids (FFA) were converted into esters using a proprietary method developed by Renewable Energy Group, Inc.

Results and discussion

Algal biomass production in raceway ponds

The consortium of wastewater isolates was cultivated in 4 raceway ponds of 950 L capacity each with 5-6% CO_2 air mixture and ~250 ppm nitrogen supplementation to improve biomass productivity. Each batch was cultivated for 10-12 days. The average productivity observed in the winter was 2.64 g/m^2/d or 9.3 tons/ha/yr of dry biomass with maximum biomass productivity being 4.9 g/m^2/d or 17.8 tons/ha/yr (Data not shown). The consortium showed remarkable resistance to predation and crashes and exhibited tolerance to low temperatures.

Biomass obtained from the algal consortium grown in raceways was analysed for its composition before and after lipid extraction (Table 6.5). Energy stored in the mixed algal consortium before and after lipid extraction was 22.87 and 20.77 MJ/kg, respectively. A 9% reduction in the energy value of fresh algal biomass was observed after lipid extraction.

Algal oil characterization and biodiesel conversion

To evaluate the feasibility of producing biodiesel from algal consortium grown in treated wastewater, about 126.7 g (144 mL) of crude algal oil was extracted from 2.3 kg of dry algal biomass for this study. The energy content of the crude algal oil was 40.2 MJ/kg. The oil was converted to methyl esters and examined for the fatty acid profile using GC. The profile showed following fatty acids: 14:0, 16:0, 16:1, 18:0, 18:1, 18:2, 18:3, 20:0, 20:1, 20:2, 20:3, 20:4, 20:5, 22:5 and 22:6 (Table 6.6). However the purified fraction of triglycerides contained fatty acids ranging from C14:0 to C18:3. Both the crude algal oil and purified fraction of triglycerides were dominated by the presence of C16:0 (Palmitic), C18:1 (Oleic), and C18:3 (Linolenic)

(Table 6.6). These results are in conformity with observations reported in the literature that microalgal lipids derived from *Chlorella*, *Spirulina*, *Nannochloropsis*, *Scenedesmus* and *Dunaliella* were mainly composed of unsaturated fatty acids (50-65%).

Table 6.5. Compositional analysis of the algal consortium before and after lipid extraction

Parameters	Biomass before lipid extraction	Biomass after lipid extraction
Proximate analysis (%)		
Moisture	7.59 ± 0.16	6.44 ± 0.73
Volatiles	68.89 ± 0.15	67.33 ± 0.86
Ashes	11.42 ± 0.11	13.39 ± 1.76
Fixed carbon	12.10 ± 0.120	12.82 ± 0.20
Ultimate analysis (%)		
Carbon (C)	49.44 ± 0.11	45.95 ± 1.08
Hydrogen (H)	6.65 ± 0.03	6.16 ± 0.13
Nitrogen (N)	9.27 ± 0.18	9.28 ± 0.88
Sulfur (S)	0.67 ± 0.03	0.76 ± 0.10
Oxygen (O)	21.62 ± 0.27	23.55 ± 0.35
Higher heating value, (HHV) (MJ kg^{-1})	22.87 ± 0.51	20.77 ± 0.42
Biochemical composition (%)		
Protein	54.50 ± 0.40	56.9 ± 4.20
Lipids	6.82 ± 0.08	0.4 ± 0.06
Carbohydrates	8.98 ± 0.87	9.15
Phosphorus	0.87	1.4

Table 6.6. Fatty acid profiles of crude and purified algal oils and algal biodiesel

Fatty acids		Crude algal oil	Refined algal oil	Algal biodiesel
			(%)	
C14:0	Myristic	1.91	1.4	0.9
C15:1	Pentadecenoic		5.9	
C16:0	Palmitic	20.62	17.6	16.3
C16:1	Palmitoleic	6.47		5.8
C18:0	Stearic	1.43		1.2
C18:1	Oleic	10.58	14.9	12.1
C18:2	Linoleic	10.54		20
C18:2n6 trans	Linoleic		9.6	
C18:2n6 cis	Linoleic		11.8	
C18:3	Linolenic	15.47	38.8	27.9
C20:0	Arachidic	0.04		
C20:1	Gadoleic	1.1		
C20:2	Eicosadienoic	1.05		
C20:3	Mead	1.05		
C20:4	Arachidonic	0.88		
C20:5	Timnodonic	1.48		
C22:0	Behenic	1.42		
C22:5	Docosapentenoic	0.41		
C22:6	Docosahexenoic	0.05		
Unknowns		25.5		15.8
Unsaturated[a]		65.88	81	78.15
Saturated[a]		34.12	19	21.85

[a]*Percentage calculated based on the total known fatty acids*

To establish proof-of-concept for biodiesel production from mixed cultures of native/wild strains growing in wastewater, conversion of extracted crude algal oil to biodiesel was attempted. The crude algal oil showed very high acid value ~99 (mg KOH/g) indicating presence of about 50% free fatty acids (FFA), an undesirable trait for biodiesel conversion process. Acid catalyzed transesterification process is normally used for feedstocks containing high FFA content. The biodiesel conversion process was carried out without degumming and chlorophyll removal. The estimate of conversion was >95%. The product yield on the acid esterification was 70.9% with losses being mainly due to oil impurities, soaps in oil and a small volume adhering to glass surface area. The ASTM specification requires that the total glycerol and free glycerin be less than 0.24 and 0.02% of the final biodiesel product, respectively as measured using a gas chromatographic method described in ASTM D 6584. The biodiesel made from mixed algal biomass was found to contain 0.0155 and 0.0001% total bound and free glycerin, respectively and met ASTM specifications.

Results from this study indicate that the algal oil produced from mixed cultures of native algae can be used for biodiesel production. However, refining of crude algal oil to remove gums, pigments and other impurities still remains a major challenge for commercial processing which needs further research.

Milestone 1: A simple, scaleable method of raceway cultivation followed by centrifugal harvesting, processing, extraction of lipids and transesterificaiton has been demonstrated. This completes the milestone on the technical feasibility, however the broader goal of economic feasibility and cost reductions remains to be addressed in the future.

Subtask 6.3: Harvesting, storage, and supply logistic modeling for biomass

Our original plan at the time of writing this proposal was to develop models that optimize the steps between harvesting and delivering biomass to a biorefinery. We set a milestone of developing a usable model for biomass management in Georgia. This was an ambitious target and at the point, it was not clear that the information needed to develop and use such models were not readily available.

Modification of plan: Because of the level at which we were beginning our work, and the relative lack of information for modeling that was available in the literature, or efforts had to be redefined. Instead of pursuing supply logistics a that point, we focused on understanding strain behavior and nutrient delivery (subtask 6.1) and biomass processing (subtask 6.2).

Task 7.0 Develop and test catalysts for biomass conversion to products.

The overall goal in this task was to develop catalysts for biomass conversion. We planned to evaluate homogeneous and heterogeneous catalysts in pyrolysis applications to increase product generation and quality. In addition we planned to focus on developing catalysts for transesterification and for syngas conversion to hydrogen (and other products). These catalysts were to be developed from biomass through thermochemical conversion processes described elsewhere in this report, thus

leading to furthering the establishment of a thermochemical biorefinery. This task also builds on the work on subtask 2.1B where levoglucosan was generated as the primary product, and here the task was to hydrolyze levoglucosan to obtain sugars that could be fermented to produce ethanol.

Modification of plan: In the original proposal we proposed to develop alkali metal impregnated catalysts for direct use in pyrolysis. That approach was based on the idea that catalysts would be developed from biomass and used in-situ in pyrolysis, thus catalyzing the pyrolysis reactions and improving product quality. Based on work in subtask 2.1, we focused on an intermediate product of pyrolysis, levoglucosan (LG) as a target instead of biomass. Our results in subtask 2.1 showed that high concentrations of LG could be produced in BioOil, and that this high sugar intermediate could be hydrolyzed further to provide an attractive substrate for fermentation. Hence, subtask 7.1 pursues this approach.

Subtask 7.1: Evaluation of alkali metal impregnated catalysts in pyrolysis

Methodology and results described and summarized below have independently been reported in the following publications:

1. *Ormsby, R.V. 2011. Levoglucosan transformation and kinetics of hemicellulose hydrolysis using carbon supported solid acid catalysts. Unpublished M.S. Thesis, Biological Engineering, The University of Georgia, Athens GA 30602.*

Here we build on previous work (subtask 2.1 A) where catalysts were developed from pine chip char (PCC, a product of pyrolysis) by sulfonation. Catalyst activity of sulfonated PCC with levoglucosan is further illustrated in Figure 7.1, which shows the change in concentration for each compound with respect to time at 120 ^{o}C. Approximately 80% conversion of LG to glucose was achieved after 2 hours.

Bio-oil Hydrolysis with PCC

An aqueous phase ILC sample with approximately 153 g/L of LG was hydrolyzed with sulfonated PCC char. The sample had an approximate water/oil ratio of 50%, and had not been filtered. Ten mL of the aqueous phase bio-oil was combined with 1 g of catalyst and heated to 120 ^{o}C over time intervals ranging from 1 to 24 hours. The resulting sugar concentrations are shown in Table 7.1. There appears to be a sharp decline in levoglucosan within the first hour of hydrolysis, but the concentration of glucose do not seem proportional to values found in the model compound trials. Furthermore, the final concentrations for all sugars after 24 hours are almost identical to the thermal control. The samples themselves developed a solid disc of particulate matter that settled on top of the solution, as well as a thick, hard film on the stir bars that can be seen in Figure 7.2. This suggests polymerization may be occurring during the hydrolysis reaction, possibly forming solid humins that inhibit the total glucose yield.

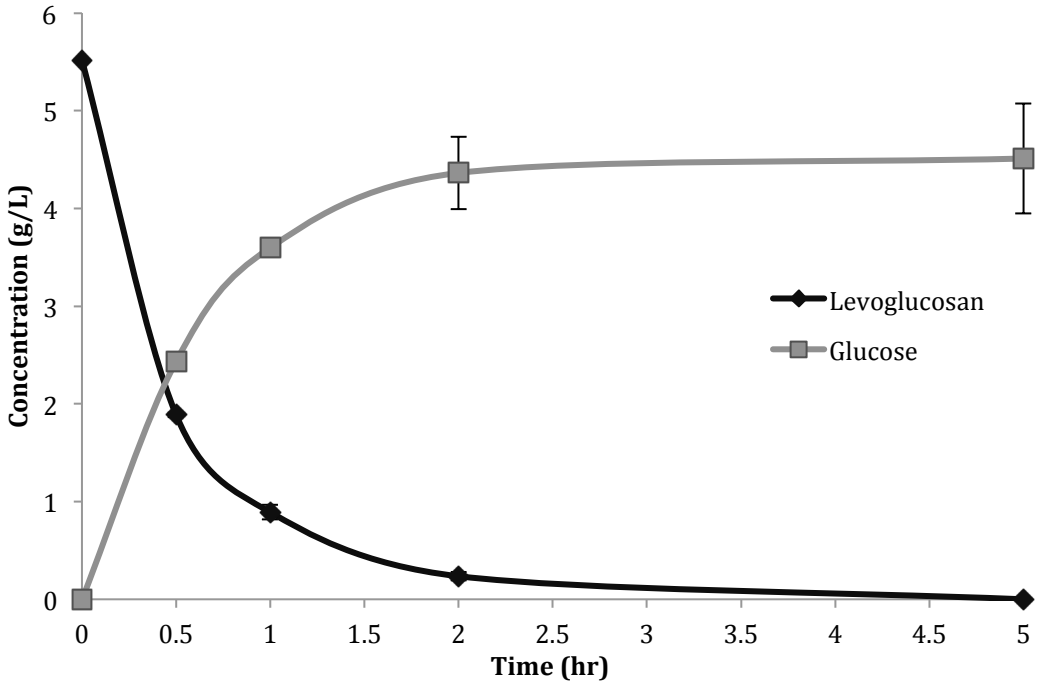

Figure 7.1. Model compound levoglucosan with sulfonated PCC hydrolysis results, 120 ^{o}C.

Table 7.1. ILC-Bio-oil hydrolysis product yield concentrations at various time intervals at 123 ^{o}C.

Time (hr)	Levoglucosan (g/L)	Glucose (g/L)	Xylose (g/L)	Arabinose (g/L)	Acetate (g/L)	5-HMF (g/L)
1	45.94	10.87	8.6	0	70.02	1.17
2	16.62	15.03	9.99	2.94	58.57	0.45
3	13.53	16.28	11.34	3.65	60.57	0.66
4	10.02	16.36	11.84	3.95	60.09	0.31
6	6.63	15.6	11.76	3.97	56.39	0
8	6.08	15.82	11.99	3.99	57.01	0
24	2.89	14.16	9.96	3.13	53.19	0
24 hr Control	3.98	14.61	10.57	3.36	56.11	0

In order to prevent polymerization, further trials included ethanol dilution of fast pyrolysis (FP) bio-oil attempting simultaneous hydrolysis of levoglucosan and esterification of organic acids and aldehydes. FP bio-oil samples were taken directly from the pyrolysis reactor and prepared for PCC hydrolysis in ethanol. Two controls were included: a thermal control consisting of only bio-oil and ethanol, and a second control consisting of only bio-oil and PCC catalyst.

Figure 7.2. Solid disc formed over the hydrolysis products of ILC aqueous phase bio-oil and PCC catalyst.

The second control group created a thick tar-like paste that could not be filtered nor analyzed. Table 7.2 shows the average concentrations of various compounds found in fast pyrolysis oil before and after solid acid catalyst hydrolysis. The first control group and both experimental groups showed little difference in final sugar concentrations. Although there was a 30 - 40%decrease in levoglucosan concentration, there was not a corresponding increase in glucose or further decomposition compounds such as 5-HMF.

HPLC analysis also showed a number of unidentified peaks for all bio-oil hydrolysis samples. These peaks may represent the formation of esters or intermediate oligosugars leading to the formation of levulinic acid. An example of these unknown peaks from an HPLC analysis of PCC bio-oil and ethanol hydrolysis reaction after 5 hours at 120 ^{o}C is shown in Figure 7.3. These peaks did not appear at any of the known retention times for any standard curves available for compound identification and quantification through HPLC analysis. Gas chromatography and

mass spectrometry analysis (GC/MS) was used in an attempt to identify these unknown compounds.

Table 7.2. Average concentration of fast-pyrolysis oil compounds before and after hydrolysis with solid acid catalysts.

Sample Group	Time (hr)	Levoglucosan (g/L)	Xylose (g/L)	Glucose (g/L)	Acetate (g/L)	5-HMF (g/L)	Furfural (g/L)
Bio-Oil	0	247.66	9.17	1.6	118.92	2.84	1.02
Bio-Oil EtOH	0	200.65	0.27	0	95.49	2.99	0.98
Bio-Oil EtOH	5	147.24	7.94	2.47	107.72	2.61	1.82
AC bio-oil EtOH	5	152.22	7.87	2.74	103.71	2.57	1.38
PCC bio-oil EtOH	5	165.05	7.66	4.61	102.79	2.82	0

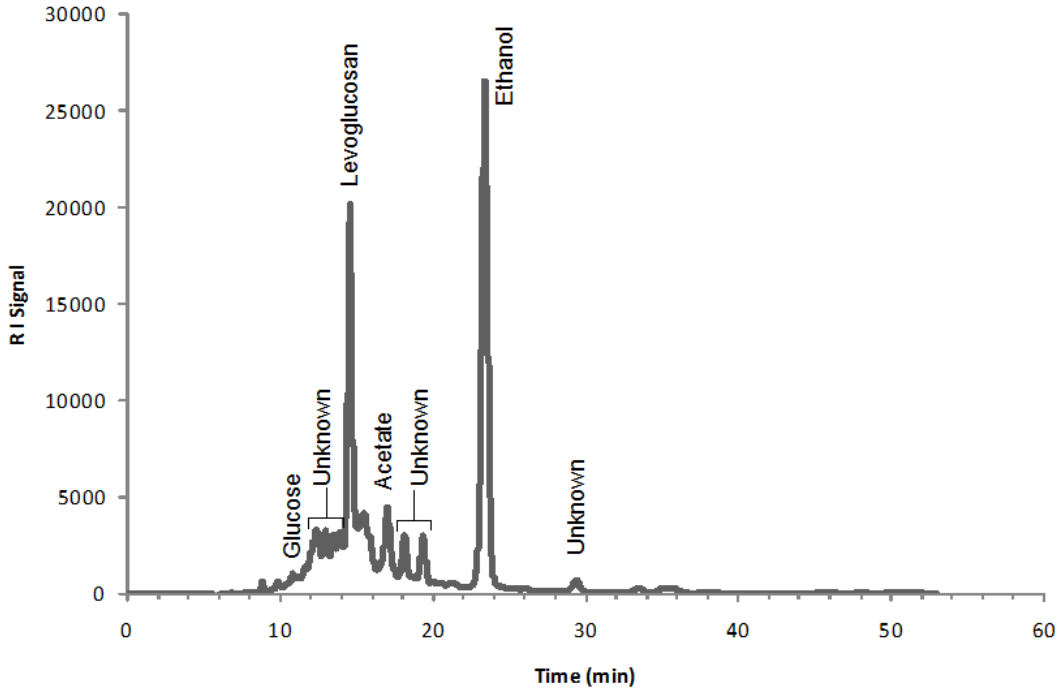

Figure 7.3. HPLC analysis of PCC Bio-oil EtOH Hydrolysis,5 hrs, 120 ^{o}C

The GC/MS chromatograph for bio-oil samples and controls before and after PCC hydrolysis is shown in Figure 7.4. All samples are fast pyrolysis bio-oil diluted to 50% in ethanol. Many of the peaks that appear in the bio-oil sample that was reacted with the PCC catalyst also appear in the bio-oil control. Peak 1 in Figure 7.4 has a retention time of 1.85 minutes with a 90% certain identity of ethyl acetate, the presence of which confirms a successful esterification reaction. Peak 2 with a retention time of 8.24 minutes has been identified as ethyl orthoformate with 78% certainty. Peak 3 has a retention time of 9.90 minutes and GC/MS analysis has determined a 59% certainty that this peak represents 1,1-diethoxy-pentane. Although peaks 2 and 3 are present in the bio-oil sample reacted with heat alone (B), the peak area is significantly larger in the reaction with PCC.

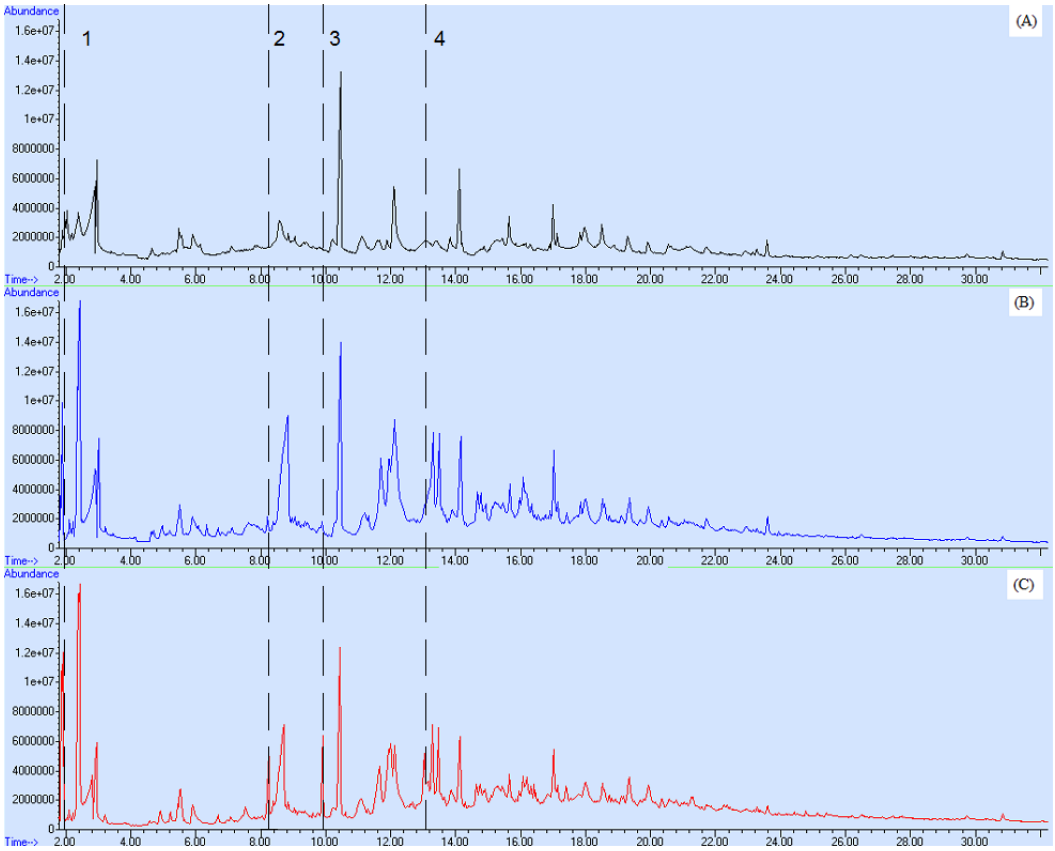

Figure 7.4. GC/MS analysis of FP bio-oil before hydrolysis 25 ^{o}C (A), FP bio-oil control 5 hr. (B), FP bio-oil and PCC 5hr. 120 ^{o}C (C)

Although GC/MS analysis could not quantify the specific concentration of the compounds associated with peaks 2 and 3, the difference in abundance suggests that PCC generated a larger concentration of these compounds. Peak 4 has a retention time or 13.15 minutes with a 32% certain identity of 1,1,1-triethoxy-ethane, which was not present in the sample reacted without PCC (B). Although the identity of these peaks is not 100% certain, all compounds appear to be ethers or esters.

Milestone 1: Identification of a catalyst that can hydrolyze levoglucoan has been completed. Further optimization and detailed process characterization would be next steps.

Subtask 7.2: Development of heterogeneous catalysts for syngas conversion and/or transesterification processes

Transesterification is typically done using a homogenous catalyst that is washed out of the final product, and typically not recovered. Solid acid or base catalysts are recoverable and reusable, can treat high free fatty acid feedstocks, and can be used in continuous processes. Solid carbon based catalysts (such as biochar based catalysts) are stable under acidic and basic conditions, are stable at high temperatures, can be made from co-products of a thermochemical biorefinery, and are non-polar and therefore prevents adsorption of polar molecules (e.g. water or glycerol).

Procedures

We produced biochars under different temperature conditions (400, 500, and 600 C) in batch reactors that were heated at 2 C/min and held at target temperature for 30-40 min. Peanul hulls, pine chips and pine pellets were pyrolyzed to obtain chars that were treated to produce the catalysts. Chars were characterized for pH, surface area, DRIFT, ATR and SEM; in addition CHNS and elemental analysis was performed.

Acid functionalization was done using sulfuric acid. At first, the chars were screened to uniform size (4-12 mesh) and treated with 99% sulfuric acid at 20 mL per 12.5 g. Subsequently the chars were heated in a muffle furnace at 100, 150, and 250 C for 12 hours. After cooling, the chars were washed with DI water until pH remained constant and then dried overnight at 110 C.

In base functionalized chars, pyrolysis was done at 500 C under similar heating rate and hold time as above. The chars were then treated with a strong organic base (4-aminophenoxide or ethylenediamine), then heated to 65-110 C and held for durations between 22 and 72 hours.

Small scale batch reactors were used for screening catalyst. Known amounts (typically 0.2 g) of catalyst was used in 5 mL volume of reactants. Palmitic acid or stearic acid at 200 to 500 mg/L, along with methanol (4 mL) was used as reactants. The mixture was heated to 55-60 C and sub-samples were taken as a function of time to determine the formation of methylesters. Fractional removal of palmitic and stearic acids were measured.

Results and discussions

Biochars generated were measured to have surface areas between 2 and 4 m^2/g. Their pH were all basic, but variable (Table 7.3). DRIFT analysis confirmed the presence of aromatic and aliphatic groups. A large peak at 1750/cm indicates the presence of carboxylic acid groups in the sulfonated chars (Figure 7.5). It was found that the acid density increased with decreasing pyrolysis temperature and sulphonation temperatures. A distinct presence of SO_3H groups was identified.

In the case of sulphonated chars the reaction was complete (90-100%) within 30 to 60 minutes at 55-60C (Figure 7.6). The 400C pyolyzed pine chip char, sulfonated

at 100 C provided the highest reaction rate and lowest reduction in conversion when reused multiple times. In general the catalytic activity declined with reuse, suggesting attrition or inactivation. Heating the catalyst to 125C allowed reuse of catalyst without decay up to 7 times.

In the case of base catalysts generated, DRIFT analysis suggests the formation of amide bonds. Reaction with glyceryl tridodecanoate showed compete conversion in 4-aminophenoxide (4-AP) treated peanut hull chars, but only 30% conversion in the ethylenediamine (EDA) treated chars. In pine pellet chars the conversion were 79% and 100%, for the 4-AP and EDA chars, respectively.

Table 7.3. Solid acid catalyst characterization.

Materials Properties	Activated* Carbon (Lignite Coal)	Peanut Hull Char (400°C)	Peanut Char (500°C)	Pine Chip Char (400°C)	Pine Chip Char (500°C)
Generation Process	Steam	Pyrolysis-N_2	Pyrolysis-N_2	Pyrolysis-N_2	Pyrolysis-N_2
Reactor/Residence Time	Unknown	Batch/40min	Batch/40min	Batch/40min	Batch/40min
pH	4.6	10.5	10.1	7.55	8.3
Surface Area, $m^2\ g^{-1}$	506 ± 34	NM	3.2±0.6	3.8 ± 0.14	2.75 ± 0.2
O_3 treated, 30 min	494 ± 57	ND	ND	ND	ND
Pore Volume ($ml\ g^{-1}$)	0.55 ± 0.005	NM	0.004± $3e^{-4}$	ND	ND
(ppm or mg kg^{-1})	Mean	Mean	Mean	Mean	Mean
Cu	ND	16	18	25	9
Mn	"	116	157	274	258
Mo	"	4.8	< 1	< 1	< 1
Ni	"	2.3	3.95	< 2	< 2.91
Fe	"	1000	1094	150	50
Ca	"	4620	4,090	1710	1850
K	"	15,200	20,700	1450	1450
Mg	"	2,190	2,478	600	590

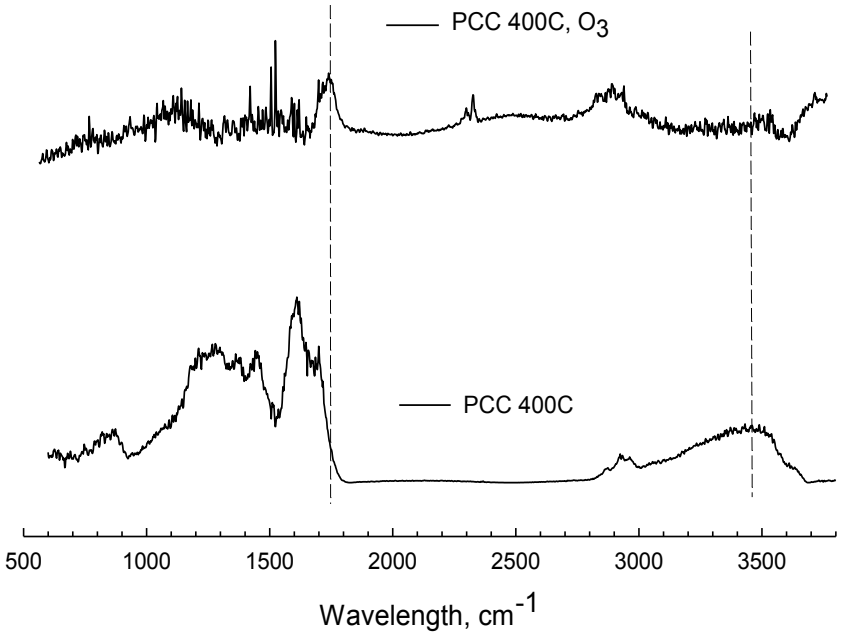

Figure 7.5. DRIFT analysis of the char catalysts generated in this project.

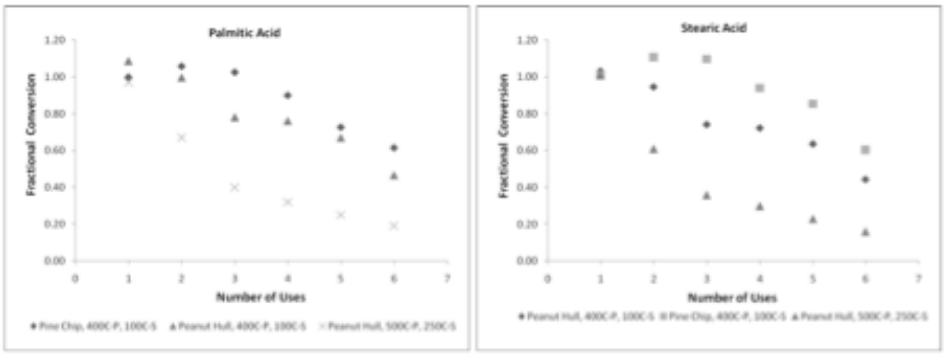

Comparison of esterification catalytic activity between different sulfonated biochars. Reactions conditions were 500 ppm palmitic and stearic acid, 0.50 g char, and 58°C for 1 hour. Catalysts were recovered, rinsed with methanol and reused without further treatment.

400C-P, is 400°C pyrolysis
100C-S, is 100°C sulfonation temperature

Figure 7.6. Catalytic Testing

Milestone 1: Several catalysts were developed and tested, completing this milestone. The base chars with EDA treatment had 100% conversion.

Task 8.0 Technology transfer and education.

The Engineering Outreach program and the research faculty involved in this program continuously performed technology outreach and education during this project. These activities include, direct one-on-one talks with industry partners and entrepreneurs interested in the areas of work in integrated biorefineries, conference presentations, site visits and presentations to larger industries, and service in state agency based outreach functions. In education, the laboratories involved in this research directly trained undergraduate and graduate students, post-doctoral fellows, technical staff, and collaborators not directly funded out of this project.

Over the period of this grant, 22 students were trained, including 5 PhD and 13 Masters degree research along with 4 formal undergraduate student research training. Also, two international exchange students from France and Thailand was trained in this project. The biorefinery research conducted provided training opportunity for 14 research technicians, 6 postdoctoral scientists and 34 research collaborators. The total persons trained in this project were 76 persons.

Listing of conference proceedings, peer reviewed journal articles and patents that came out of this work are listed in the following sections.

Milestone: A total of 22 students were trained in this project who were awarded a B.S., M.S., or PhD degree.

Products developed under the award and technology transfer activities

Publications (list journal name, volume, issue), conference papers

1. Vishwanathan, T., S. Mani, K.C. Das, S. Chinnasamy, and A. Bhatnagar. 2011. Thin layer drying kinetics and chemical composition of microalgae consortium. Transactions of the ASABE, 54(6):2245-2252
2. Hilten, R., R. Speir, J. Kastner and K.C. Das. 2011. Production of gasoline-like fuel via catalytic pyrolysis of acidulated peanut oil soap stock. Bioresource Technology 102(17):8288-8294
3. Doydora, S., M. Cabrera *, K.C. Das, J. Gaskin, L. Sonon, and W. Miller. 2011. Release of nitrogen and phosphorus from poultry litter amended with acidified biochar. IJERPH Special issue: Soil Pollution – Preventaion and Mitigation, 8(5):1491-1502.
4. Das, K.C., K. Singh, B.P. Bibens, R. Hilten, S.A. Baker, W.D. Greene and J.D. Peterson. 2011. Pyrolysis characteristics of forest residues obtained from different harvesting methods. Applied Engineering in Agriculture, 21(1):107-113.
5. Ormsby, R.V. 2011. Levoglucosan transformation and kinetics of hemicellulose hydrolysis using carbon supported solid acid catalysts. Unpublished M.S. Thesis, Biological Engineering, The University of Georgia, Athens GA 30602.

6. Lakshmanaswamy, A., E. Rajaraman, M. A. Eiteman, E. Altman. 2011. Microbial removal of acetate selectively from sugar mixtures. *Journal of Industrial Microbiology and Biotech.,* in press (2011) doi: 10.1007/s10295-010-0932-1

7. Garcia-Perez, M., T.T. Adams, J.W. Goodrum, K.C. Das, and D.P. Geller. 2010. DSC studies to evaluate the impact of bio-oil on cold flow properties and oxidation stability of biodiesel. Bioresource Technology, 101(15):6219-24.

8. Chinnasamy, S., A. Bhatnagar, R. Claxton and K.C. Das. 2010. Biomass and bioenergy production potential of microalgae consortium in open and closed bioreactors using untreated carpet industry effluent as growth medium. Bioresource Technology, 101(17):6751-60.

9. Hilten, R., R. Speir, J.R. Kastner, and K.C. Das. 2010. Production of fuel from the catalytic cracking of pyrolyzed poultry DAF skimmings. Journal of Analytical and Applied Pyrolysis 88(1):30-38.

10. Hilten, R. and K.C. Das. 2010. Comparison of three accelerated aging procedures to assess bio-oil stability. Fuel 89(10): 2741-2749.

11. Steiner, C., K.C. Das, N.D. Melear, and D. Lakly. 2010. Reducing nitrogen losses during poultry litter composting using biochar. Journal of Environmental Quality, 39(4):1236-42.

12. Chinnasamy, S., A. Bhatnagar, R.W. Hunt, and K.C. Das. 2010. Microalgae cultivation in wastewater dominated by carpet mill effluents for biofuel applications. Bioresource Technology 101(9):3097-3105.

13. Bhatnagar, A., M. Bhatnagar, S. Chinnasamy and K.C. Das. 2010. *Chlorella minutissima*-A promising fuel alga for cultivation in municipal wastewaters. Applied Biochemistry and Biotechnology 161(8):523-536.

14. Gaskin, J.W., R.A. Speir, D. Lee, K. Harris, L.A. Morris, K.C. Das and D. Fisher. 2010. Effect of peanut hull and pine chip biochar on soil nutrients, corn nutrient status and yield. Agronomy Journal, 102, 623-633.

15. Hilten, R., B. Bibens, J.R. Kastner and K.C. Das. 2010. In-line esterification of pyrolysis vapor with ethanol improves bio-oil quality. Energy & Fuel 24(1):673-682.

16. Risse, L. M., K. Singh, K.C. Das, J. Worley and S. Thompson, 2010. Value Added Poultry Litter Products through Fractionation and Pyrolysis. Poster abstract for the National Animal and Poultry Waste Management Symposium, Greensboro, NC, September 26-28, 2010.

17. Das, K.C., M. Singh, M. Garcia-Perez, and S. Chinnasamy. 2010. Biorefinery Technologies – an overview. International Conference on Bioengineering, SRM University, Chennai, India, July 29-31 [Presentation and Proceedings]

18. Chinnasamy, S., M. Singh, and K.C. Das. 2010. Microalgae technology for integrated waste management with bioenergy production. International

Conference on Bioengineering, SRM University, Chennai, India, July 29-31 [Presentation and Proceedings]

19. Almeida, A., K.C. Das, and N. Balagurusamy. 2010. Biochemical methane potential of desert plants: *Aloe vera* and *Opuntia robusta* in Comarca Lagunera, Mexico. Proceedings of the 3rd Intl Symposium on Energy from Biomass and Waste, Venice, Italy, Nov 8-11.
20. Alvarado, A., S. Chinnasamy, K.C. Das, and N. Balagurusamy. 2010. Opportunities for co-digestion of industrial and agricultural substrates for anaerobic digestion. Proceedings of the 3rd Intl Symposium on Energy from Biomass and Waste, Venice, Italy, Nov 8-11.
21. Steiner, C., K.C. Das, N. Melear, J. Gaskin, K. Harris, and D. Lakly. 2010. Biochar use in the poultry industry. 3rd Intl Biochar Conference, Rio de Janeiro, Brazil, Sept 12-15.
22. Viswanathan, T., S. Mani, S. Chinnasamy, K.C. Das. 2010. Effect of cell rupturing methods on the drying characteristics of microalgae. Society of Industry Microbiology, 32nd Symposium on Biotechnology for Fuels and Chemicals, Clearwater beach FL, April 19-22.
23. Novak, J.M., I. Lima, B. Xing, J.W. Gaskin, C. Steiner, K.C. Das, M. Ahmedna, D. Rehrah, D.W. Watts, W.J. Busscher, and H. Schomber. 2009. Characterization of designer biochar produced at different temperatures and their effects on a loamy sand. Annals of Environmental Science, 3, 195-206.
24. Hunt, R.W., A. Zavalin, A. Bhatnagar, S. Chinnasamy and K.C. Das. 2009. Electromagnetic biostimulation of living cultures for biotechnology, biofuel, and bioenergy applications. International Journal of Molecular Science 10, 4515-4558.
25. Chinnasamy, S., B. Ramakrishnan, A. Bhatnagar, S.K. Goyal and K.C. Das. 2009. Carbon and nitrogen fixation under elevated levels of CO_2 and temperature by Anabena fertilissima. Journal of Freshwater Ecology 24(4):587-596.
26. Singh, K., M. Risse, J. Worley, K. C. Das, and S. Thompson. 2009. Studying compaction behavior of fractionated poultry litter and use of pyrolysis condensate as a binder during pelletizing. Transactions of ASABE 52(3):949-956.
27. Smith, J.S., M. Garcia-Perez, and K.C. Das. 2009. Producing fuel and specialty chemicals from the slow pyrolysis of poultry DAF skimmings. Journal for Analytical and Applied Pyrolysis 86(1):115-121
28. Chinnasamy, S., B. Ramakrishnan, A. Bhatnagar, and K.C. Das. 2009. Biomass production potential of a wastewater alga Chlorella vulgaris ARC 1 under elevated levels of CO2 and temperature. International Journal of Molecular Sciences 10(2):518-532.
29. Kastner, J.R., J. Miller, P. Kolar, and K.C. Das. 2009. Catalytic ozonation of ammonia using biomass char and wood fly ash. Chemosphere 75, 739-744.

30. Gaskin, J.W., C. Steiner, K.R. Harris, K.C. Das, and B. Bibens. 2008. The effect of low-temperature pyrolysis conditions on the characteristics of poultry litter, peanut hull, and pine chip biochars for agricultural use. Transactions of the ASABE 51(6):2061-2069

31. Das, K.C., S. Chinnasamy, G. Hawkins and C. Steiner. 2009. Organic waste management - Bioproducts and Biofuel Opportunities. AgriINTEX International Conference - Next Generation of Indian Agriculture, Coimbatore, India, October 2-5, 2009 [International Invited Keynote Presentation]

32. Singh, K., K.C. Das, M. Risse, and J. Worley. 2009. Determination of Composition of Cellulose and Lignin Mixture using Thermo Gravimetric Analysis (TGA). Journal of Energy Resource Technology 131(2): DOI: 10.1115/1.3120349

33. Kastner .J.R, J. Miller, and K.C. Das. 2009. Pyrolysis conditions and ozone oxidation effects on ammonia adsorption in biomass generated chars. Journal of Hazardous Materials, 164(2-3):1420-1427.

34. Jena, U., and K.C. Das. 2009. State of the art thermochemical liquefaction of biomass for biofuel generation. Annual meeting of American Society Agricultural and Biological Engineering, Reno, Nevada, USA. June 20-24.

35. Eiteman, M.A., S. A. Lee, R. Altman, E. Altman. 2009. A substrate-selective co-fermentation strategy with *Escherichia coli* produces lactate by simultaneously consuming xylose and glucose. *Biotechnology and Bioengineering*, 102(3):822-827.

36. Vairavapandian, D. 2009. Formation of platinum thin films by electrochemical ALD and 2nd network of carbon nanotubes for electrochemical applications. PhD Dissertation, The University of Georgia, Department of Chemistry.

37. Das, K.C., M. Garcia-Perez, B. Bibens, and N.D. Melear. 2008. Slow pyrolysis of poultry litter and pine woody biomass -impact of chars and BioOils on microbial growth. Journal of Environmental Science and Health - Part A, 43(7):714-724.

38. Singh, K., L.M. Risse, J. Worley, K.C. Das, and S. Thompson. 2008. Effect of fractionation on fuel properties of poultry litter. Applied Engineering in Agriculture 24(4): 383-388. [ASABE Graduate Student Research Award Winning Paper. 2007]

39. Garcia-Nunez, J.A., M. Garcia-Perez, and K.C. Das. 2008. Determination of kinetic parameters of thermal degradation of palm oil mill byproducts using thermogravimetric analysis and differential scanning calorimetry. Transactions of the ASABE, 51(2):547-557.

40. Steiner, C., K.C. Das, M. Garcia, B. Forster, and W. Zech. 2008. Charcoal and smoke extract stimulate the soil microbial community in a highly weathered xanthic ferralsol. Pedobiologia, 51(5-6):359-366.

41. Brandon, S.K., M.A. Eiteman, K. Patel, M.M. Richboug, D.J. Miller, W.F. Anderson, and J. Doran Peterson. 2008. Hydrolysis of Tifton 85 bermudagrass in a pressurized batch hot water reactor. Journal of Chemical Technology and Biotechnology, 83(4):505-512
42. Das, K.C. 2008. Review of biorefinery concepts and opportunities in the palm oil sector. [Revision del concepto de biorefineria y oportunidades en el sector palmero]. In: Tertulias Palmeras, Document 93, Biomasa, una oportunidad mas para la agroindustria de la palma de aceite en Colombia. Bogota, DC, 29 July 2008. Published by Fedepalma, Carrera 10A, No. 69A-44, Bogota, Colombia.
43. Gaskin, J, K.C. Das, A. Tasistro, L. Sonon, K. Harris, and B. Hawkins. 2008. Characterization of biochar for agricultural use in the soils of the southeastern United States. In: Terra Preta Nova: A Tribute to Wim Sombroek. William Woods (Ed.), Springer Publishers.
44. Eiteman, M.A., S. A. Lee, E. Altman, "A Co-Fermentation Strategy to Consume Sugar Mixtures Effectively," *Journal of Biological Engineering*, 2:3 (2008) doi: 10.1186/175-1611-2-3
45. Mudhoo, A., V.K. Garg, R. Mohee, K.C. Das, and G.D. Unmar (Eds.) Special issue on "Treatment processes for mixed organic wastes, residual biosolids and wastewater", International Journal of Environment and Waste Management (2008).
46. Baker, S.A., W.D. Greene, K.C. Das and J. Peterson. 2008. Logging residues show promise for biofuel production. Forest Resources Association, Rockville MD 20852, Technical Release 08-R-6 [Peer reviewed technical notes].
47. Singh, K., M. Risse, J. Worley, K. C. Das, and S. Thompson. 2008. Effect of fractionation and pyrolysis on fuel properties of poultry litter. Peer reviewed proceedings. Air and Waste Management Annual Meeting and Expo, Portland, Oregon. [Nominated for Young Professional Best Paper Award 2008 Air and Waste Management Association]
48. Singh, K., E. W. Tollner, S. Mani, L. M. Risse, K. C. Das, and John Worley. 2008. Transforming solid wastes into high quality bioenergy products: Entropy analysis. ASME Paper No. 1924. Peer reviewed proceedings, North American Waste to Energy Conference (NAWTEC-16), Philadelphia, PA. May 19-21.
49. Singh K., E. W. Tollner, S. Mani, L. M. Risse, K. C. Das, and J. Worley. 2008. Emergy analysis of a pyrolysis process. Peer review proceedings, Fifth Biennial Energy Research Conference, University of Florida, Gainesville, Florida, January 31 - February 2.
50. Jena, U., S. Chinnasamy, S. Mani, and K. C. Das. 2008. Thermochemical liquefaction of microalgae into biofuels. Annual Environmental Conference, Atlanta, Georgia, October 9.

51. Jena, U., and K. C. Das. 2008. Kinetic study of catalytic decomposition of paper mill sludge, paulownia wood waste and micro algae using thermo gravimetric analyzer. Annual meeting of American Society Agricultural and Biological Engineering. Providence, Rhode Island, USA. June 29- July 2.
52. Jena, U., S. Chinnasamy, and K. C. Das. 2008. Transformation of algae into biofuel and chemicals. Annual meeting of Georgia section of American Society Agricultural and Biological Engineering, Georgia section of Soil and Water Conservation Engineering, Georgia section of International Erosion Control Engineering, Athens, GA, USA. June 4-6.
53. Jena, U., and K. C. Das. 2008. Gasification study of paper mill sludge, paulownia wood waste and micro algae using thermo gravimetric analyzer. Annual meeting of Institute of Biological Engineering, Chapel Hill, NC, USA. March 6-8.
54. Das, K.C., B. Bibens, J.R. Kastner, and R.Hilten. 2008. Biorefinery and Carbon Cycling – Producing biochar along with biofuels. Paper presented at the 2008 Conference of the International Biochar Initiative – Biochar, Sustainability and Security in a Changing Climate, Sept 8-10, Newcastle, United Kingdom.
55. Das, K.C. 2008. Pyrolysis based biorefinery – Multiple co-products and their utilization. Beneficial use of industrial materials summit. Organized by the United States Environmental Protection Agency and the United States Department of Agriculture, Denver, Colorado, USA, March 31.
56. Singh, K., M. Risse, J. Worley, K. C. Das, and S. Thompson. 2008. Effect of fractionation and pyrolysis on fuel properties of poultry litter. Peer reviewed proceedings. Air and Waste Management Annual Meeting and Expo, Portland, Oregon. [Nominated for Young Professional Best Paper Award 2008 Air and Waste Management Association]
57. Singh, K., E. W. Tollner, S. Mani, L. M. Risse, K. C. Das, and John Worley. 2008. Transforming solid wastes into high quality bioenergy products: Entropy analysis. ASME Paper No. 1924. Peer reviewed proceedings, North American Waste to Energy Conference (NAWTEC-16), Philadelphia, PA. May 19-21.
58. Jena, U., S. Chinnasamy, S. Mani, and K. C. Das. 2008. Thermochemical liquefaction of microalgae into biofuels. Annual Environmental Conference, Atlanta, Georgia, October 9.
59. Jena, U., S. Chinnasamy, and K. C. Das. 2008. Transformation of algae into biofuel and chemicals. Annual meeting of Georgia section of American Society Agricultural and Biological Engineering, GA Soil and Water Conservation Engineering, Georgia section of International Erosion Control Engineering, Athens, GA, USA. June 4-6.
60. Joshee, N., S. Corbett, K.C. Das, and A.K. Yadav. 2008. Paulownia: A multipurpose tree. Conference presentation at The VI International

Symposium of Floriculture and Silviculture in Arid Zones, 2008. La Paz, Baja California, Mexico. March 12-15.

61. Gaskin, J.W., A. Speir, K. Harris, D. Lee, And K.C. Das. 2008. Effect Of Pyrolysis Chars On Corn Yield And Soil Quality In A Loamy Sand Soil Of The Southern United States. Paper Presented At The Conference Of The International Biochar Initiative -Biochar, Sustainability And Security In A Changing Climate, 2008, Newcastle, United Kingdom, Sept 8-10.
62. Steiner, C., K. Harris, J. Gaskin, And K.C. Das. 2008. Pyrolytic Char Characterization For Its Use As A Soil Amendment. Paper Presented At The Conference Of The International Biochar Initiative -Biochar, Sustainability And Security In A Changing Climate. Newcastle, United Kingdom, Sept 8-10.
63. Baker, S.A., M.D. Westbrook., W.D. Greene, K.C. Das, J.D. Peterson, And R.L. Izlar. 2008. Evaluation Of Integrated Harvesting Systems In Pine Stands Of The Southern United States. Paper Presented At The World Bioenergy Conference, Jonkoping, Sweden, May 23-25.
64. Das, K.C. 2008. Catalytic Processes For Conversion Of Biomass To Liquid Fuels. Forestry Resources Association Annual Conference, Myrtle Beach, Sc, April 14.
65. Das, K.C. 2008. Pyrolysis Based Biorefinery -Multiple Coproducts And Their Utilization. Beneficial Use Of Industrial Materials Summit. Denver, Colorado, March 31- 10.
66. Garcia-Perez, M., T.T. Adams, J.W. Goodrum, D.P. Geller, and K.C. Das. 2007. Production and fuel properties of pine chip biooil/biodiesel blends. Energy and Fuels, 21 (4): 2363-2372.
67. Singh, K., K.C. Das, M. Risse, And J. Worley. 2007. Determination Of Composition Of Cellulose And Lignin Mixture Using Thermo Gravimetric Analysis (TGA). ASME Paper No. 32222. Peer Reviewed Proceedings, North American Waste To Energy Conference (Nawtec-15). Three Park Avenue. NY: ASME.
68. Das, K.C. 2007. Biorefining And Thermochemical Conversion Of Biomass To Energy And Products. [International Invited Presentation], University Of South Australia, Mawson Lakes Camus, South Australia, May 7.
69. Mani, S. And K.C. Das. 2007. Life Cycle Analysis Of Charcoal Production From Biomass. Aiche Annual Conference, Salt Lake City, Utah, USA.
70. Das, K.C. 2007. Thermochemical Biorefineries And The Use Of Products For Fuels, Biochar And Chemicals. [International Invited Presentation], Shanghai Academy Of Environmental Sciences, Shanghai, China, July 11.
71. Steiner, C., W.G. Texiera, J. Lehmann, B. Glaser, K.C. Das, M. De Arruda, And W. Zech. 2007. Agrichar Charcoal Use -Studies In The Humid Tropics. Poster Presented At The International Agrichar Initiative Conference, Terrigal, NSW, Australia. April 29-May2.

72. Das, K.C. 2007. Biorefinery And Hydrogen Fuel Cells Research And Education Program. Doe Biomass Program - Integrated Biorefineries Program Peer Review, Denver Co, August 10.

73. Singh, K., L.M. Risse, J. Worley, K.C. Das, And S. Thompson. 2007. Energy And Biooil Production From Poultry Litter Using Fractionation And Pyrolysis -A Quality Assurance Project Plant (QAPP). Paper No. 078021 Presented At ASABE Annual International Meeting, Minneapolis, Minnesota, June 17-20.

74. Singh, K., L.M. Risse, J. Worley, K.C. Das, And S. Thompson. 2007. Adding Value To Poultry Litter Using Fractionation, Pyrolysis, And Pelleting. Paper No. 074064 Presented At ASABE Annual International Meeting, Minneapolis, Minnesota, June 17-20.

75. Hunt, R., S. Chinnasamy, And K.C. Das. 2007. Microalgae Based Biodiesel Production Using Poultry Litter. Presented At The "Incredible Anaerobes - From Physiology To Genomics To Fuels". The Georgia Center, University Of Georgia, March 2-3.

76. Cyetkovic, Z., Y. Genest, E.T. Davies, K.C. Das, And J. Doran Peterson. 2007. Ethanol Production From Pulp And Paper Sludge. Presented At The "Incredible Anaerobes -From Physiology To Genomics To Fuels". The Georgia Center, University Of Georgia, March 2-3.

77. Das, K.C. 2007. Pyrolysis Processes And Products. Presentation At The "Biomass: Dispelling Myths And Advancing The Truth About This Valuable Resource" Workshop, Forsyth Ga. The Georgia Forestry Association. Feb 27.

78. Gaskin, J., A. Speir, K. Harris, D. Lee, L. Morris, And K.C. Das. 2007. Effect Of Two Types Of Pyrolysis Chars On Corn Yield, Soil Nutrient Status, And Soil C In A Loamy Sand Soil Of The Southeastern United States. Abstracts Of American Society Of Agronomy, Crop Science Society Of America, And Soil Science Society Of America International Annual Meetings. New Orleans, La. Nov. 4-8.

79. Harris, K., J. Gaskin, And K.C. Das. 2007. Effect Of Feedstock And Production Method On Pyrolysis Char Properties For Use As An Agricultural Soil Amendment. Abstracts Of American Society Of Agronomy, Crop Science Society Of America, And Soil Science Society Of America International Annual Meetings. New Orleans, La. Nov. 4-8.

80. Gaskin, J.W., A. Speir, L.M. Morris, L. Ogden, K. Harris, D. Lee, And K.C. Das. 2007. Potential For Pyrolysis Char To Affect Soil Moisture And Nutrient Status Of A Loamy Sand Soil. Proceedings Of The 2007 Georgia Water Resources Conference. University Of Georgia. Athens, Ga. March 27-29.

81. Garcia-Perez., M., C-Z. Li, M. Rhodes, And K.C. Das. 2007. Challenges And Opportunities For The Use Of Crude Bio-Oils As Source Of Fuels And Chemicals. Bioenergy Australia, Fremantle Western Australia, Dec 6-7.

82. Garcia-Perez, M., T.T. Adams, J.W. Goodrum, D.P. Geller and K.C. Das. 2007. Production and fuel properties of pine chip BioOil/biodiesel blends. Energy and Fuels 21, 2363-2372.

83. Kim, Y-G, J.Y. Kim, C. Thambidurai, and J.L. Stickney. 2007. Pb deposition on I coated Au (111), UHV-EC and EC-STM studies. Langmuir, 23, 2539-2545.

84. Garcia-Perez, M., K.C. Das, T.T. Adams. 2006. Thermochemical conversion of biomass in biorefineries. Book Chapter (In Press), In: Charcoal and biomass technologies for energy and agriculture, Translated to Portuguese and scheduled for publication in Brazil.

85. Das, K.C. 2006. Biorefining Principles And Opportunities. Presentation To The State Of Georgia Animal Waste Roundtable Meeting, October 3, Georgia Center, The University Of Georgia, Athens, Georgia, USA.

86. Das, K.C. 2006. Biorefinery Engineering – Bioconversion, Composting And Other Processing, For Value Added Production. Presentation At The National Agricultural Research Institute, Georgetown, Guyana, June 13. [International Invited Presentation]

87. Das, K.C. 2006. Biorefining Principles And Opportunities. [Invited Presentation] The University Of Georgia Academy Of The Environment Symposium, October 24, Georgia Center, The University Of Georgia, Athens, Georgia USA.

88. Gaskin, J., L. Morris, D. Lee, R. Adolphson, K. Harris, And K.C. Das. 2006. Effect Of Pyrolysis Char On Corn Growth And Loamy Sand Soil Characteristics. Abstracts Of American Society Of Agronomy, Crop Science Society Of America, And Soil Science Society Of America International Annual Meetings. Indianapolis, In. Nov. 12-16.

89. Harris, K., J.W. Gaskin, L.S. Sonon, And K.C. Das. 2006. Characterization Of Pyrolysis Char For Use As An Agricultural Soil Amendment. American Society Of Agronomy, Crop Science Society Of America, And Soil Science Society Of America International Annual Meetings. Indianapolis, In. Nov. 12-16.

90. Sonon, L. K. Harris, J. Gaskin, And K.C. Das. 2006. Phosphorus Sorption Characteristics Of Tifton Soil Amended With Pyrolysis-Derived Chars. Abstracts Of American Society Of Agronomy, Crop Science Society Of America, And Soil Science Society Of America International Annual Meetings. Indianapolis, In. Nov. 12-16.

91. Das, K.C., J.A. Garcia-Nunez, And M. Garcia-Perez. 2006. Overview Of A Biorefinery And Opportunities In The Palm Oil Sector. Plenary Address At The 15th International Palm Oil Conference, Cartagena, Colombia, Sept 19-25 [Memorias: Xv Conferencia International Sobre Palma De Aceite, Cartagena Colombia, Sept 19-22]

92. Garcia-Nunez, J.A., M. Garcia-Perez, And K.C. Das. 2006. Determination Of Kinetic Parameters Of Thermal Degradation Of Palm Oil Mill Byproducts

Using Thermogravimetric Analysis And Differential Scanning Calorimetry. Paper Presented At The International ASABE Conference, Portland, Oregon, July 9-12.

93. Greene, W.D., And K.C. Das. 2006. Forest Biomass Potential For Pyrolysis - Raw Material Issues And Potential Products. Paper Presented At The 60th International Convention Of The Forest Products Society Of America. Newport Beach Ca June 25-29.
94. Das, K.C. 2006. Biorefining Principles And Opportunities. Presentation To The State Of Georgia Animal Waste Roundtable Meeting, Georgia Center UGA. October 3.
95. Das, K.C., T.T. Adams, and E.D. Threadgill. 2006. Update On Research And Outreach In Biorefining At The University Of Georgia. ASABE State Section Meeting. Athens Ga. April 21.
96. Kim, Y-G., J.Y. Kim, D. Vairavapandian, and J.L. Stickney. 2006. J. Phys. Chem. B. 110, 17998-18006.
97. Kim,J.Y., Kim, Y-G, and J.L. Stickney. 2006. Studies of Cu atomic layer replacement, formed by underpotential deposits, to form Pt nanofilms using electrochemical atomic layer epitaxy. ECS Transactions, 1(3):41-48.
98. Das, K.C., T.T. Adams, and E.D. Threadgill. 2005. Biorefinery And Carbon Cycling Engineering. Poster Presentation At The Renewable Resources And Biorefineries Conference, Ghent Belgium, Sept 19-21.
99. Barczak, S., K.C. Das, And R. Kilpatrick. 2005. Water Quality Implications Of Bio-Fuels Development In Georgia. Proceedings Of The 2005 Georgia Water Resources Conference, Held At The University Of Georgia. Kathryn J. Hatcher, Editor, Institute Of Ecology, The University Of Georgia, Athens, Georgia. April 25-27.
100. Das, K.C., And E.D. Threadgill. 2005. Biorefinery- Integrated Processing Of Biomass To Multiple Products. Presentation To The SAF Meeting, Macon Ga. [Continuing Education Credits] Aug 23.
101. Das K.C. 2005. Principles Of Biomass Conversion Through Thermochemical Processes. Lecture At The Horticulture College, Tamil Nadu Agricultural University, Theni, India. Dec 2005 [International Invited Presentation]
102. Das K.C. 2005. Biorefining Technologies: Overview And Assessment. Biocycle Conference, Charlotte, North Carolina, USA, Nov 13-16 [Invited Presentation].
103. Threadgill, E.D., And K.C. Das. 2005. Challenges To Biomass Conversion: Biomass Opportunities And Realities In The Southeast United States. Warnell School and NCAD Conference. Aug 29.
104. Das, K. C., T.T. Adams, And E.D. Threadgill. 2005. Biorefinery - Integrated System For The Conversion Of Biomass To Chemicals, Fuels, And Bio-Products. SC-NC-GA State Section ASABE Meeting. Charleston Sc, June 2-3.
105. Das, K.C., T.T. Adams, R. Adolphson, And E.D. Threadgill. 2005. Biorefinery - Integrated System For The Conversion Of Biomass To

Chemicals, Fuels, And Bio-Products. Alternate Energy Technology Innovation, Georgia Tech Savannah Conference, Savannah Ga, May 12.
106. Das, K.C., T.T. Adams, R. Adolphson, And E.D. Threadgill. 2005. Biorefinery - Integrated System For The Conversion Of Biomass To Chemicals, Fuels, And Bio-Products. Georgia Industrial Technology Partnership Conference, Atlanta Ga, April 27.
107. Day, D., J. Lehmann, C. Steiner, K.C. Das. 2005. Long-Term Sequestration Of Carbon In Soils Using Charcoal From Renewable Energy Production. Third USDA Symposium On Greenhouse Gases & Carbon Sequestration In Agriculture And Forestry; Wyndham Baltimore - Inner Harbor, Baltimore, Maryland March 21 -24. [Abstract And Presentation]

Web site or other Internet sites that reflect the results of this project

This project hosted a website www.biorefinery.uga.edu that was intended to provide an overview of activities in the project. Listing of publications are provided on this site, however no direct description of research results are shown.

Networks or collaborations fostered

Through this project we fostered a very effective partnership with USDA-ARS represented by laboratories/centers in Georgia, South Carolina and Illinios. Several publications have resulted from this partnership and research work is continuing in a partnership at the time of writing this report.

Several on-campus partnerships between Engineering (lead), Crop and Soil Science, Microbiology, Forestry, and other fields have resulted.

Technologies/Techniques

Technologies developed in activities that included this grant were in pyrolysis, algal production in wastewaters and in fermentation. Briefly, between 2005 and 2008, Dr. Das (PI on this grant) and others on this team worked with Eprida Inc. (a private company based out of Georgia, USA) in pre-commercial testing of biomass pyrolysis and conversion of pyrolysis gases, through catalytic conversion, to hydrogen. The technology was developed by the National Renewable Energy Laboratory (Golden, Colorado) and the University of Georgia provided technology-transfer. Dr. Das served as the technical lead from the University of Georgia on this project.

Since 2007, University of Georiga has been partnering with Dalton Utilities (Dalton, Georgia) in developing a method of removing phosphorus from wastewater while cultivating algae for biofuel applications. The work includes laboratory scale testing and onsite pilot testing at the company site.

Inventions/Patent Applications, licensing agreements

A listing of patent applications that came out of this effort is shown below. Of these applications, some have been licensed and are described later.

1. U.S. Utility Patent Application 2011. Biological optimization systems for enhancing photosynthetic efficiency and methods of use. Publication No. US

2011/0179706A1; Application No: 13/014,464 Filed Jan 26, 2011. UGARF. Inventors: R.W. Hunt, S. Chinnasamy, K.C. Das, and E.R de Mattos.

- U.S. Provisional Patent Application. 2010. Biostimulants for enhancing biomass productivity and other metabolites in algae for biofuel and other commercial applications. K.C. Das, R.W. Hunt, S. Chinnasamy. Docket No. 222102-8990. Utility Patent Application Filed, Jan 16, 2011 (listed above).
- Patent Disclosure: 2010. Biostimulants for enhancing biomass productivity and other metabolites in algae for biofuel and other commercial applications. Inventors: K.C. Das, R.W. Hunt, S. Chinnasamy. Provisional Patent Application Field (listed above).

2. U.S. Utility Patent Application. 2011. Method and system of culturing an algal mat. Application No. 13/089, 380 (DOE #S-119,210). Filed April 19, 2011. US Department of Energy. Inventors: K.C. Das, B.R. Cannon, A. Bhatnagar, and S. Chinnasamy.
   - Patent Disclosure: 2009. Fog Supported Algal Mat Generator (FAM-Generator): A novel algal production technology for biofuel, bioenergy, and added value products. Inventors: B.R. Cannon, S. Chinnasamy, A. Bhatnagar, K.C. Das.
3. U.S. Utility Patent Application. 2010. Algal lipid harvest using mollusk for biofuel production. Publication No. US 2011/0045556; Application No. 12/862,246. Filed Aug 24, 2010. UGARF. Inventors: K.C. Das, S. Chinnasamy, J. Shelton, S.B. Wilde, R.S. Haynie and J.A. Herrin.
   - Patent Disclosure: 2009. A novel biobased method of harvesting microalgae for biofuels production. Inventors: K.C. Das, S. Chinnasamy, J. Shelton, S. Wilde, R. Haynie, J. Herrin.
4. U.S. Utility Patent Application. 2010. Method of increasing biomass productivity, lipid induction, and controlling metabolites in algae for production of biofuels using biochemical stimulants. Publication No. US 2011/0091945 A1; Application No. 12/907,206. Filed Oct 19, 2010. UGARF. Inventors: K.C. Das, R.W. Hunt, S. Chinnasamy, R. Claxton, and P. Raber.
5. U.S. Utility Patent Application. 2010. Production of higher quality bio-oil by in-line esterification of pyrolysis vapors. Filed Sept 2, 2010; Application No. WO 2010099058; Inventors: R.N. Hilten, K.C. Das, J.R. Kastner and B.P. Bibens.
   - Patent Disclosure: 2009. Production of higher quality bio-oils by in-line esterification of pyrolysis vapor with ethyl alcohol. Inventors: R.N. Hilten, K.C. Das, J.R. Kastner, B.P. Bibens.
6. U.S. Utility Patent Application. 2010. Microalgae cultivation in a wastewater dominated by carpet mill effluents for biofuel application. Filed April 8, 2010; Publication No. US 2010/0267122 A1; Application No. 12/756,371;

Inventors: S. Chinnasamy, A. Bhatnagar, R.W. Hunt, R. Claxton, M. Marlowe, and K.C. Das.

- Patent Disclosure: 2009. Animal waste derived organic plankton booster as low-cost renewable nutrient source for algaculture to produce biofuels. Inventors: K.C. Das, A. Bhatnagar, R.W. Hunt, S. Chinnasamy.
- Patent Disclosure: 2009. Mixotrophic algae and their consortia for the production of algae biofuel feedstock in wastewater fed open ponds. Inventors: A. Bhatnagar, S. Chinnasamy, K.C. Das.
- Patent Disclosure: 2009. Renewable biomass, biofuel, and bioproducts production from carpet industry wastewater (treated and untreated) using mixotrophic alga(e). Inventors: S. Chinnasamy, A. Bhatnagar, R.W. Hunt, R. Claxton, M. Marlowe , K.C. Das.

7. PCT International Patent Application. Filed 12 Aug 2010. Application No. PCT/US2010/045266. Biochars, methods of using biochars, methods of making biochars, and reactors. UGARF. Inventors: K.C. Das, N. Balagurusamy, S. Chinnasamy, G.J. Martinez Castro and C.A. Espino Lopez.
    - Patent Disclosure: 2009. Biochar as biostimulant to enhance biomethane production from animal waste. K.C. Das (3/10), S. Chinnasamy (3/10), N. Balagurusamy (2/10), G. Castro (1/10), C. Lopez (1/10).
8. Patent Disclosure: 2009. Process and product for minimizing nitrogen losses, enhancing microbial activity and accelerating stabilization of organic wastes during composting. Inventors: C. Steiner (4/10), K. C. Das (4/10), N.D. Melear (2/10).
9. Utility Patent Application Filed: 2008. "Substrate-Selective Co-Fermentation Process," U.S. Patent filed April 9, 2008. M. A. Eiteman, E. Altman.
10. Utility Patent Application Filed: 2007. Method for controlling the cooling rate and composition of condensing vapors from biomass pyrolysis. Inventors: T.M. Lawrence and K.C. Das.
    - Patent Disclosure: 2005. Method for controlling the cooling rate and composition of condensing vapors from biomass pyrolysis. Inventors: T.M. Lawrence and K.C. Das.